East & West Nishnabotna Watershed Coalition

West Nishnabotna River Watershed

Hydrologic Assessment Report

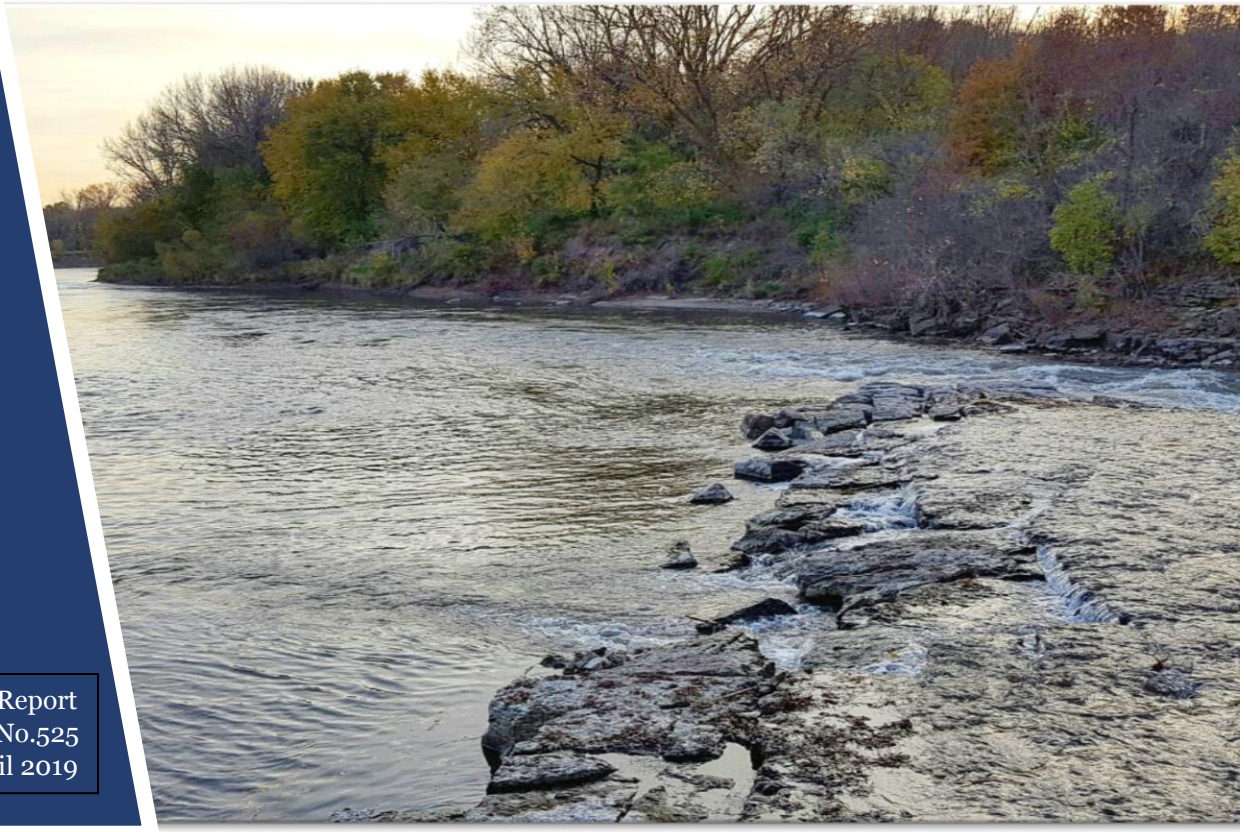

IIHR Report
No.525
April 2019

Prepared by:
Iowa Flood Center / IIHR — Hydroscience & Engineering

Sponsored by:
West Nishnabotna River Watershed Management Coalition

Iowa Watershed Approach
Phase I Report

IIHR — Hydroscience & Engineering
The University of Iowa
C. Maxwell Stanley Hydraulics Laboratory
Iowa City, Iowa 52242

Hydrologic Assessment of the West Nishnabotna River Watershed

April 2019

IIHR Technical Report No. 525

Prepared by:
Iowa Flood Center | IIHR—Hydroscience & Engineering
The University of Iowa
C. Maxwell Stanley Hydraulics Laboratory
Iowa City, Iowa 52242

Executive Summary

The Iowa Watershed Approach (IWA) is a vision for Iowa's future that voluntarily engages stakeholders throughout the watershed to achieve common goals, while moving toward a more resilient state. It is a scalable and replicable model for other watersheds and communities where the landscape has lost its natural resilience to floods. This program is not only about Iowans helping Iowans, but also about demonstrating Iowans' commitment to agricultural stewardship, to the environment, to their neighbors, and to the future. This report focuses on understanding the hydrology of the West Nishnabotna River Watershed and the potential impacts of large-scale land cover changes and the addition of flood detention structures throughout the watershed.

To better understand the watershed's hydrology, an overview of relevant data describing hydrology, geology, topography, land use, instrumentation, and historic water cycle, as well as a summary of previous floods of records was presented.

A computer model of the entire West Nishnabotna River Watershed was developed using the U.S. Army Corps of Engineers Hydrologic Engineering Center Hydrology Modeling System (HEC-HMS). Development of the model utilized the best available GIS data to characterize the terrain, land cover, soils, and overland flow network. Once calibrated, the model was used to investigate potential flow reductions resulting from several what-if scenarios exploring changes in land use, soil health, and distributed detention ponds. The what-if scenarios included conversion of all agricultural land to prairie grass, 100% utilization of cover crops to realize soil infiltration improvements, the addition of multiple detention ponds derived from Agricultural Conservation Planning Framework (ACPF) data, and a combination of all the ACPF detention ponds and 50% utilization of cover crops. Full implementation of these scenarios is not feasible, however, the maximum potential benefits of the what-if scenarios provide some context for achievable watershed improvement goals.

Overall, the largest reductions in flow and river stage were achieved by broad-scale land use changes or soil health improvements. Simulated flows were generally 20-40% lower with all agricultural areas converted to prairie grass. Simulated flows with 100% utilization of cover crops to improve soil health were generally 5-20% lower. A more feasible set of improvements, but ambitious nonetheless, was the distributed detention pond scenario that incorporated an additional 24,930 acre-feet of detention storage across 1153 pond structures. The pond scenario generally reduced flows along the main river segment less than 5%. While reductions along the main stem were much smaller, the impact of the ponds is highly dependent on the amount of pond storage added and upstream drainage area intercepted by the ponds. Flow reductions were generally substantial just downstream of ponds located in upland locations, but deceased with increasing drainage area. Using a combination of cover crops and detention storage generally reduced peak flows along the main river segment by 2-10%.

Realistic implementation of the watershed's improvement plan will likely draw upon combinations of land use changes, soil health improvement, and structural measures to achieve flood reduction goals. It is important to recognize that these modeling scenarios evaluate the hydrologic effectiveness of the flood mitigation strategies and not their effectiveness in other ways. For instance, while certain strategies are more effective in terms of hydrology, they may not be as effective economically. As part of the flood mitigation planning process, other factors should be considered in addition to the hydrology, such as the cost and benefits of alternatives, landowner willingness to participate, and more.

Acknowledgements

The Iowa Flood Center and IIHR—Hydroscience & Engineering would like to thank the following agencies and organizations for providing data and engaging in discussions that contributed to this assessment:

Iowa Department of Natural Resources
Natural Resources Conservation Service
Members of the West Nishnabotna Watershed Coalition
Golden Hills Resource Conservation & Development
Mills County
Fremont County

Table of Contents

List of Figures

List of Tables

Introduction

From 2011–13, Iowa suffered eight Presidential Disaster Declarations encompassing 73 counties and more than 70% of the state. As devastating as these events were, this period is but a small portion of Iowa's long history of enduring and recovering from major floods. Figure 1 shows just one example of devastation caused by the historic floods of 2008. Long-term data shows that heavy precipitation and flood events are increasing in frequency across the Midwest, and Iowans need to be prepared for the economic, social, and environmental impacts of these changing trends.

In January 2016, the state of Iowa received a $97 million award for the Iowa Watershed Approach (IWA). The grant was part of the U.S. Department of Housing and Urban Development's (HUD) National Disaster Resilience Competition, which funds cutting-edge projects to address unmet needs from past natural disasters and reduce Americans' vulnerability to future disasters. The project will end in September 2021.

Figure 1. Flooding at the confluence of the East and West Nishnabotna rivers during the June 2008 event. Photo taken on June 13, 2008, by the U.S. Army Corps of Engineers.

The Iowa Watershed Approach (IWA) program takes a holistic approach to address flooding at the watershed scale, recognizing that upstream and downstream communities need to voluntarily work together to increase community flood resilience.

The IWA will accomplish six specific goals:

1) Reduce flood risk;
2) Improve water quality;
3) Increase community flood resilience;
4) Engage stakeholders through collaboration, outreach, and education;

5) Improve quality of life and health for Iowans, especially for vulnerable populations; and
6) Develop a program that is scalable and replicable throughout the Midwest and United States.

The IWA brings Iowans together to address factors that contribute to floods. Nine distinct watersheds are involved in the project, including the Upper Iowa River, Upper Wapsipinicon River, Middle Cedar River, Clear Creek, English River, North Raccoon River, East Nishnabotna River, West Nishnabotna River, and Bee Branch Creek. In addition, urban projects in the cities of Dubuque, Coralville, and Storm Lake will focus on infrastructure improvements to mitigate flood risk.

Figure 2. Tour of a flood mitigation project in the Soap Creek Watershed, which was one of the basins that participated in the Iowa Watersheds Project (2010–16).

Each watershed has formed a Watershed Management Authority (WMA) that brings local stakeholders together to prioritize their watershed improvement needs, share resources, and foster new partnerships and collaborations. IIHR—Hydroscience & Engineering (IIHR) and the Iowa Flood Center (IFC) are developing a hydrologic assessment of each watershed that will provide WMAs, local leaders, landowners, and residents with an understanding of the hydrology – the movement of water – within their watershed. This assessment will deliver valuable information to stakeholders to help guide strategic decision-making to efficiently address flooding and water-quality concerns.

IIHR and IFC have developed this report for the West Nishnabotna River Watershed. Information in this report will be integrated into a comprehensive watershed resiliency plan. The watershed resiliency plan will guide long-term watershed management initiatives and planning efforts, as

well as identify goals and objectives to meet the current and future needs of local stakeholders and community members.

WMAs in the IWA watersheds have identified eligible sub-watersheds (e.g., HUC 12s) for practice implementation efforts. This report will help guide the implementation of small-scale flood mitigation projects. Through the IWA, volunteer landowners will be eligible to receive 75% cost-share assistance to implement best management practices (BMPs) such as ponds, wetlands, and water and sediment control basins (WASCOBS) to reduce the magnitude of downstream flooding and improve water quality during and after flood events. The implementation of BMPs is an essential step toward the long-term recovery to improve Iowa's future flood resiliency.

Figure 3. Flood mitigation structure in the Soap Creek Watershed.

The success of the IWA depends on collaborative partnerships among many statewide organizations and local stakeholders who together will carry out the work necessary to achieve the goals of the IWA. Partnerships include, but are not limited to:

- U.S. Department of Housing and Urban Development (HUD)
- U.S. Army Corps of Engineers
- Iowa Silver Jackets Flood Risk Management Team
- Iowa Economic Development Authority
- Iowa Homeland Security and Emergency Management
- University of Iowa (IIHR—Hydroscience & Engineering, Iowa Flood Center, Center for Evaluation and Assessment)
- Iowa State University (Iowa Nutrient Research Center, Iowa Water Center, Daily Erosion Project, ISU Extension & Outreach)
- University of Northern Iowa (Tallgrass Prairie Center)

- Watershed Management Authorities and their member entities
- Iowa Department of Natural Resources
- Iowa Department of Transportation
- Iowa Association of Counties
- Iowa Department of Agriculture and Land Stewardship
- Iowa Soybean Association
- Iowa Natural Heritage Foundation
- Iowa Corn Growers Association
- Iowa Farm Bureau
- Iowa Agricultural Water Alliance
- Cities of Dubuque, Coralville, and Storm Lake
- Local Resource Conservation and Development Offices
- Benton, Buena Vista, Fremont, Iowa, Johnson, Mills, Winneshiek, and Howard counties

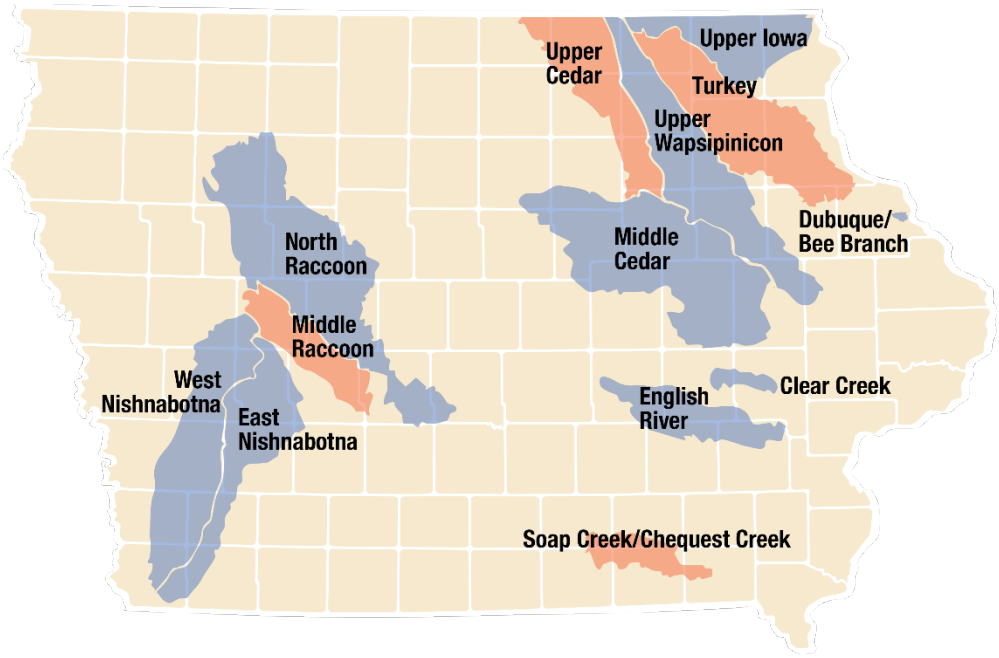

Figure 4. Current IWA watersheds in blue and completed IWP watershed in red.

The IWA is an expansion of the Iowa Watersheds Project (IWP) (Weber et al. 2018), a similar effort in the five Iowa watersheds (Upper Cedar River, Turkey River, Soap Creek, Middle Raccoon, and Chequest Creek) shown in Figure 4. HUD funded the IWP in the aftermath of the devastating 2008 floods; and the project was active from 2010–16. The success of the IWP served as a significant source of leverage for the state of Iowa to receive funding for the IWA, providing a framework to build upon, continuing Iowa's leadership and commitment to working together and improving flood resiliency. For more information on the Iowa Watersheds Project, visit http://iowafloodcenter.org/projects/watershed-projects/. For more information about the Iowa Watershed Approach, visit www.iowawatershedapproach.org.

1. Iowa's Hydrology and Water Quality

This chapter summarizes Iowa's water cycle, geology, land use, hydrology, and water quality across the state. The authors examined precipitation, streamflow, and shallow groundwater records to describe how much precipitation falls, how that water moves through the landscape, when storms typically produce river flooding, and how Iowa's hydrology, land use, and water quality have changed over the past decades and century. In addition, this chapter includes an overview of two novel web-based platforms that allow access to Iowa's flood and water-quality data. The information presented in this chapter is valid for the entire state, but some sub-sections place emphasis on the eight IWA watersheds shown in Figure 1.1.

Figure 1.1. Iowa Watershed Approach study areas.

a. Land Surface and Use

Iowa has a unique and diverse landscape that is the culmination of geologic processes occurring over millennia. Iowa has been subdivided into seven distinct landform regions, shown in Figure 1.2. The Iowa Watershed Approach projects are primarily contained within four of these regions: the Paleozoic Plateau, the Iowan Surface, the Southern Iowa Drift Plain, and the Des Moines Lobe landform regions. Surficial materials are underlain by a host of sedimentary bedrock formations including carbonate (limestone and dolomite), sandstone, and shale. Most of these rocks were deposited during the Paleozoic Era (541–299 million years ago), with others being deposited during the earlier Mesozoic Era (201–66 million years ago).

Following an extensive period of non-deposition and erosion, Iowa was glaciated numerous times during the Quaternary Period. At least seven episodes of glaciation occurred between 2.6 and 0.5 million years ago. These are collectively known as the Pre-Illinoian glacial advances. More recently, the Des Moines Lobe glacier advanced into north-central Iowa, reaching its maximum extent approximately 14,000 years ago. Subsequent loess (wind-blown silt) deposition occurred during and after this time, mantling much of the state. These glacial processes and erosional periods shaped the landform regions of Iowa.

The Southern Iowa Drift Plain encompasses the southern portion of the state and consists of several layers of Pre-Illinoian till deposits mantled by loess. Landscape development following the ice retreat eroded most of the features typically associated with glaciers and created the well-developed drainage network we see today. The Loess Hills landform region in the western part of the state has the same stratigraphic units as the Southern Iowa Drift Plain, but with thicker loess deposits because of its proximity to the source – the Missouri River alluvial plains.

In contrast, northeastern Iowa experienced a period of extreme cold (21,000 to 16,500 years ago) during the last glacial maximum, resulting in extensive erosion of the landscape and the formation of the Iowan Surface landform region. Characteristic features include gently rolling topography, common glacial “erratics” (rocks and boulders not native to Iowa transported here by glaciers), and loess-mantled paha (northwest to southeast trending uneroded upland remnants of the former landscape). The depth to bedrock is often shallow on this landform region. Surficial materials consist of poorly consolidated glacial deposits with the potential for extensive local sand bodies. In areas where the depth to bedrock is shallow, these materials provide limited protection from surface water infiltrating into bedrock.

The Paleozoic Plateau borders the Iowan Surface and experienced many of the same processes. The primary difference is that shallow bedrock dominates the Paleozoic Plateau. Characteristic features include steep sided, deeply entrenched valleys; abundant rock exposures; and common karst features. The unconsolidated materials consist of relatively thin glacial deposits with a loess mantle. Carbonate bedrock is susceptible to the formation of karst features, and numerous caves, springs, and sinkholes are identified throughout this landform region.

The younger Des Moines Lobe landform region is in north-central Iowa. This region was glaciated between approximately 15,000 and 12,000 years ago, with several advances and retreats before the glacier finally receded. Because of the relative youth of this region, erosional processes have not erased the surficial features typical of glacial landscapes. Characteristic features include glacial moraines (arcuate ridges associated with stationary periods), ice contact features (knobs, kettles, and hummocky terrain), fine-grained lake and pond deposits, and outwash (coarse sand and gravel carried by rivers draining glaciers). Natural drainage on the Des Moines Lobe is typically very poor.

Figure 1.2. Landform regions of Iowa.

Prairies covered Iowa before the arrival of European settlers, as depicted in historical vegetation shown in Figure 1.3. Forests and wetlands created a diverse set of habitats for animals, and prairies contained up to 300 species of grasses and flowers. As settlers tilled the prairie and planted crops such as wheat, corn, and buckwheat, the land cover of Iowa shifted to a majority agricultural state (Schilling et al., 2008).

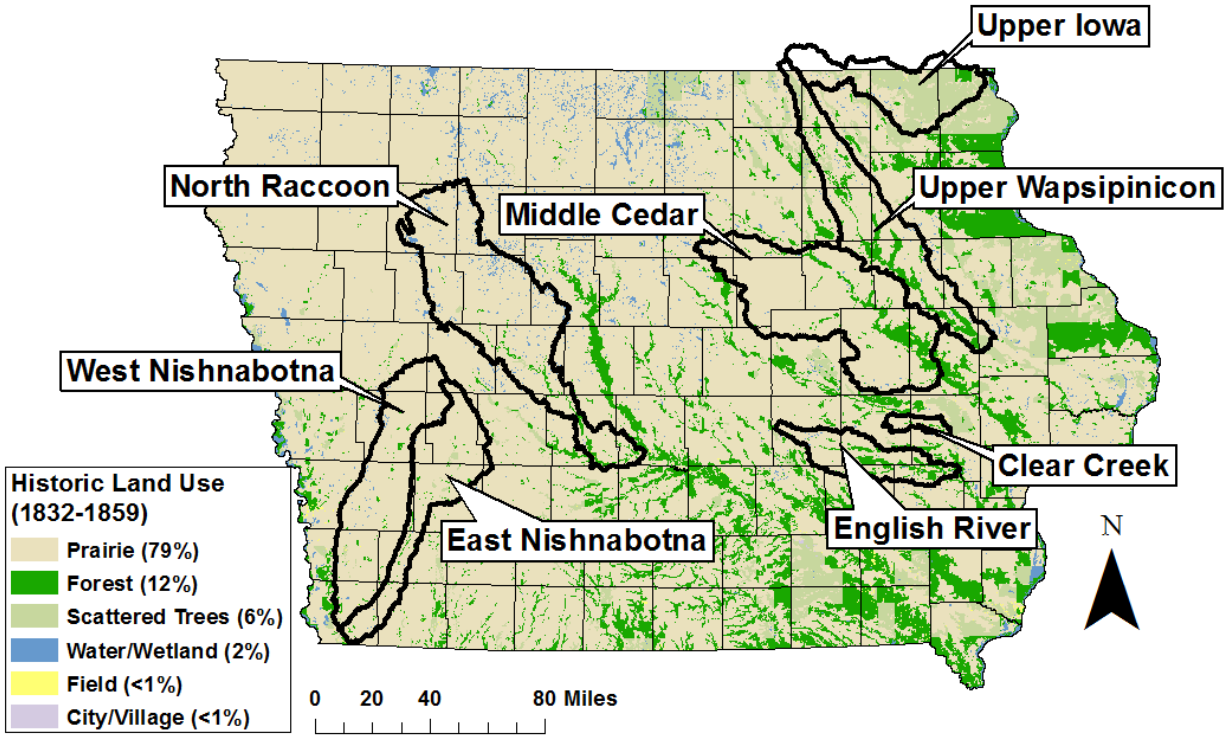

Figure 1.3. Historic vegetation of Iowa 1832–59. Raw data downloaded from the Iowa Geographic Map Server (https://ortho.gis.iastate.edu/).

Today, corn and soybeans cover 64% of Iowa, with only small prairie remnants remaining, which are shown in Figure 1.4. Several factors make Iowa an excellent place to sustain agricultural activities, including the rich topsoil left behind by the prairies; advances in farming technology including fertilizers, pesticides, and herbicides; and rainfall patterns, among others. Over the past 15 years, the percentage of Iowa's land used for growing corn and soybeans has stayed relatively stable at near 60%. The percentage of Iowa land area devoted to growing corn or soybeans is shown in Figure 1.5.

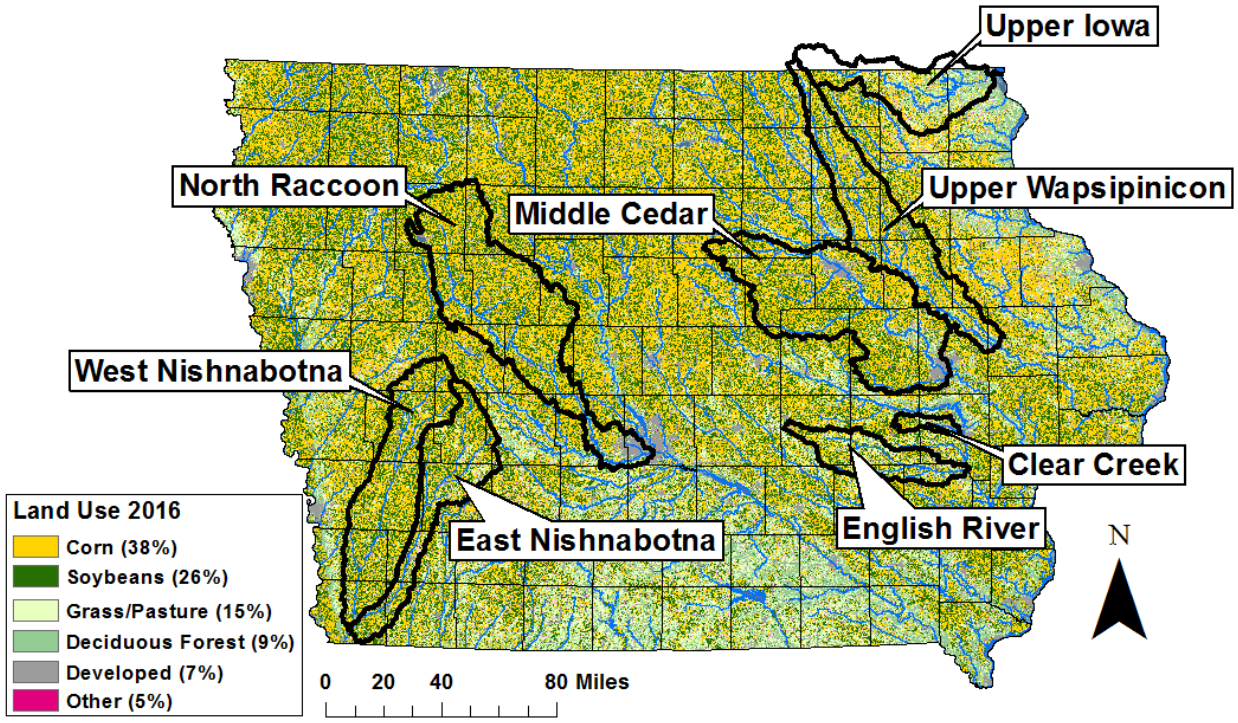

Figure 1.4. Land use composition in the state of Iowa 2016. Cropland Data Layer.

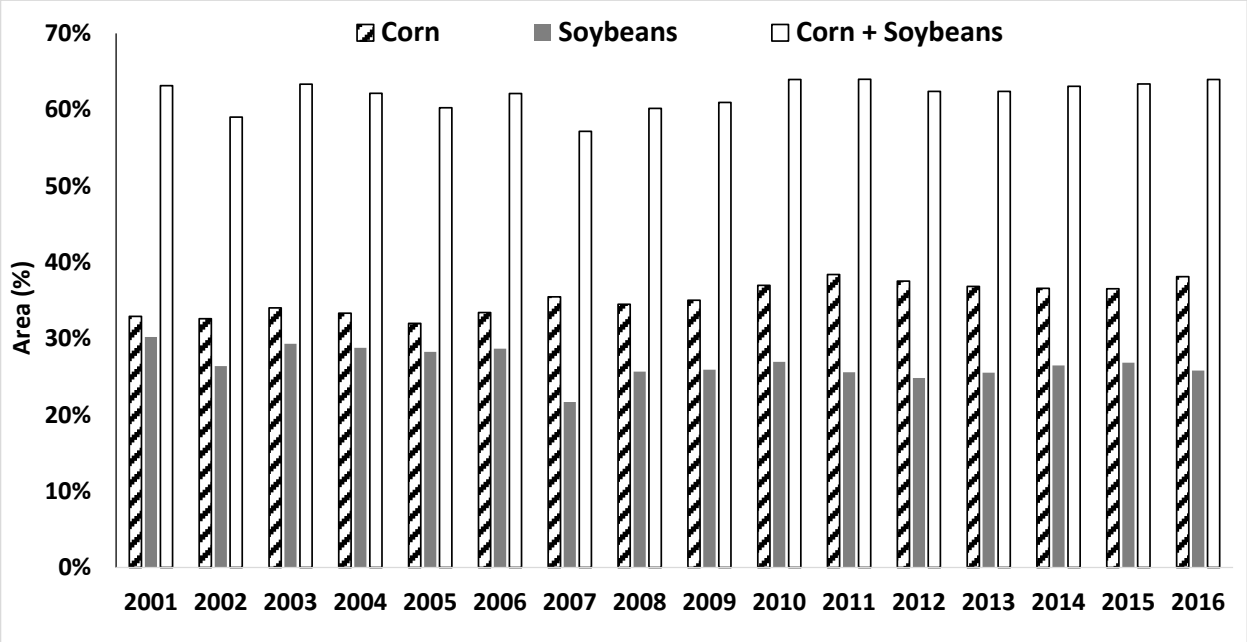

Figure 1.5. Percent of Iowa's total area planted with row crops between 2001 and 2016. Cropland Data Layer.

A significant portion of Iowa soils require sub-surface drainage to achieve optimal yields for row crops. Areas that likely require tile drainage are shown in Figure 1.6. It is estimated that installation of tile drainage peaked between the late 1800s and the mid-1900s, but today landowners continue to expand and upgrade drainage systems. In some areas (mostly in the Des Moines Lobe), public drainage districts were created to facilitate drainage over large areas. Drainage districts, also shown in Figure 1.6, have the power to tax and bond and are governed by trustees.

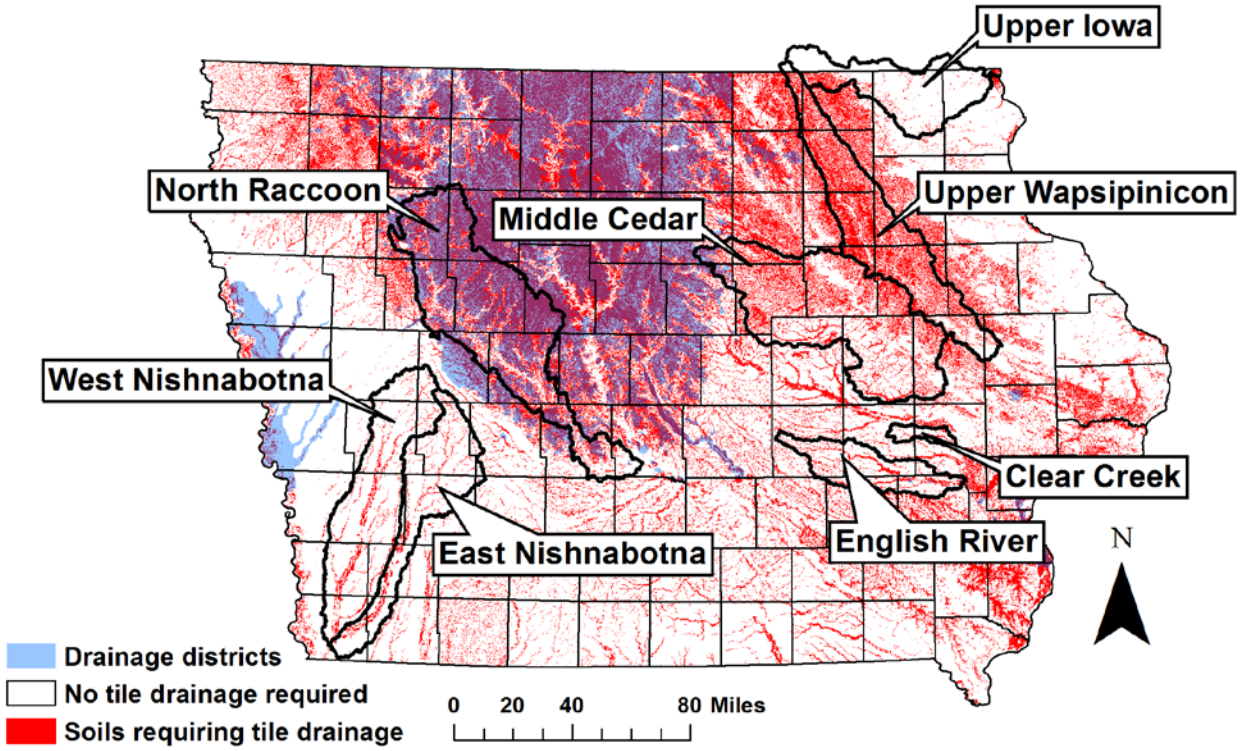

Figure 1.6. Soils requiring tile drainage for full productivity and drainage districts.

b. Climate and Water Cycle

Iowa is characterized by a humid continental climate with marked seasonal temperature variations, typically experiencing hot summers and cold winters. Annual average temperatures range between approximately 40°F and 60°F. Severe weather can impact regions of the state between the spring and fall; heavy rains and tornados are the most common of these events. Precipitation records show that Iowa typically receives the bulk of its annual precipitation in the spring and the summer.

i. Statewide Precipitation

Iowa's precipitation spatial patterns are marked by a smooth transition of annual precipitation across its landscape from the southeast to the northwest, as shown in Figure 1.7. The average annual precipitation reaches 40 inches in the southeast corner and decreases to 26 inches in the northwest corner.

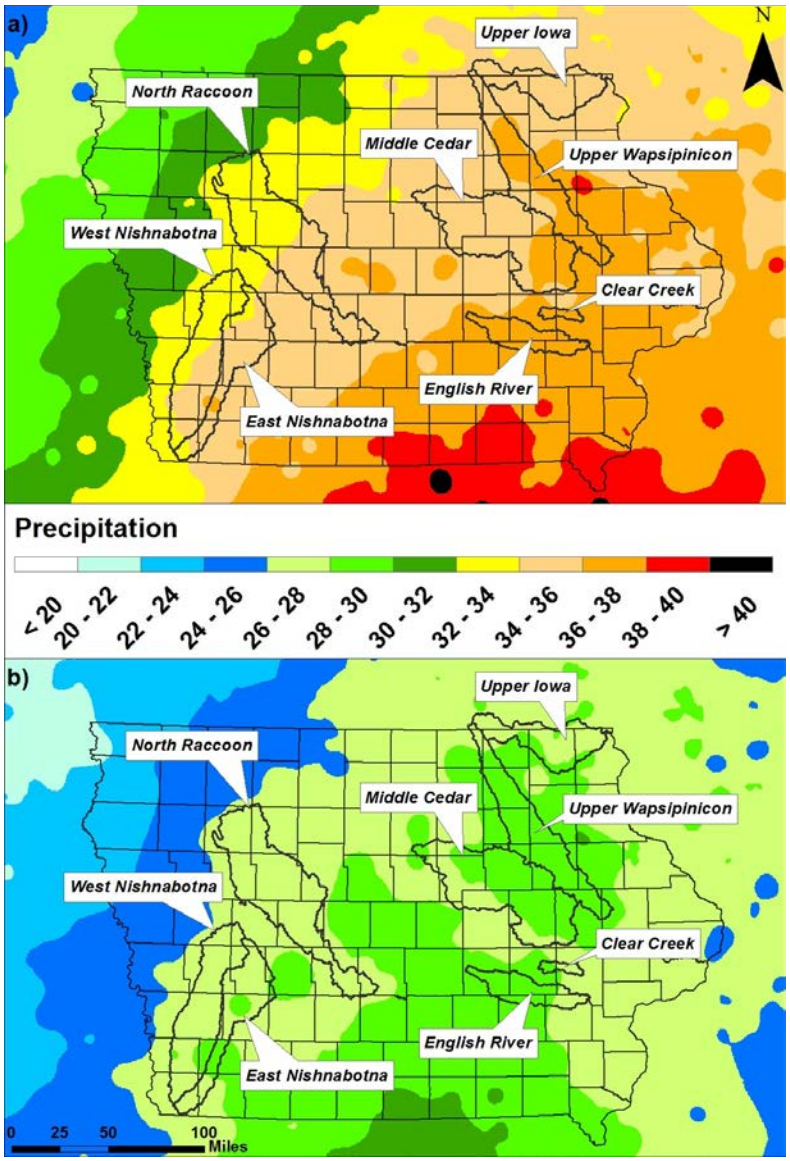

Figure 1.7. Average precipitation (inches): (a) annual; and (b) growing season (April–October). Precipitation estimates are based on the 30-year annual average (1981–2010). (Raw data downloaded from: http://www.prism.oregonstate.edu/).

Records show small variations in average annual precipitation among the eight IWA watersheds; the North Raccoon receives the least (33.8 inches), and the English River the most (36.6 inches). Historically, the quantity of annual precipitation presented in Figure 1.7b has been ideal for agricultural needs, such that Iowa has not required irrigation systems like other parts of the country. The state average precipitation between April and October is approximately 27 inches, and the months with highest precipitation accumulation (May, June, and July) occur during the peak of the growing season. These climatological characteristics make Iowa an ideal place for agriculture.

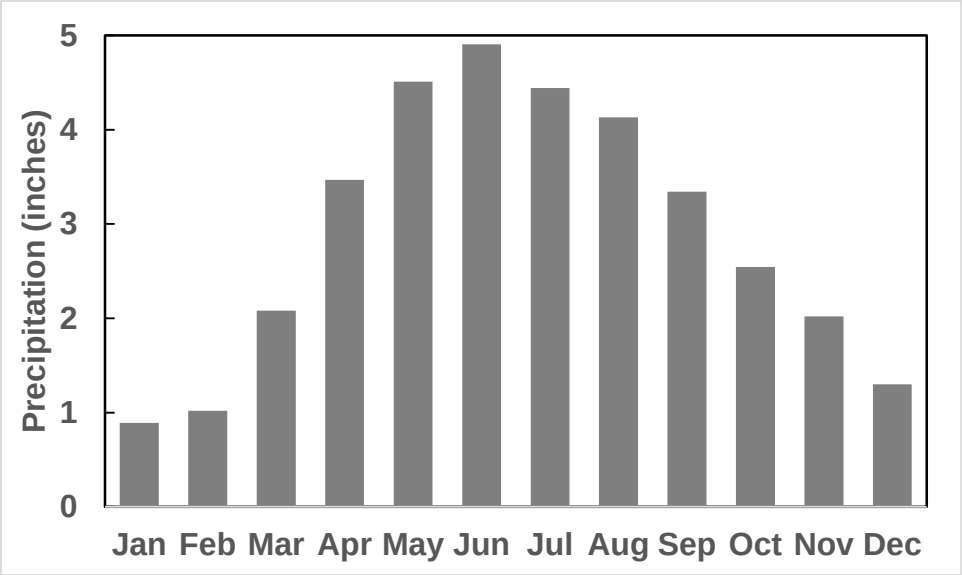

Figure 1.8. Statewide average monthly precipitation. Precipitation estimates are based on the 30-year annual average (1981–2010). (Raw data downloaded from: http://www.prism.oregonstate.edu/).

ii. The Water Cycle in Iowa

A large portion of Iowa's precipitation evaporates into the atmosphere — either directly from lakes and streams, or by transpiration from crops and vegetation. What doesn't evaporate drains into streams and rivers. The average annual partitioning of precipitation into evapotranspiration, surface flow, or base flow in each IWA watershed is shown in Figure 1.9.

Evapotranspiration

In Iowa, most precipitation leaves by evapotranspiration; for the IWA watersheds, evapotranspiration accounts for between 66% and 79% of precipitation. Moving westward in the state, a larger fraction of the precipitation evaporates, as can be seen in Table 1.1.

Surface Flow

The precipitation that drains into streams and rivers can take two different paths. During rainy periods, some water quickly drains across the land surface, causing streams and rivers to rise in the hours and days following the storm. This portion of the flow is often called "surface flow," even though some of the water may soak into the ground and discharge later (e.g., through a tile drainage system).

Baseflow

The rest of the water that drains into streams and rivers takes a longer, slower path; first it infiltrates into the ground, percolates down to the groundwater, and then slowly moves toward a stream. The groundwater eventually reaches the stream, maintaining flows in a river even during extended dry periods. This portion of the flow is often called "baseflow." In hydrologic analyses, sub-surface drainage flows are typically lumped with groundwater flows.

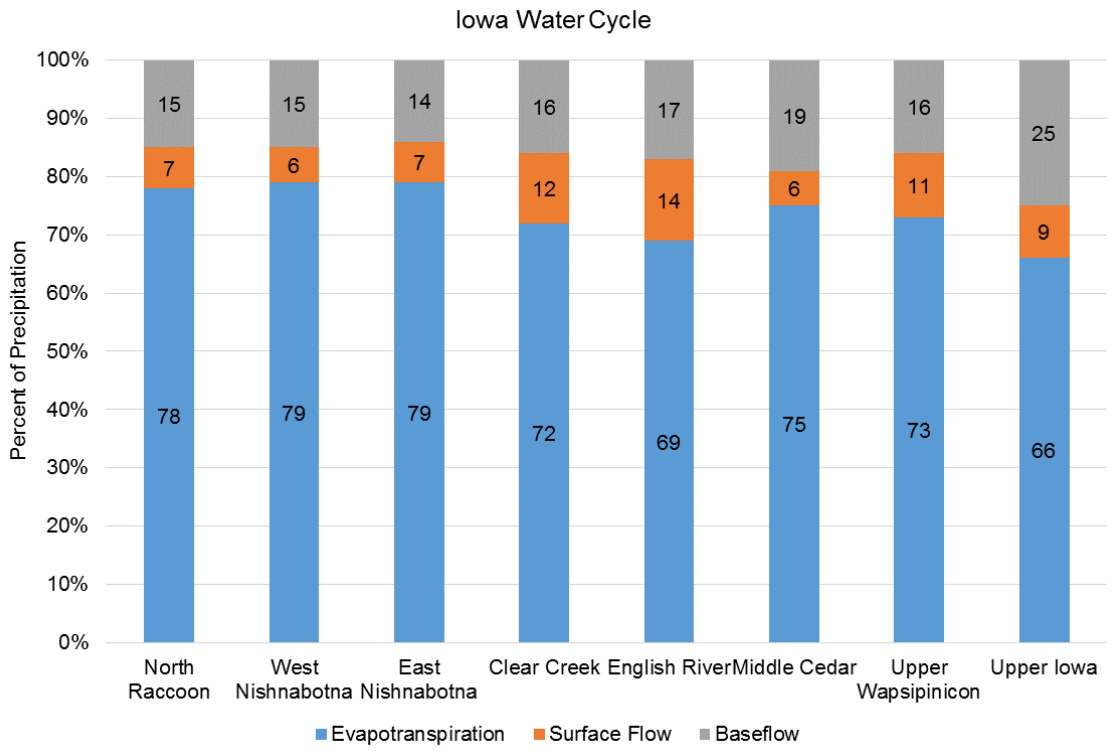

Figure 1.9. Iowa water cycle for the IWA watersheds. This shows the partitioning of average precipitation into evapotranspiration, surface flow, and baseflow components.

iii. Shallow Groundwater and Soil Moisture Trends

Shallow groundwater and soil moisture conditions can play an important role in the transformation of rainfall into runoff. For example, several studies have identified the occurrence of very wet winters and springs (and the subsequent high soil moisture and groundwater levels) as contributing factors to the major floods in 1993 and 2008 (Linhart and Eash, 2010; Mutel, 2010; Bradley, 2010; Smith et al., 2013). Across the state, almost 400 sensors continuously monitor the condition (e.g., streamflow and stage) of the Iowa rivers. In contrast, long-term continuous data on groundwater levels or soil moisture are sparse. Figure 1.10 displays shallow groundwater information from two United States Geological Survey (USGS) wells located in two different Iowa counties. The location of the water table is influenced by several factors, such as location on the landscape, land cover, soil type, etc. In Iowa, it is very common to find the location of the water table within the first 25 feet of the soil column, except in the deep loess hills in western Iowa and incised bedrock valleys of northeast Iowa.

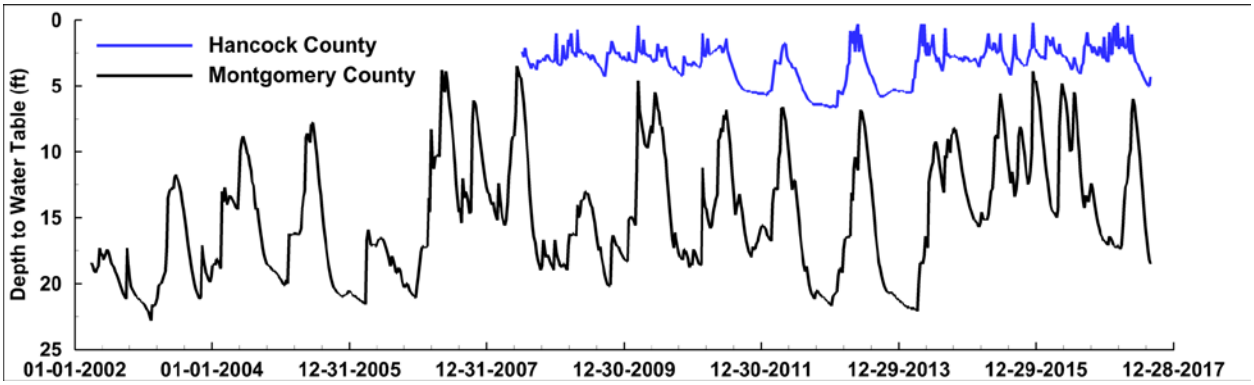

Figure 1.10. Shallow groundwater data (USGS wells).

iv. Floods

Rivers and streams have a finite capacity to convey water within their banks. When the amount of water surpasses that capacity, flooding occurs. Floods are typically related to large amounts of precipitation or snow melt and saturated or frozen soil. In Iowa, historic records show that the great majority (>90%) of floods occur in the spring and summer; the month of June shows the highest number of flood events. Precipitation records show that heavy rains occurred in the fall as well; however, Iowa soils have a larger capacity to infiltrate water late in the year, and therefore fall floods are less common. In Iowa's flood history, the events of 1993 and 2008 are on an entirely different scale than the others. These two events stand out from the rest when looking at the extent of the area impacted, recovery costs, precipitation amounts, and stream flows recorded (Bradley 2010; Smith et al., 2013). Figure 1.11 shows the extent of the flooding during the flood events of 1993 and 2008. In both years, flooding impacted the eight IWA watersheds.

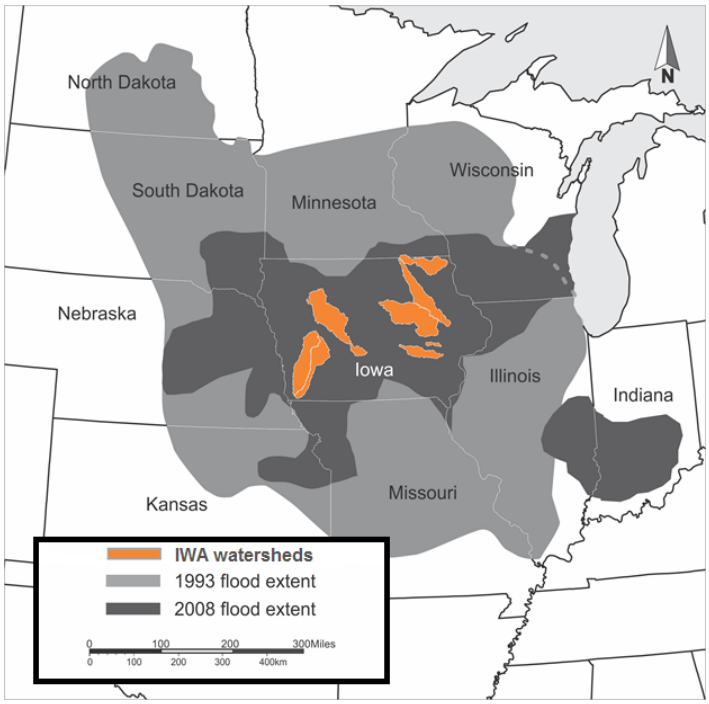

Figure 1.11. The extent of the flooding during the 1993 and 2008 floods (Bradley, 2010).

Federal disaster declarations give impacted regions access to federal recovery assistance. Current regulation permits two kinds of disaster declarations: emergency declarations and major disaster declarations (Stafford Act). Both are granted at the discretion of the president of the United States after the governor of the impacted state makes the request. FEMA records on disaster declarations are open to the public and were used to write the text and create the figures below.

- FEMA records show 952 flood-related disaster declarations (FRDD) in Iowa between 1988 and 2016. Of these, 951 were reported for Iowa counties (see Figure 1.12) and one for the Sac and Fox Tribe of the Mississippi in Iowa. All the FRDD in Iowa have been major disaster declarations except the 99 related to Hurricane Katrina evacuation (see Table 1.), which were classified as emergency disaster declarations.

Table 1.1. FEMA disaster declarations in Iowa (1988–2016).

DISASTER TITLE	COUNT 1988-2016
SEVERE STORMS, TORNADOES, AND ***FLOODING***	223
SEVERE STORMS & ***FLOODING***	195
SEVERE STORMS, TORNADOES AND ***FLOODING***	106
HURRICANE KATRINA EVACUATION	99
SEVERE STORMS AND ***FLOODING***	98
SEVERE STORMS, ***FLOODING*** , AND TORNADOES	97
SEVERE STORMS, TORNADOES, STRAIGHT-LINE WINDS, AND ***FLOODING***	79
SEVERE WINTER STORM	62
SEVERE WINTER STORMS	48
ICE STORM	44
SEVERE STORMS, STRAIGHT-LINE WINDS, AND ***FLOODING***	34
SNOW	30
SEVERE WINTER STORMS AND SNOWSTORM	27
SEVERE STORMS, AND ***FLOODING***	15
SEVERE SNOWSTORMS	13
FLOODING	6
SEVERE STORMS, TORNADOES, AND STRAIGHT-LINE WINDS	6
RAIN, WINDS, & TORNADOES	1
SEVERE STORM	1
	1184

- In the last 30 years, every county in Iowa has experienced sufficiently large and severe flood events to warrant a presidential disaster declaration. The number of FRDDs for each Iowa county from 1988–2016 is shown in Figure 1.12.

- The eastern half of the state has received more FRDDs than the western part. In addition, most counties in Northeast Iowa have received at least 10 FRDDs in the last three decades. The two counties with the lowest and highest number of FRDDs are O'Brien (4) and Clayton (17), respectively.

- Since 1988, the longest period with no FRDDs in Iowa was two years, which can be seen in Figure 1.13. The years with the highest number of FRDDs were 1993, 2005, and 2008. Remarkably, the number of FRDDs in 1993 is higher than the number of counties in Iowa. In that year, 15 counties received two FRDDs, one in late April and the second in early July (Buchanan, Butler, Des Moines, Linn, Black Hawk, Muscatine, Benton, Cedar, Louisa, Tama, Webster, Floyd, Mitchell, Kossuth, and Scott counties).

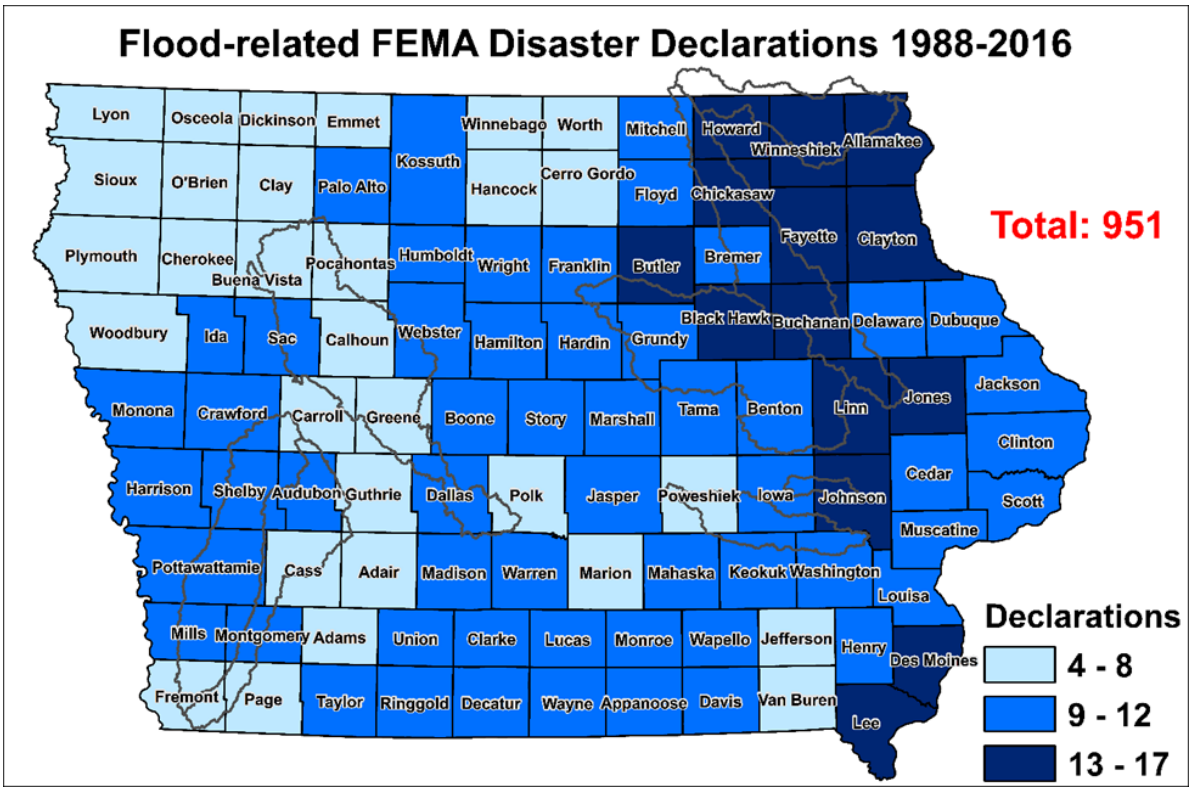

Figure 1.12. Number of flood-related federally declared disasters in Iowa counties (1988–2016). Data source: https://www.fema.gov/.

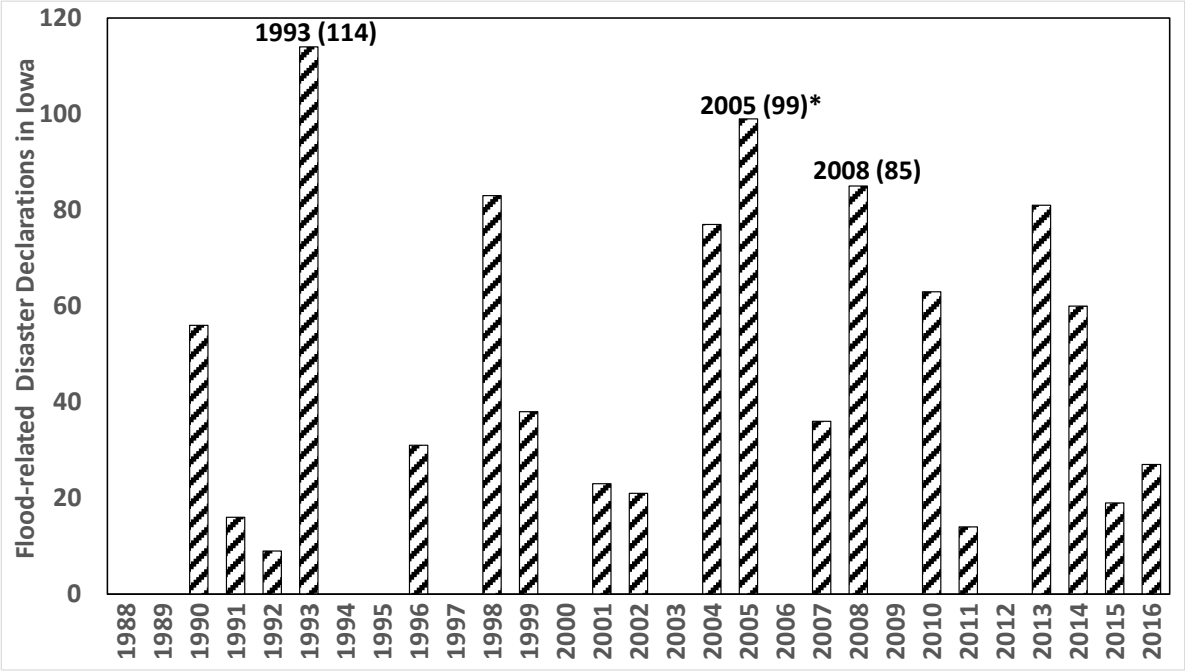

Figure 1.13. The number of flood-related federally declared disasters in Iowa (1988–2016). Data source: https://www.fema.gov/.

v. Droughts

Like floods, droughts are a recurrent phenomenon and part of the Earth's climate. Droughts are characterized by periods with precipitation deficits; depending on their severity, these can also include very low streamflows as well as reduced soil moisture and groundwater levels.

Unlike floods, droughts tend to progress slowly, and their onset is not easily identifiable. The extremely dry period of the 1930s (known as the "Dust Bowl") is still considered the unsurpassable benchmark against which all other droughts will be measured. In Iowa's recent history, both 1988 and 2012 stand out as drought years. Overall, comparisons of these two droughts reveal some similarities. In 1998, Iowa had its 4th hottest and 14th driest summer; whereas the 2012 summer was the 14th hottest and 5th driest in the observational record (Harry Hillaker, state climatologist).

Since 1999, several federal agencies and academic institutions partnered to create the U.S. Drought Monitor (USDM, http://droughtmonitor.unl.edu/), which releases a weekly map of drought conditions for the United States. Drought conditions are classified in five categories: Abnormally Dry (D0), Moderate Drought (D1), Severe Drought (D2), Extreme Drought (D3), and Exceptional Drought (D4). The map presented in Figure 1.14, shows the extent of 2012 drought in Iowa using data generated by the USDM.

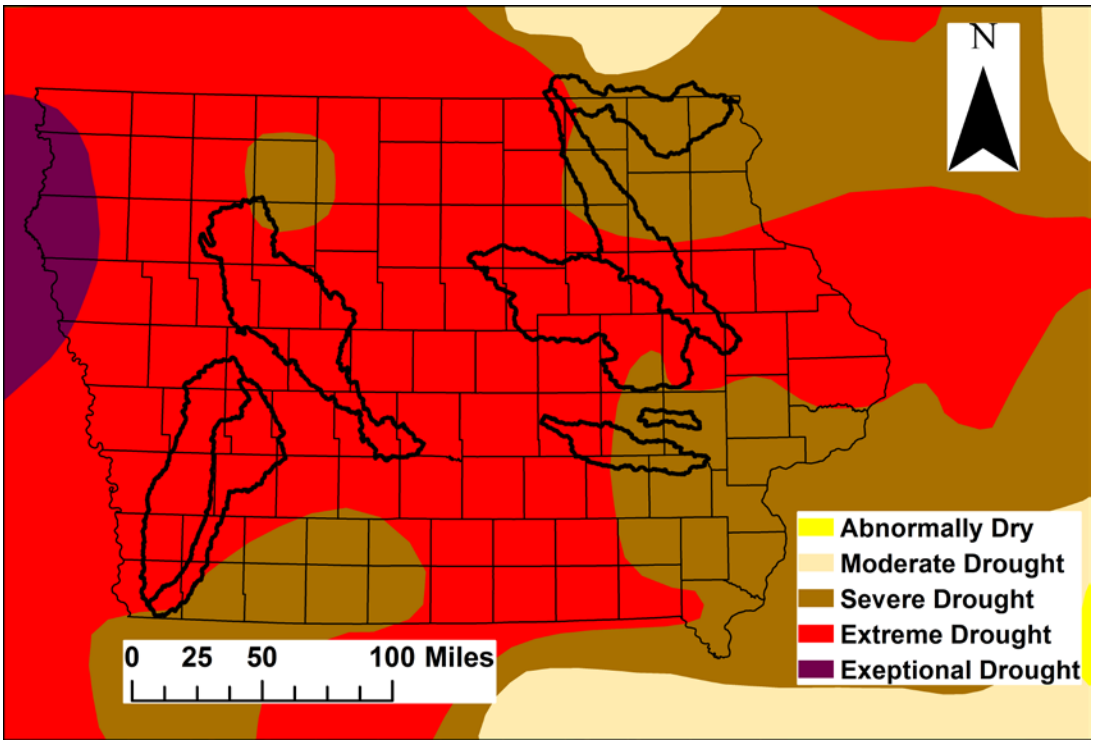

Figure 1.14. Drought conditions, October 09, 2012. (Source: http://droughtmonitor.unl.edu/).

c. Hydrological Alterations in Iowa and the Iowa Watershed Approach Study Areas

Although the hydrologic conditions presented for the Iowa Watershed Approach study areas illustrate the historical water cycle, the watersheds themselves are not static; historical changes have occurred that have altered the water cycle. In this section, we discuss the hydrological alterations of Iowa's watersheds.

i. Hydrological Alterations from Agricultural-Related Land Use Changes

The Midwest, with its low-relief poorly-drained landscape, is one of the most intensively managed areas in the world (Schilling et al., 2008). With European-descendent settlement, most of the land was transformed from low-runoff prairie and forest to higher-runoff farmland (see Figure 1.3 and 1.4). Within Iowa, the land cover changes in the first decades of settlement occurred at an astonishing rate (Wehmeyer et al., 2011). Using land cover information obtained from well-documented studies in 1859, 1875, and 2001, Wehmeyer et al. (2011) estimated that the increase in runoff potential in the first 30 years of settlement represents the majority of predicted change in the 1832 to 2001 study period.

Still, other transformations associated with an agricultural landscape have also impacted runoff potential (see Table 1.2). For example, the introduction of conservation practices in the second half of the 20th century tend to reduce runoff, as suggested by a recent study of an Iowa watershed (Papanicolaou et al., 2015). The Conservation Reserve Program (CRP) originally began in 1950s. The federal government established many programs in the 1970s to remove lands from agricultural production and establish native or alternative permanent vegetative cover; in an effort to reduce erosion and gully formation, government agencies also encouraged practices such as terraces, conservation tillage, and contour cropping. The Farm Bill of 1985 was the first act that officially established the CRP as we know it today; the Farm Bills of 1990, 1996, 2002, and 2008 expanded these activities. The 2014 Farm Bill gradually reduced the CRP cap from 32 million acres to 24 million acres, although the 2018 Farm Bill is expected to increase the CRP cap to 29 million acres. Table 1.2 summarizes the timeline of agriculture-driven land use changes and their impacts on local hydrology.

Table 1.2. Agricultural-Related Alterations and Hydrologic Impacts.

Timeline	*Land use status, change, & interventions*	*Hydrologic effect(s)*	*Source*
1830s–Prior	Native vegetation (tall-grass prairies and broad-leaved flowering plants) dominate the landscape	Baseflow dominated flows; slow response to precipitation events	Petersen (2010)
1830–1980	Continuous increase in agricultural production by replacement of perennial native vegetation with row crops 1940: <40% row crop (Raccoon) 1980: 75% row crop (statewide)	Elimination of water storage on the land; acceleration of the upland flow; expanded number of streams; increased stream velocity	Jones & Schilling (2011); Knox (2001)
1820–1930	Wetland drainage, stream channelization (straightening, deepening, relocation) leading to acceleration of the rate of change in channel positioning	Reduction of upland and in-stream water storage, acceleration of stream velocity	Winsor (1975); Thompson (2003); Urban & Rhoads (2003)
1890–1960 2000–present	Reduction of natural ponds, potholes, wetlands; development of large-scale artificial drainage system (tile drains)	Decrease of water storage capacity, groundwater level fluctuations, river widening	Burkart (2010); Schottler et al. (2013)
1940–1980	Construction of impoundments and levees in Upper Mississippi Valley	Increased storage upland	Sayre (2010);
1950–present	Modernization/intensification of the cropping systems	Increased streamflow, wider streams	Zhang & Schilling (2006); Schottler et al. (2013)
1970–present	Conservation practices implementation: Conservation Reserve Program (CRP); Conservation Reserve Enhancement Program (CREP); Wetland Reserve Program (WRP)	Reduction of runoff and flooding; increase of upland water storage	Castle (2010); Schilling (2000); Schilling et al. (2008);
2001–present	62% of Iowa's land surface is intensively managed to grow crops (dominated by corn and soybeans up to 63% of total)	About 25% to 50% of precipitation converted to runoff (when tiling is present)	Burkart (2010)

ii. Hydrological Alterations Induced by Climate Change

The U.S. goverment recently released The Climate Science Special Report (Wuebbles et al., 2017) summarizing the state-of-the-art science on climate change and its physical effects. The CSSR writing team is comprised of three coordinating lead authors from the National Science Foundation and U.S. Global Change Research Program, NOAA Earth System Research Laboratory, and NASA Headquarters. In addition, more than 50 experts from federal agencies, departments, and universities are listed as lead authors, review editors, and contributing authors. CSSR is "designed to be an authoritative assessment of the science of climate change, with a focus on the United States, to serve as the foundation for efforts to assess climate-related risks and inform decision-making about responses." The information below presents text and figures taken from the CSSR that are relevant to the IWA watersheds, Iowa, and the Midwest.

"Heavy rainfall is increasing in intensity and frequency across the United States (see Figure 1.15) and globally and is expected to continue to increase over the next few decades (2021–2050, see Figure 1.16), annual average temperatures are expected to rise by about 2.5°F for the United States, relative to the recent past (average from 1976–2005), under all plausible future climate scenarios."

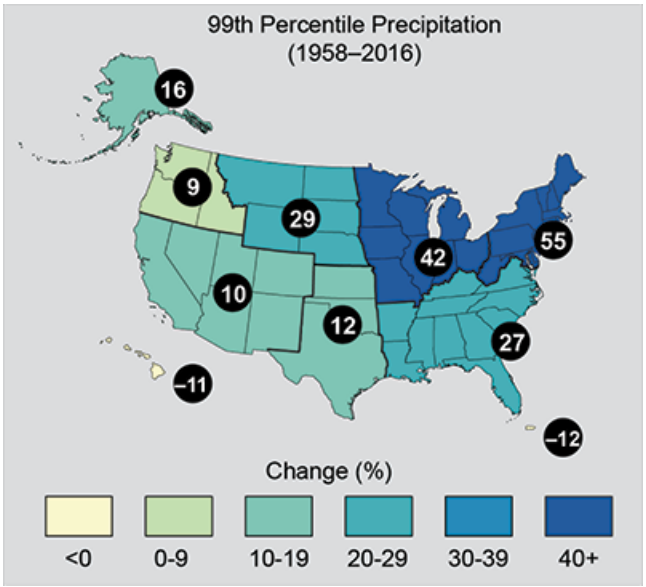

Figure 1.15. Observed change in heavy precipitation (the heaviest 1%) between 1958 and 2016. Figure taken from The Climate Science Special Report (Easterling et al. 2017) (https://science2017.globalchange.gov/).

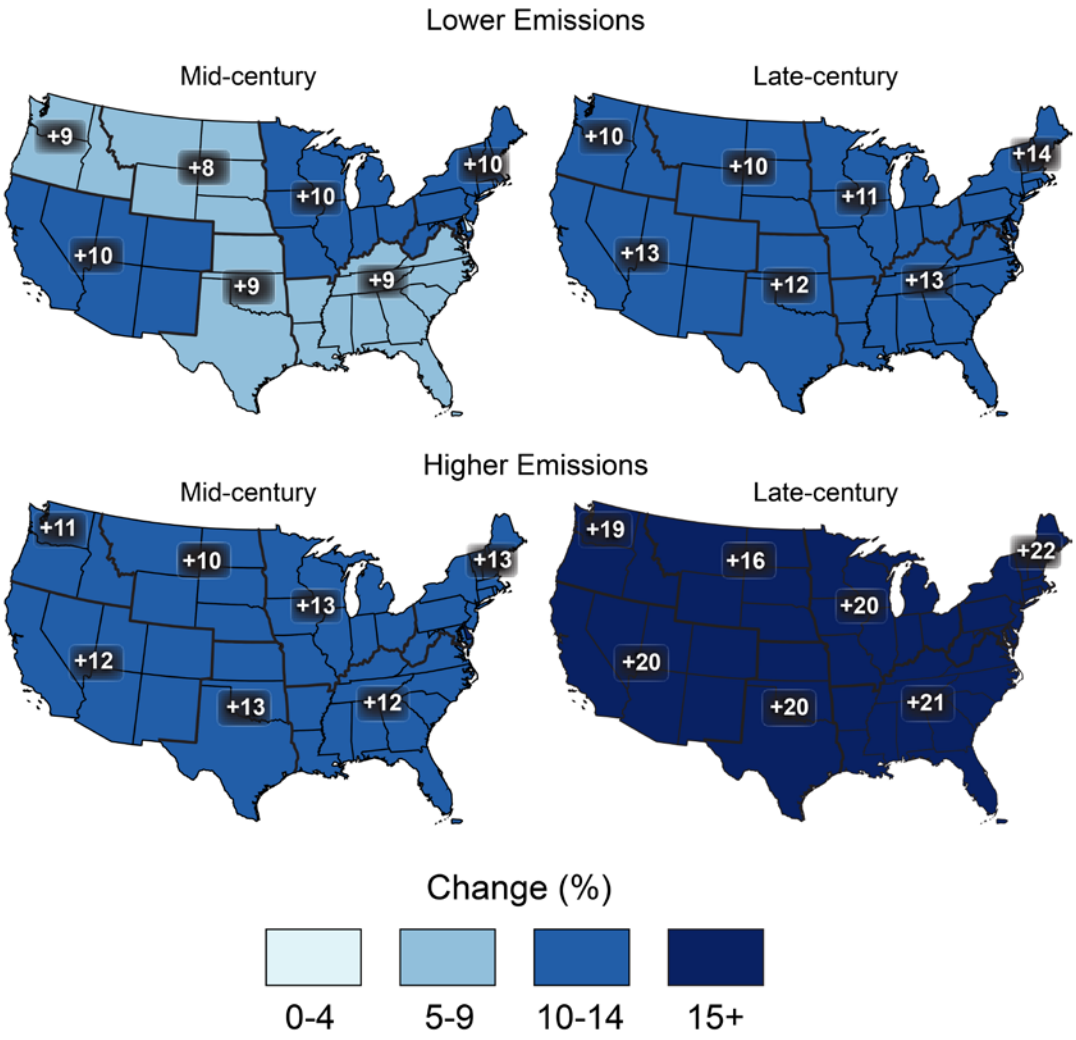

Figure 1.16. Projected change in heavy precipitation. Twenty-year return period amount for daily precipitation for mid- (left maps) and late-21st century (right maps). Results are shown for a lower emissions scenario (top maps; RCP4.5) and for a higher emissions scenario (bottom maps, RCP8.5). Figure taken from The Climate Science Special Report (Easterling et al. 2017) (https://science2017.globalchange.gov/).

iii. Hydrological Alterations Induced by Urban Development

Although Iowa remains an agricultural state, a growing portion of its population resides in urban areas. The transition from agricultural to urban land uses has a profound impact on local hydrology, increasing the amount of runoff, the speed at which water moves through the landscape, and the magnitude of flood peaks. The factors that contribute to these increases (Meierdiercks et al., 2010) are the increase in the percentage of impervious areas within the drainage catchment and its location (Mejia et al., 2010), and the more efficient drainage of the landscape associated with the constructed drainage system — the surface, pipe, and roadway channels that add to the natural stream drainage system. Although traditional stormwater

management practices aim to reduce increased flood peaks, urban areas have long periods of high flows that can erode stream channels and degrade aquatic habitat.

d. Assessment of Iowa's Water Quality

i. Iowa Water-Quality History

Prior to European settlement in the 19th century, Iowa was covered with prairies, oak savannahs, wetlands, and forests (see Figure 1.3). Much of the landscape was internally drained, meaning that rainfall and snowmelt drained to small depressional areas, rather than streams. Groundwater-fed streams meandered across the landscape and likely ran shallow and clear, carrying low levels of sediment and nutrients. Rivers easily spilled out into the flood plain after heavy rains, and river banks re-vegetated during drought, reducing streambank erosion.

Over several decades, the native prairie was broken and cultivated for corn, oats, and alfalfa, as well as a few other minor crops. Soil erosion was intense in the first years following a field's cultivation. From the period of 1880 to 1920, pervious clay pipes drained many of Iowa's wettest areas. This was most common in the recently-glaciated area of north-central Iowa known as the Des Moines Lobe, shown in Figure 1.2. Many new streams were constructed in ditches to drain water externally to the river network. Many existing streams were straightened to facilitate crop production.

The post-World War II era brought new developments to agriculture. The emergence of chemical fertilizers, soybeans, and continued drainage of the landscape with plastic drainage tiles helped Iowa become a world leader in crop and livestock production.

The loss of the native ecosystems, stream straightening and incision, artificial drainage, and discharges from industries and municipalities degraded water quality. Although the decline in water quality probably subsided in the early 1980s, Iowa's streams still carry more nutrients and sediment than most people find acceptable.

ii. Water Quality in the Post-Clean Water Act Era

The Federal Water Pollution Control Act of 1948 was the first major U.S. law to address water pollution. Growing public awareness and concern for controlling water pollution led to sweeping amendments in 1972. The amended law became commonly known as the Clean Water Act (CWA). The 1972 Amendments achieved the following: (1) established the basic structure for regulating pollutant discharges into the waters of the United States; (2) gave EPA the authority to implement pollution control programs, such as setting wastewater standards for industry; (3) maintained existing requirements to set water-quality standards for all contaminants in surface waters; (4) made it unlawful for any person to discharge any pollutant from a point source into navigable waters, unless a permit was obtained under its provisions; (5) funded the construction of sewage treatment plants under the construction grants program; and (6) recognized the need for planning to address the critical problems posed by nonpoint source pollution.

After passage of the CWA, construction began on many new wastewater treatment facilities in Iowa, and upgrades were implemented on many existing treatment works. Undoubtedly these efforts improved water quality in several of Iowa's major interior rivers, in addition to the Missouri and Mississippi rivers on its borders. Improvements in the levels of ammonia, oxygen demand, Kjeldahl (organic) nitrogen, and dissolved oxygen were particularly important. These improvements made river water quality much more suitable for recreation and aquatic life, especially near Iowa's larger cities. However, the CWA provisions to address non-point source pollution (i.e., pollution from diffuse areas) proved relatively ineffective in reducing levels of nutrients and sediment in Iowa streams. The main CWA program designed to address non-point source pollution was the 319 Grant Program.

The Food Security Act of 1985 (Farm Bill) required farmers participating in most programs administered by the Farm Service Agency (FSA) and the Natural Resources Conservation Service (NRCS) to abide by certain conditions on any highly erodible land owned or farmed, or land considered a wetland. To comply with the highly erodible land conservation and wetland conservation provisions, farmers were required to certify that they would not: (1) produce an agricultural commodity on highly erodible land without a conservation system; (2) plant an agricultural commodity on a converted wetland; and (3) convert a wetland to produce an agricultural commodity. As result of these requirements, sediment levels in Iowa streams declined and water clarity improved (Jones and Schilling, 2011). Phosphorus levels also declined in unison with the improvements in sediment transport and water quality (Wang et al., 2016). However, conservation compliance, as these requirements are known, has not had a similar beneficial effect on stream nitrate levels (Sprague et al., 2011; Jones et al., 2017).

Iowa policy-makers and watershed stakeholders look to the Impaired Waters list, Section 303(d), as a common reference point to gauge statewide water quality. According to Section 303(d) of the CWA, from "time to time" states must submit a list of lakes, wetlands, streams, rivers and portions of rivers for which effluent limits will not be sufficient to meet all state water-quality standards. The EPA has defined "time to time" to mean April 1 of even numbered years. The failure to meet water-quality standards might be due to an individual pollutant, multiple pollutants, "pollution," or an unknown cause of impairment. The 303(d) listing process includes waters impaired by point sources and non-point sources of pollution. States must also establish a priority ranking for the listed waters, considering the severity of pollution and uses. In 2016, there were 608 category 5 Iowa waterbodies with 818 impairments. In 2014, there were 571 impaired waterbodies with 754 impairments. Category 5 waterbodies are those where a Total Maximum Daily Load assessment is required. About 58% of Iowa streams are considered "impaired"; 23% are considered "potentially impaired"; and 19% are considered to have "good" water quality. Indicator bacteria (i.e., *E. coli*) are the most common cause of impairment, causing about half of all such designations. Biological impairments are next, followed by fish kills. Figure 1.17 lists the main causes. Figure 1.18 shows historical numbers of impaired Iowa waters.

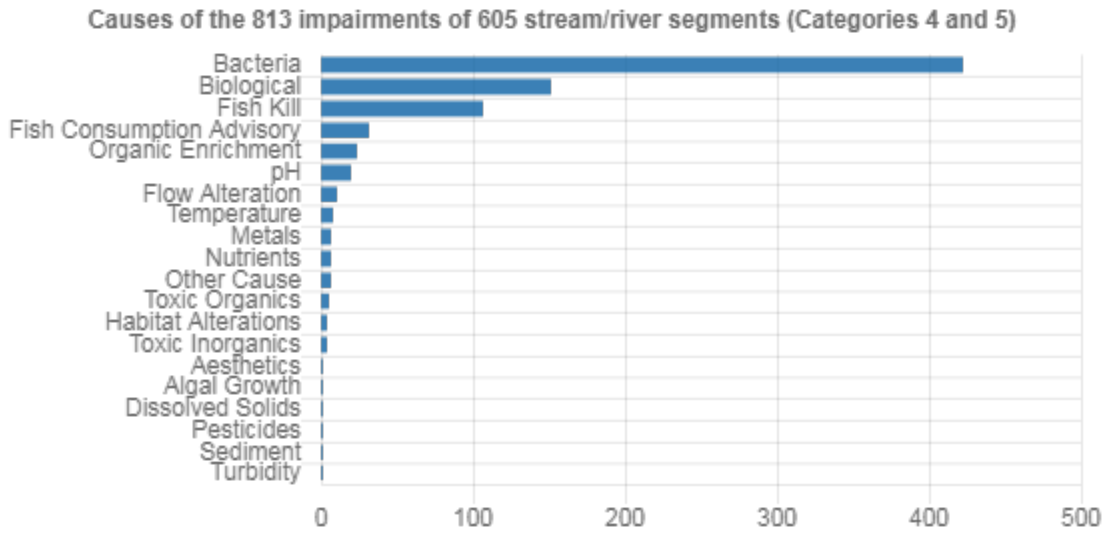

Figure 1.17. Causes of impairments in Iowa's impaired waters. (Iowa Department of Natural Resources, 2018).

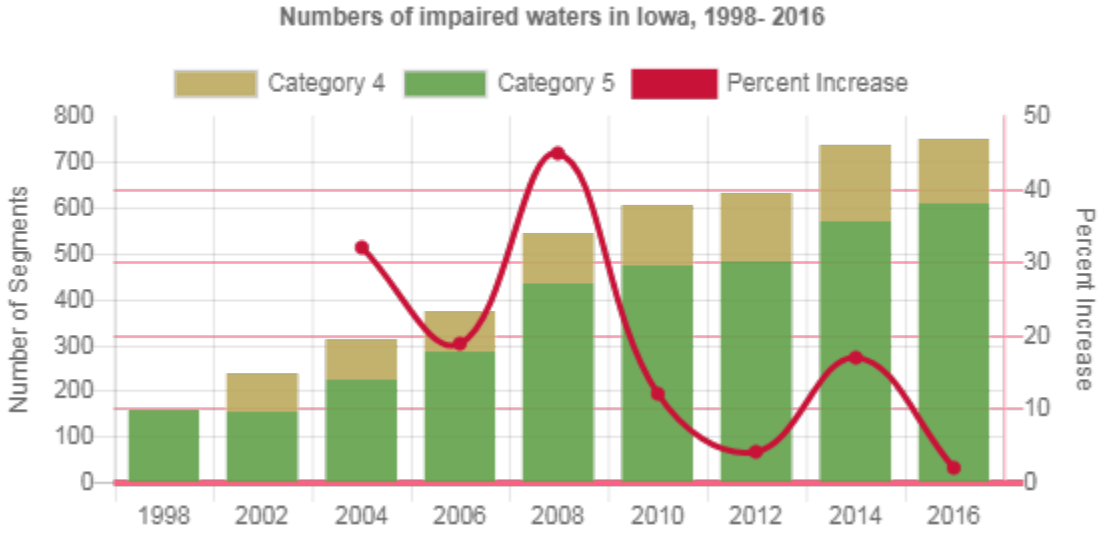

Figure 1.18. Number of impaired Iowa waterbodies 1998–2016. (Iowa Department of Natural Resources, 2018).

e. Web-Based Information Systems of Flood and Water-Quality Data

IIHR—Hydroscience & Engineering and the IFC at the University of Iowa have pioneered the creation of user-friendly, interactive, web-based information systems (WBIS) to communicate environmental information in Iowa and the United States. These two institutions also have expertise in the installation of real-time environmental monitoring systems and currently administer and maintain extensive networks that record flood and water-quality data in Iowa. WBIS displays this information, along with data collected by other federal institutions.

i. The Iowa Flood Information System (IFIS)

The Iowa Flood Information System (IFIS) is a one-stop web-platform to access community-based flood conditions, forecasts, visualizations, inundation maps, and flood-related information, visualizations, and applications. IFIS can be accessed using this URL: http://ifis.iowafloodcenter.org/ifis/. Below is an overview on some of the information available on IFIS.

Floodplain inundation maps

In partnership with the IDNR, the IFC has created statewide floodplain maps that estimate flood hazard extents and depths for every stream in the state of Iowa draining greater than one square mile. The maps depict flood boundaries and depths for eight different annual probabilities of occurrence: 50-, 20-, 10-, 4-, 2-, 1-, 0.5-, and 0.2-%, allowing Iowans to better understand their flood risks and make informed land management decisions. The statewide floodplain maps can be accessed through IFIS or at http://www.iowafloodmaps.org/. Figure 1.19 shows an example of statewide floodplain map data.

Community-based inundation maps

The IFC has also developed online inundation map libraries for more than 20 Iowa communities that relate forecasted or observed flow conditions to flood extents and depths. These inundation map libraries use detailed computer models that consider small-scale floodplain and channel features, bridges, and dams to better simulate the physics of flowing water. The maps allow a user to "translate" a forecasted river stage at a USGS gauge to flood extents and depths in the community, to better anticipate and respond to immediate flood hazards, and to consider "what-if" scenarios for long-term planning. Community inundation map libraries can be accessed on IFIS. Figure 1.20 shows the inundation map library interface for the city of Des Moines.

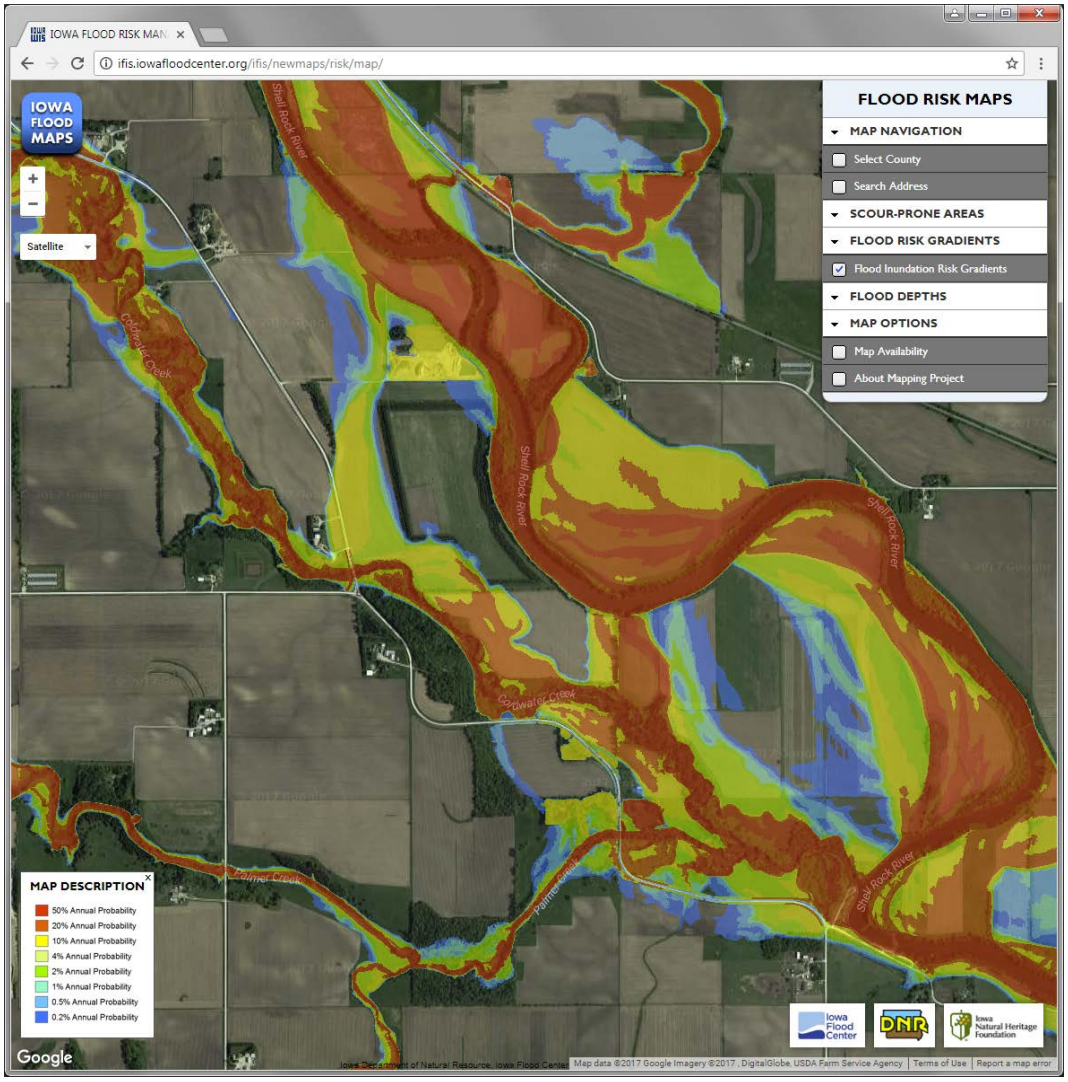

Figure 1.19. Statewide floodplain map data showing different levels of annual flood risk.

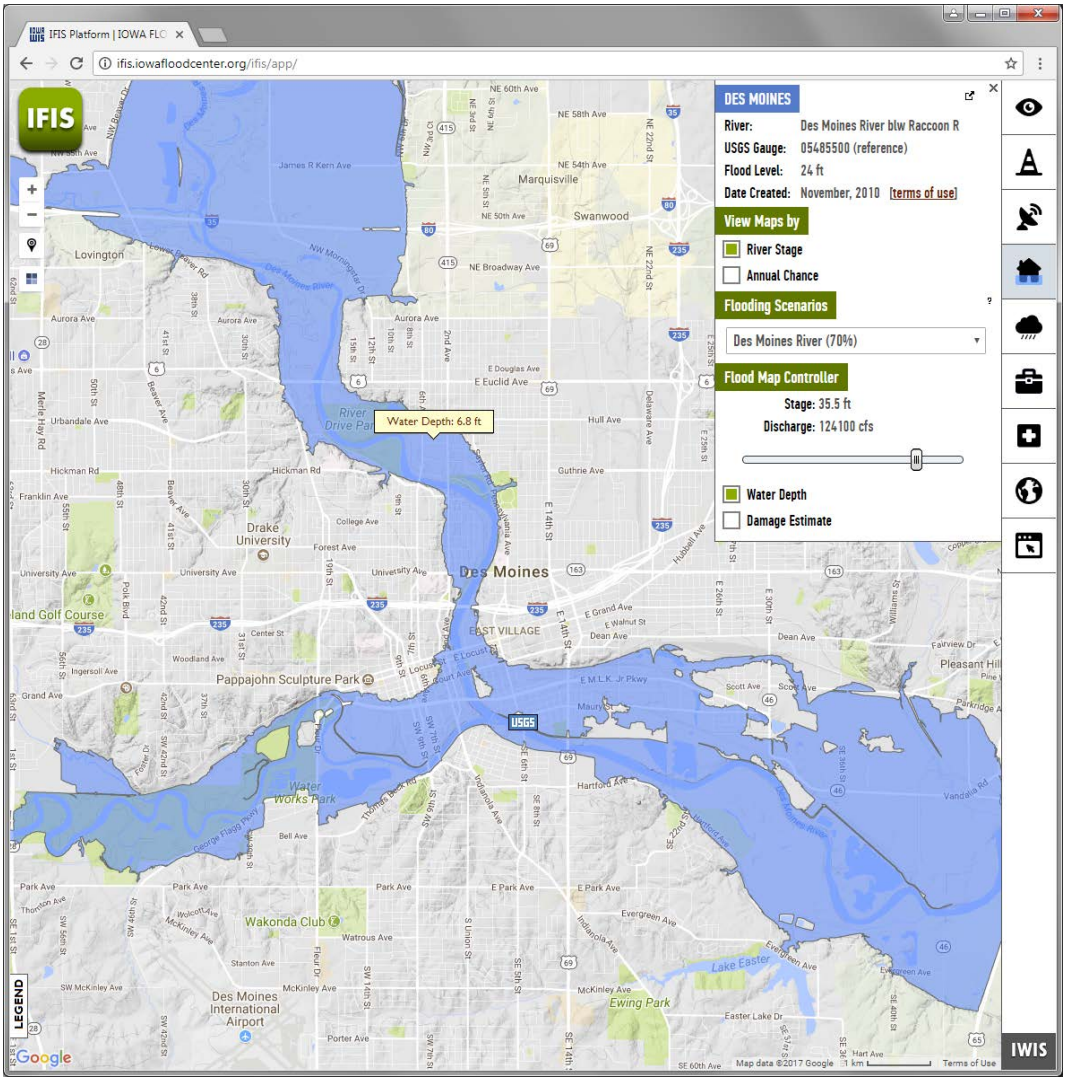

Figure 1.20. Flood inundation map library for the Des Moines and Raccoon rivers in the city of Des Moines.

Observed stream conditions

IFIS displays data from more than 400 sensors continuously monitoring Iowa stream conditions in real-time, which is shown in Figure 1.21. Currently, the USGS collects streamflow data at approximately 200 locations, and the IFC administers and maintains a growing network of more than 250 stream-stage sensors that record stage conditions.

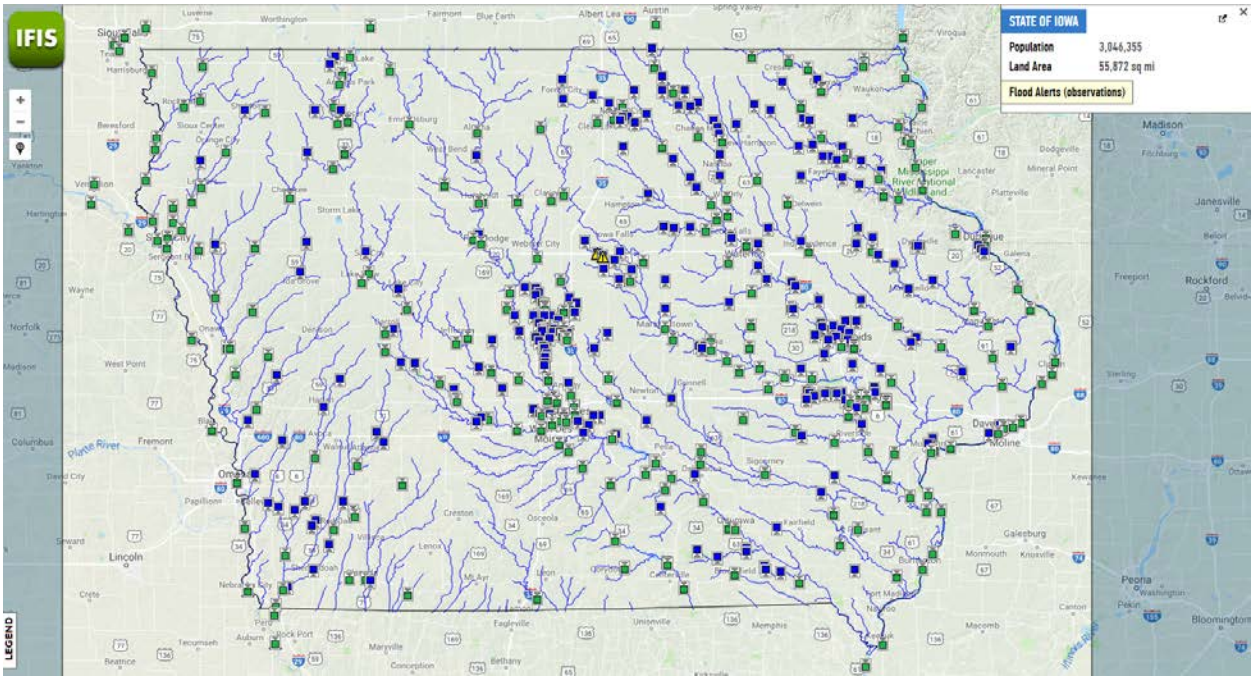

Figure 1.21. USGS (green) and Iowa Flood Center (blue) stream-stage monitoring locations displayed in the Iowa Flood Information System (IFIS).

Flood alerts, warnings, and forecasts

IFIS provides flood alerts for stream sensors with stage values higher than the threshold values for the four flood levels defined by National Weather Service (NWS) and the IFC. Different colors represent the four flood stage levels (action, flood, moderate flood, and major flood). The flood forecast products included in IFIS are the NWS six-hourly forecast for 48 hours and the NWS seasonal forecast for 90 days. IFIS integrates short-term NWS forecasts into real-time data series and more-info views. The NWS shares a seasonal forecast probability for minor, moderate, and major flooding for a three-month period. The Iowa Flood Center has developed a real-time, high-performance computing–based flood forecasting model that provides quantitative stage and discharge forecasts and a five-day flood risk outlook in IFIS for more than 1,500 locations (e.g., communities and stream gauges) in Iowa.

The IFC system complements the operational forecasts issued by the NWS and is based on sound scientific principles of flood genesis and spatial organization. At its core is a continuous rainfall-runoff model based on landscape decomposition into hillslopes and channel links. The input to the system comes from a radar-rainfall algorithm, developed in-house, that maps rainfall every 5 min with high spatial resolution.

ii. The Iowa Water-Quality Information System

The Iowa Water-Quality Information System (IWQIS) integrates real-time water-quality data collected by IIHR and the USGS, along with a variety of watershed-related information such as precipitation, stream flow and stage, soil moisture, and land use. IWQIS (https://iwqis.iowawis.org/) provides useful information for researchers, agencies, landowners,

and other watershed stakeholders as they study, analyze, and work to better understand the fate and transport of nutrients in Iowa's waterways. Iowa WQIS also helps Iowa monitor progress toward achieving the goals of the Iowa Nutrient Reduction Strategy. Iowa has the largest concentration of continuous nutrient and water-quality sensors in the United States; as of 2018, the state has a water-quality network comprised of:

- 74 nitrate sensors (14 operated by USGS)
- 27 hydrolabs (pH, SC, DO, temp)
- 26 turbidimeters
- 4 ortho-P sensors
- 4 ISCOs

This network generates data for science and policy-making, facilitates individual BMP performance assessments, and allows Iowa to quantify the nutrient loads leaving the state. Figure 1.22 is a screenshot of IWQIS displaying the WQ network (2018).

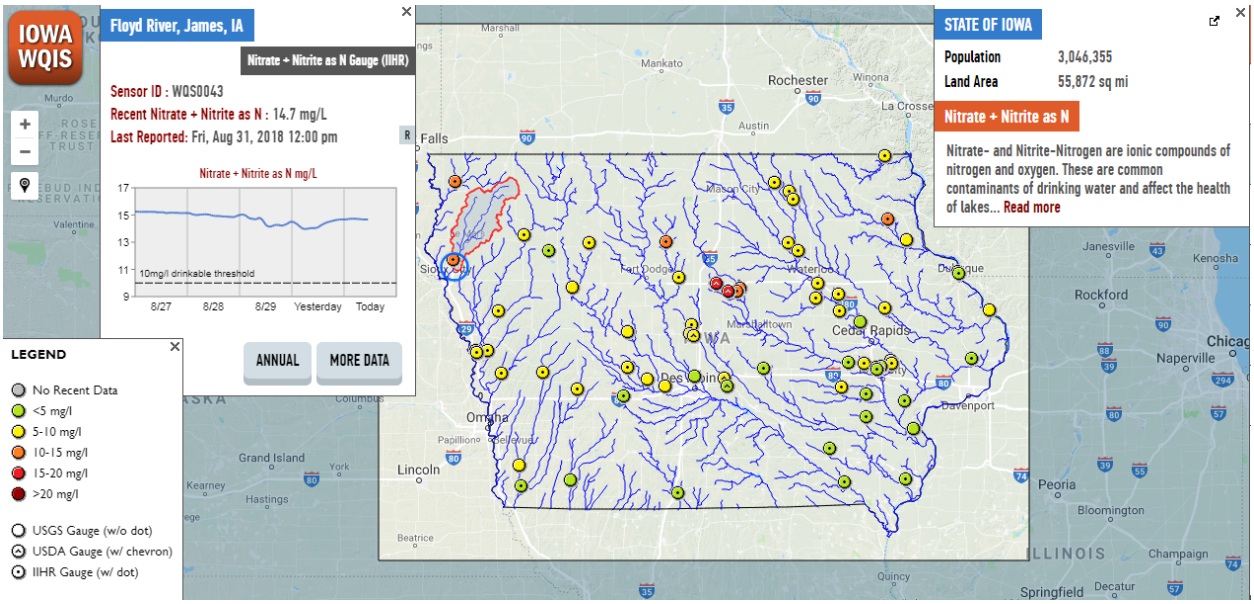

Figure 1.22. IIHR—Hydroscience & Engineering and USGS surface water-quality monitoring locations as displayed in the Iowa Water Quality Information System (IWQIS).

iii. The Iowa Watershed Approach Information System (IWAIS)

IIHR and IFC are developing a web-based information system to provide public access to general information and updates on the IWA project, existing and potential BMPs in IWA watersheds, hydrologic and water-quality data collected in the IWA watersheds, and resources to improve flood resiliency. The website can be accessed at: http://iowawatershedapproach.org. Figure 1.23 shows an example view of the IWAIS interface showing the number of existing ponds within each HUC 12 in the Middle Cedar River Watershed.

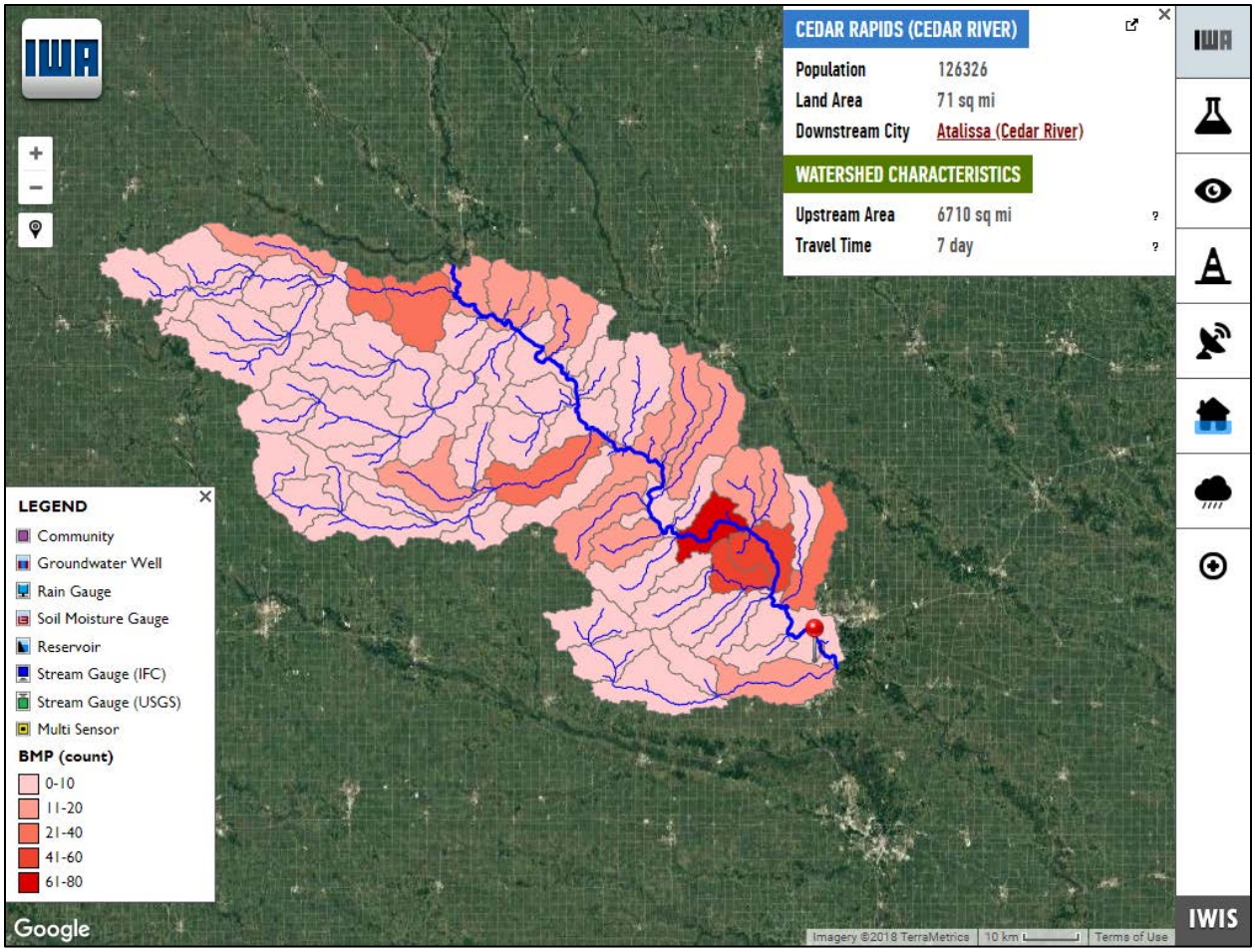

Figure 1.23. Example IWAIS interface view showing the number of existing ponds within each HUC 12 in the Middle Cedar River Watershed.

2. Conditions in the West Nishnabotna River Watershed

This chapter provides an overview of current West Nishnabotna River Watershed conditions, including hydrology, geology, topography, land use, and hydrologic/meteorologic instrumentation, and historic water cycle, as well as a summary of previous floods of record.

a. Hydrology

The West Nishnabotna River Watershed as defined by the boundary of eight-digit Hydrologic Unit Code (HUC 8) 10240002 is in southwest Iowa and encompasses approximately 1,650 square miles (mi^2). The West Nishnabotna River is joined by the East Nishnabotna River (HUC 8 10240003) near Riverton, Iowa, becoming the Nishnabotna River. The total drainage area of the Nishnabotna River at Riverton is approximately 2,800 mi^2. The West Nishnabotna River Watershed boundary falls within 10 counties in total, as shown in Figure 2.1; however, most of the watershed area lies within Shelby, Pottawattamie, Mills, and Fremont counties.

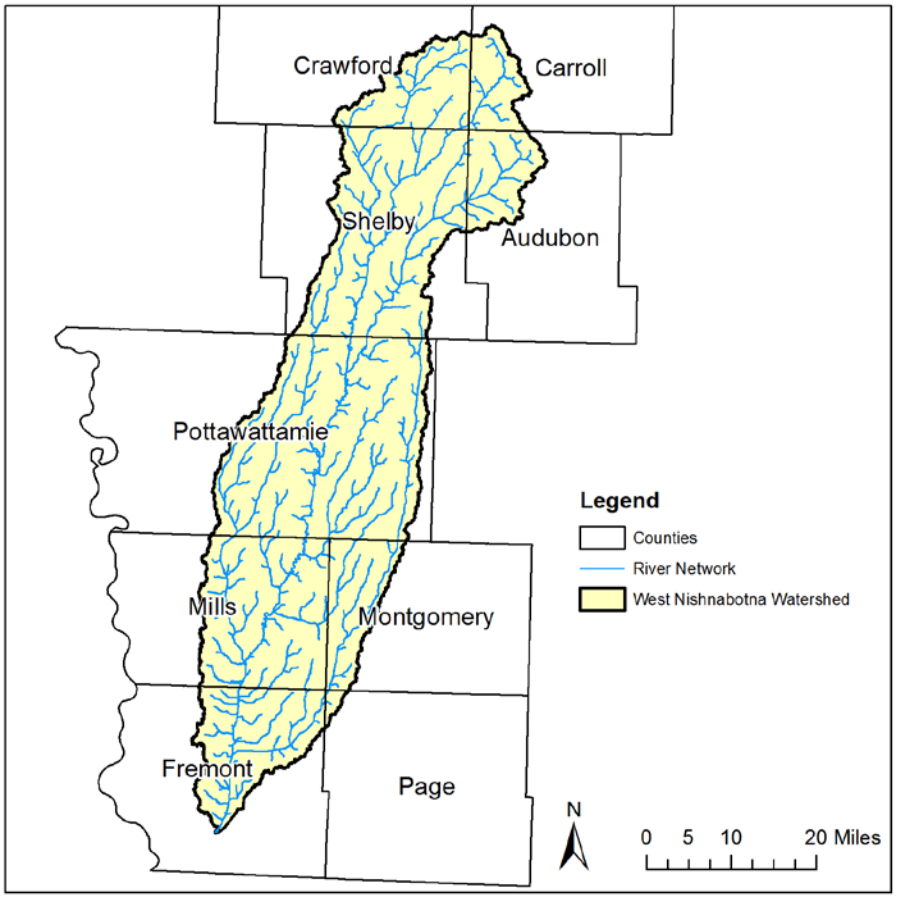

Figure 2.1. The West Nishnabotna River Watershed (HUC 8 10240002) drains 1650 mi^2. The West Nishnabotna River joins the East Nishnabotna River near Riverton, Iowa.

Average annual precipitation in Iowa ranges from 26–40 inches, with the lowest precipitation in the northwest corner of the state and the highest in the southeast corner. The average annual

precipitation ranges from roughly 33–36 inches in the West Nishnabotna River Watershed (PRISM, 1981–2010). About 70% of the annual precipitation falls as rain during the months of April–September. During this period, thunderstorms capable of producing torrential rains are possible, with the peak frequency of such storms occurring in June. Southwest Iowa has experienced increased variability in annual precipitation since 1975, along with a general increase in the amount of spring rainfall (U.S. Department of Agriculture — Iowa State University, 2011).

b. Geology and Soils

A landscape is a collection of terrain features, or landforms (Iowa Geological & Water Survey, 2017). These combinations of surface features and underlying soils influence how water moves through the landscape.

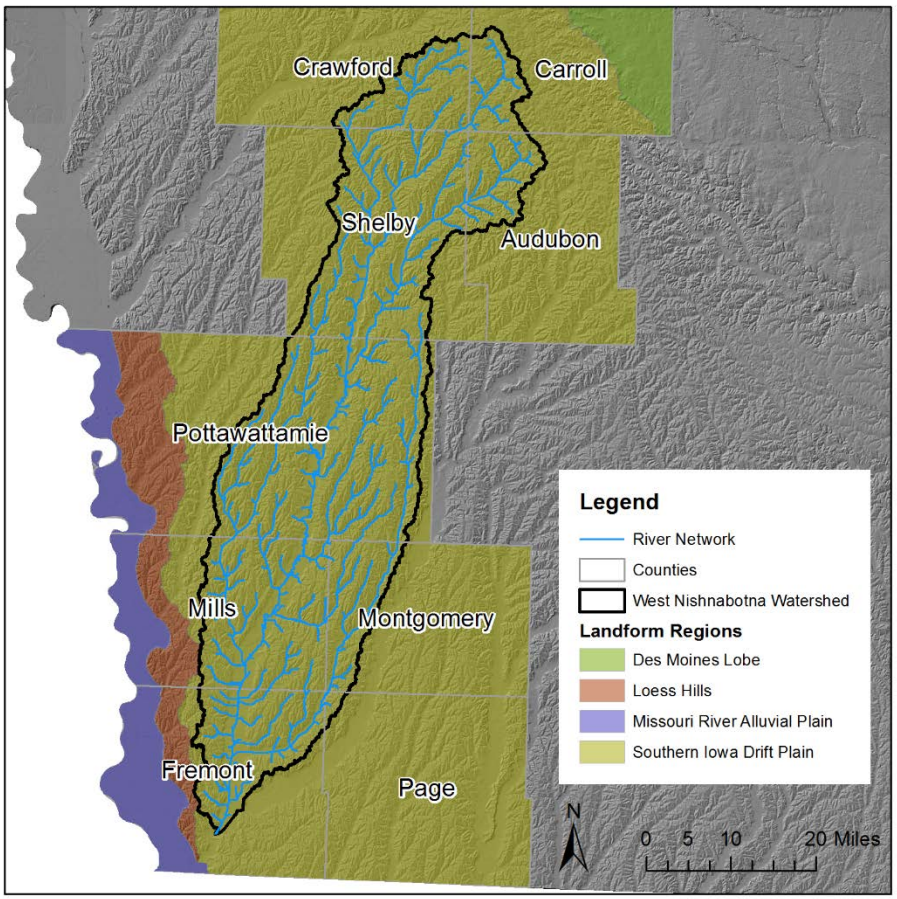

Figure 2.2. Defined Landform Regions of the West Nishnabotna River Watershed.

The West Nishnabotna River Watershed is located entirely within the Southern Iowa Drift Plain landform region (Figure 2.2). The southernmost portion of the watershed is immediately adjacent to the Loess Hills landform region. The characteristics of each landform region have an influence on the rainfall-runoff potential and hydrologic properties of the watershed.

The West Nishnabotna River Watershed is located entirely within the Southern Iowa Drift Plain landform region (Figure 2.2), which includes most of southern Iowa. This region experienced numerous episodes of glaciation between 500,000 and 2.6 million years ago. Since that time, periods of relative landscape stability and soil formation have alternated with episodes of erosion, shaping the land surface we see today. The landscape is characterized by steeply rolling topography and well-developed drainage divides (Figure 2.3). Glacial till deposits provide a thick confining unit on top of the bedrock surface and are generally mantled with a relatively thick package of loess (wind-blown silt). In the northern reaches of the watershed (Crawford and Carroll counties), the thickness of unconsolidated materials may exceed 500 feet. Very limited areas of bedrock outcrop may be present in steep valley locations along the West Nishnabotna River, primarily in the central portion of the watershed. The Loess Hills landform region to the west has a similar geologic history to the Southern Iowa Drift Plain, but the loess deposits are much thicker. Loess thickness may exceed 150 feet near the Missouri River and thin to the east in the direction of the Southern Iowa Drift Plain. Figure 2.3 shows a typical Southern Iowa Drift Plain cross-section.

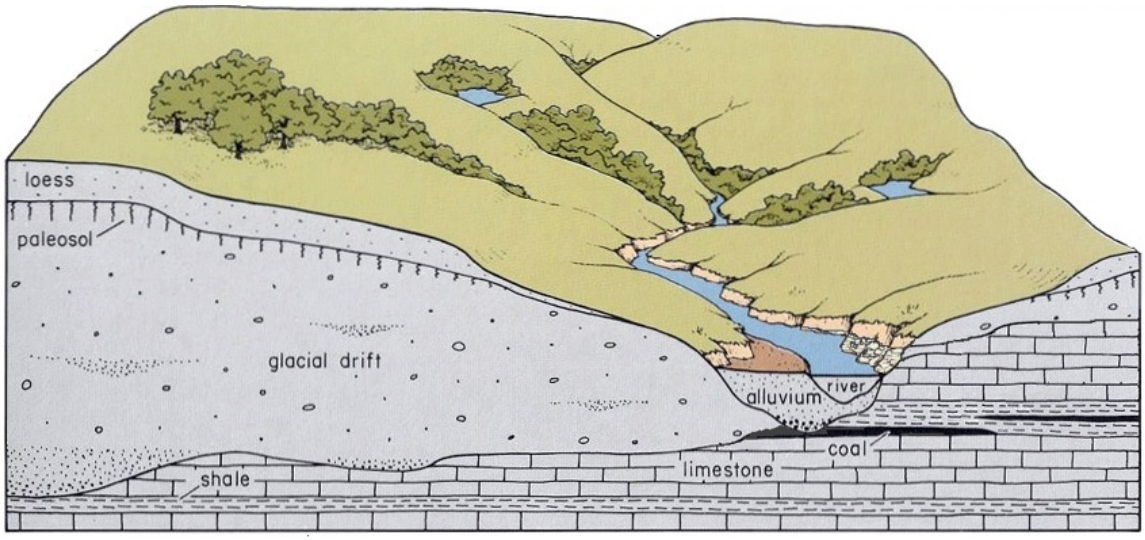

Figure 2.3. Typical Southern Iowa Drift Plain cross-section (Prior 1991).

Depth to bedrock varies from 0–600 feet throughout the watershed, as seen in Figure 2.4. Isolated areas of shallow depth to bedrock are located throughout much of the watershed, with most of these locations in Mills and Pottawattamie counties. A shapefile developed by IGS showing likely locations of bedrock exposed or within 30 inches of the surface is shown in the inset of Figure 2.4 However, surficial geology maps created by IGS indicate there are no known areas of exposed bedrock within West Nishnabotna River Watershed.

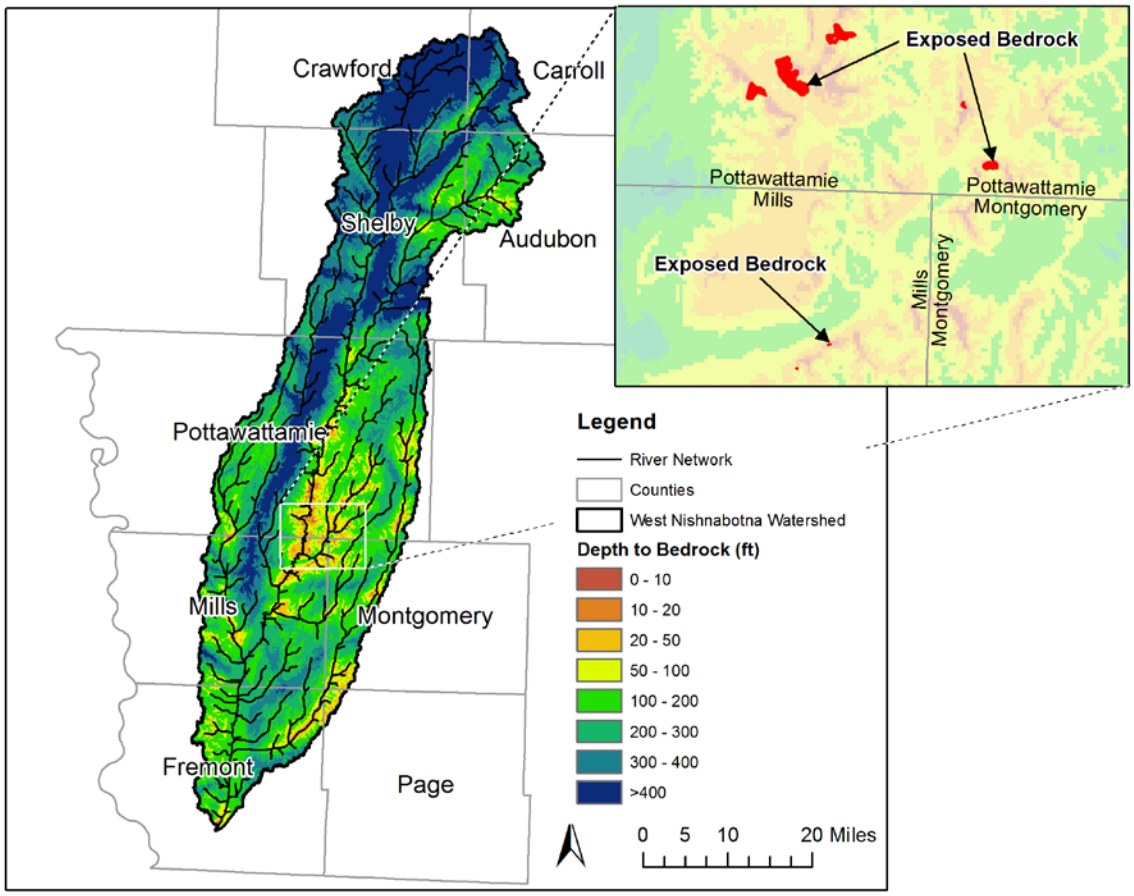

Figure 2.4. Depth to bedrock in the West Nishnabotna River Watershed.

The Natural Resources Conservation Service (NRCS) classifies soils into four hydrologic soil groups (HSG) based on the soil's runoff potential. The four HSGs are A, B, C, and D, where A-type soils have the lowest runoff potential and D-type have the highest. In addition, there are dual code soil classes A/D, B/D, and C/D that are assigned to certain wet soils. For these soil groups, even though the soil properties may be favorable to allow infiltration (water passing from the surface into the ground), a shallow groundwater table (within 24 inches of the surface) typically prevents much from doing so. For example, a B/D soil will have the runoff potential of a B-type soil if the shallow water table were to be drained away, but the higher runoff potential of a D-type soil if it is not. Table 2.1 summarizes some of the properties generally true for each HSG (A-D). This table is meant to provide a general description of each HSG and is not all-inclusive. Complete descriptions of the HSGs can be found in USDA-NRCS National Engineering Handbook, Part 630 – Hydrology, Chapter 7.

Table 2.1. Soil properties and characteristics generally true for Hydrologic Soil Groups A-D.

Hydrologic Soil Group	Runoff Potential	Soil Texture	Composition	Minimum Infiltration Rate[1] (in/hr)
A	Low	Sand, gravel	< 10% clay > 90% sand/gravel	>5.67
B	Moderately low	Loamy sand, sandy loam	10-20% clay 50-90% sand	1.42-5.67
C	Moderately high	Loam containing silt and/or clay	20-40% clay <50% sand	0.14-1.42
D	High	Clay	>40% clay <50% sand	<0.14

[1] For HSG A-C, infiltration rates based on a minimum depth to any water impermeable layer and the ground water table of 20 and 24 inches, respectively.

Figure 2.5 shows the soil distribution of the West Nishnabotna River Watershed using digital soils data (SSURGO) available from the USDA-NRCS Web Soil Survey (WSS). The map illustrates spatial variation and the noticeable difference in soil type near drainage ways versus upland areas. The watershed is dominated by HSG type C soils with moderately high runoff potential. The majority of HSG type B soils, with moderately low runoff potential, occur along the western border of the watershed, near the Loess Hills landform region. The slightly lower runoff potential of these HSG type B soils is likely a result of the presence of windblown Loess soil. The infiltration properties of these soil types and their spatial distribution in the watershed largely dictate identification runoff prone areas, presented in Chapter 4.

Table 2.2 defines the HSGs as a percentage of watershed area. The second most common HSG is type B, which can be seen along the areas west of the West Nishnabotna River valley. Dual code HSGs, such as C/D, indicate a shallow groundwater table would inhibit infiltration, creating type D soil behavior; however, if drained, the soil would behave as type C.

Table 2.2. Approximate Hydrologic Soil Group percentages by area of the West Nishnabotna River Watershed

Hydrologic Soil Group	Percentage (%)
A	0.0
A/D	0.0
B	19.1
B/D	0.2
C	62.1
C/D	14.8
D	3.8

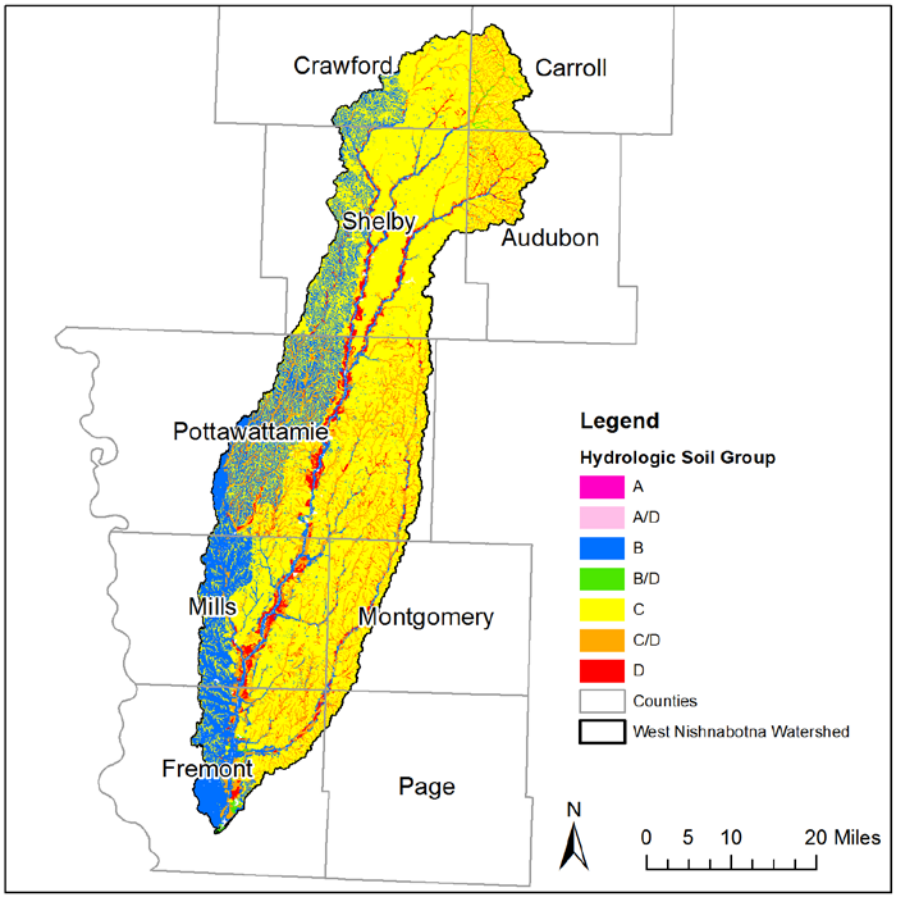

Figure 2.5. Distribution of Hydrologic Soil Groups in the West Nishnabotna River Watershed. Hydrologic Soil Groups reflect the degree of runoff potential a particular soil has, with Type A representing the lowest runoff potential and Type D representing the highest runoff potential.

c. Topography

The topography of the West Nishnabotna River Watershed reflects its geologic past. As previously mentioned, the watershed lies within the Southern Iowa Drift Plain, which is characterized by numerous steeply rolling hills and valleys. Figure 2.6 shows topography provided by Iowa DNR in the form of bare-earth light detection and ranging (LiDAR) data. Numerous rills, creeks, and rivers cover the landscape, and these are evident in the LiDAR data. Elevations range from approximately 1,560 feet above sea level in the northernmost part of the watershed to 900 feet at the mouth of West Nishnabotna River. Typical land slopes are between 0.4 and 8.0% (25th and 75th percentiles), with the steepest areas occurring in uplands in the northern portion of the watershed. A slope of 8.0% is equivalent to eight feet of rise for 100 feet of run. Many existing terraces have been constructed on terrain with slopes between 5.0% and 10.0%. The major river valleys contain the flattest terrain, which is conspicuous in Figure 2.7.

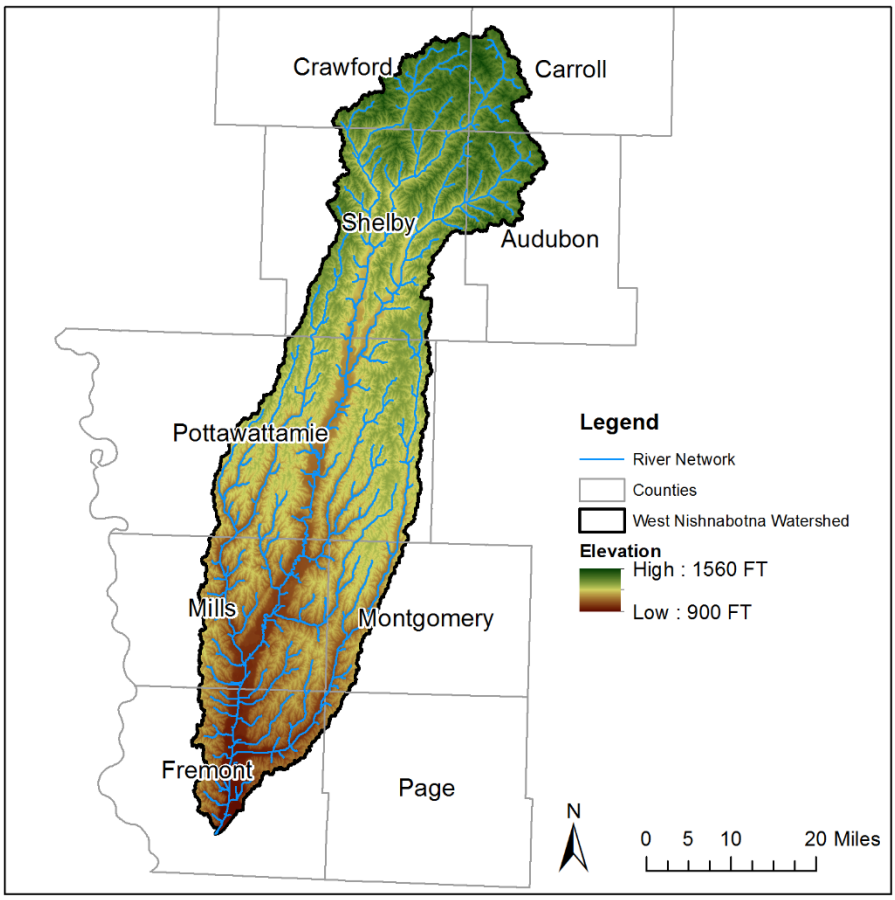

Figure 2.6. Topography of the West Nishnabotna River Watershed.

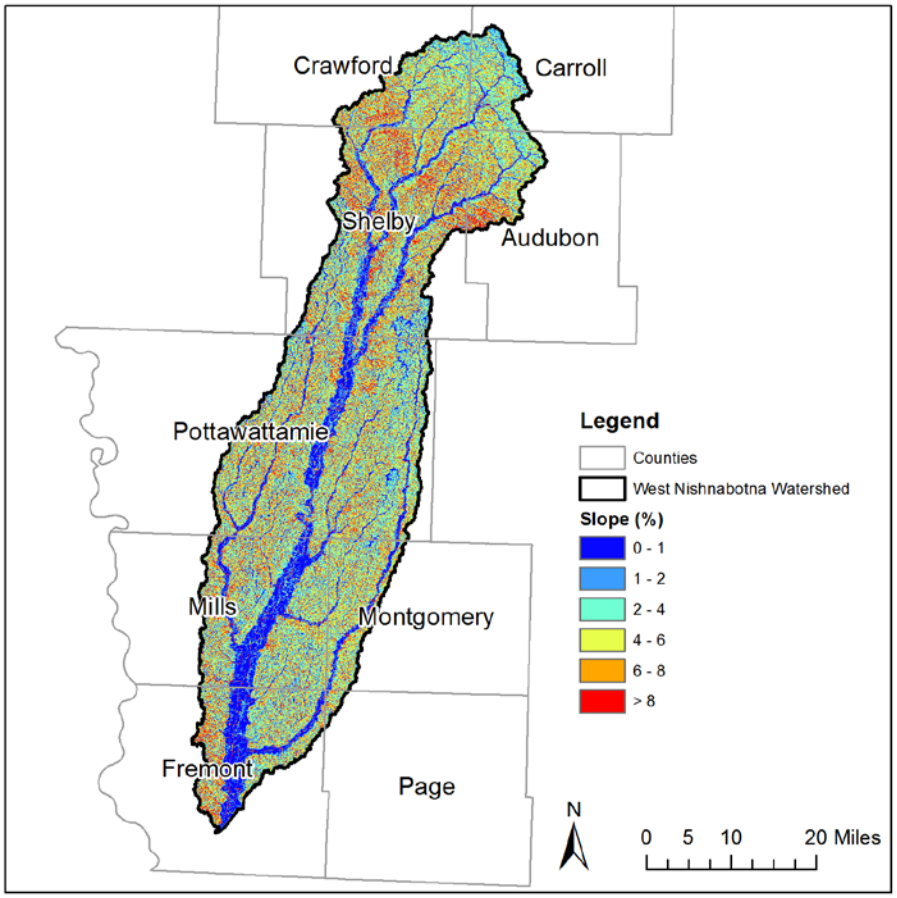

Figure 2.7. Terrain slopes derived from LiDAR data.

d. Land Use and BMP Mapping Project

Land use in the West Nishnabotna River Watershed is predominantly agricultural, dominated by cultivated crops (corn/soybeans) on approximately 76.8% of the acreage (approximately 510,000 acres), followed by grass/hay/pasture on approximately 16.9%. The remaining acreage in the watershed is about 3.5% forest (primarily deciduous forest), 1.7% developed land, and 0.5% open water and/or wetlands, per the 2009 High Resolution Land Cover (HRLC) dataset provided by Iowa DNR. Figure 2.8 shows the spatial distribution of land cover in the watershed.

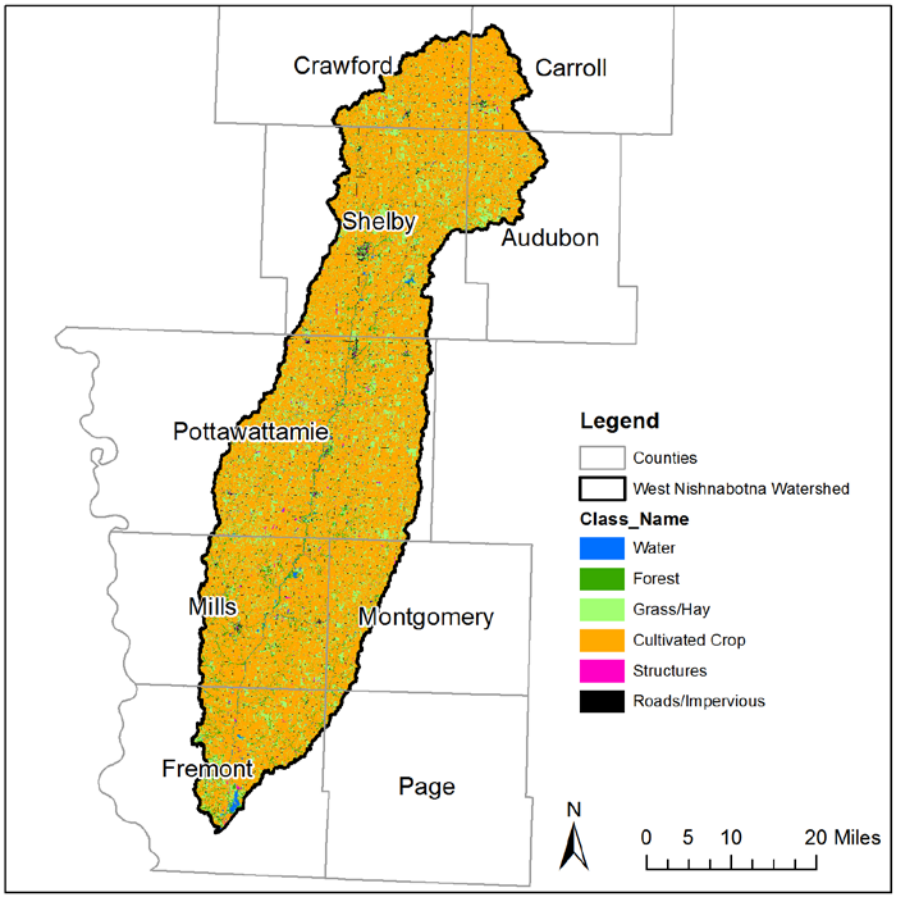

Figure 2.8. Land use composition in the West Nishnabotna River Watershed according to the 2009 HRLC dataset provided by Iowa DNR.

The Iowa Best Management Practices (BMP) Mapping Project is a collaborative effort led by the Iowa State University Geographic Information Systems (GIS) Facility, in association with the Iowa DNR, Iowa Flood Center, Iowa Department of Agriculture and Land Stewardship, Iowa Nutrient Research Center, National Laboratory for Agriculture and the Environment, and the Iowa Nutrient Research and Education Council. The goal of the project is to provide a complete baseline set of BMPs during the 2007–10 timeframe for use in watershed modeling, historic documentation, and future practice tracking. These practices include terraces, water and sediment control basins (WASCOBs), grassed waterways, pond dams, contour strip cropping, and contour buffer strips. The data has been manually digitized for each HUC 12 using LiDAR products, color-infrared (CIR) imagery, National Agriculture Imagery Program imagery, and historic aerial photography.

Appendix A shows individual BMPs and practices aggregated based on HUC 12 area.

e. Potential BMPs – Agricultural Conservation Planning Framework

Development of an effective watershed planning document will require identification of potential conservation practices and viable locations to implement them. One cutting-edge tool available for practical conservation planning is the Agricultural Conservation Planning Framework (ACPF) watershed planning toolbox, developed by Mark Tomer and his research team at the USDA-ARS in Ames, Iowa (Tomer et al., 2013). ACPF is a watershed approach to conservation planning facilitated with a set of semi-automated tools within ArcGIS software. Freely available and pre-packaged GIS data can be used for terrain analyses to determine which fields within the watershed are most prone to runoff into streams. Users can apply the ACPF toolbox to identify locations where field-scale and edge-of-field practices could be installed based on general design criteria. These practices include controlled drainage, surface intake filters or restored wetlands, grassed waterways, contour buffer strips, WASCOBs, nutrient removal wetlands (NRWs), or edge-of-field bioreactors (North Central Region Water Network 2018).

Using the ACPF toolbox, potential BMPs have been generated for all of the 44 HUC 12s in the West Nishnabotna River Watershed. Of the 44 ACPF databases generated, 33 were developed by IFC, and 11 were developed by JEO Consulting Group Inc. Appendix A shows the locations of these BMPs and aggregations based on HUC 12 area.

f. Instrumentation/Data Records

The West Nishnabotna River Watershed has instrumentation installed to collect and record stream-stage, discharge, and precipitation measurements. Three USGS-operated stage and discharge gauges and eight IFC stream-stage sensors are located within the watershed. In addition, there are 10 National Oceanic and Atmospheric Administration (NOAA) 15-minute/hourly precipitation gauges and an additional 19 NOAA-partnered hourly or sub-hourly precipitation gauges within or near the watershed. The operational period of record varies for each of these gauges. The following figure and tables detail the instrumentation and its period of record.

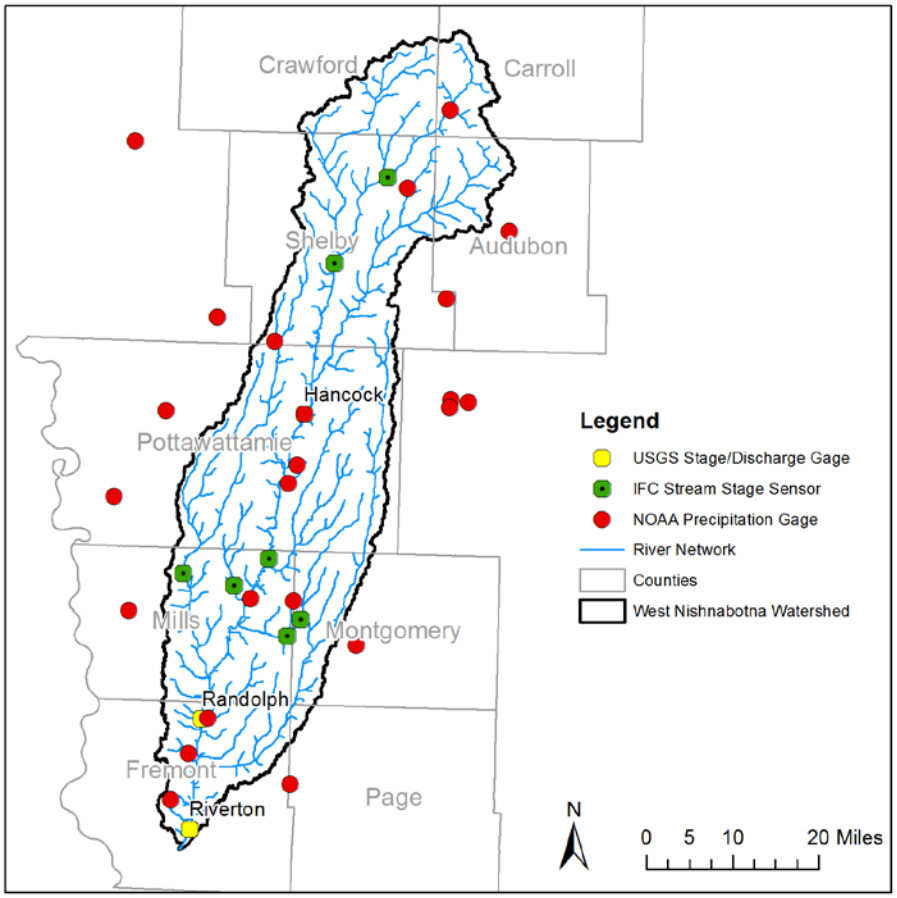

Figure 2.8. Hydrologic and meteorologic instrumentation in the West Nishnabotna River Watershed. Stage/discharge gauges (11) are shown in yellow or green, while NOAA-partnered daily- or sub-hourly measuring precipitation gauges (29) are shown in red.

Table 2.3. Stage/Discharge Gauges and Precipitation Gauges in the West Nishnabotna River Watershed.

Gauge Type	Location	Period of Record
State/Discharge Gauges (11)		
USGS Stage/Discharge	West Nishnabotna River at Hancock, Iowa 06807410	1959–Present
USGS Stage/Discharge	West Nishnabotna River at Randolph, Iowa 06808500	1948–Present
USGS Stage/Discharge	West Nishnabotna River near Riverton, Iowa 06808820	2010–Present
IFC Stream Sensor (stage)	West Nishnabotna River, Cora St., near Irwin, Iowa, WNISH04	2011–Present

IFC Stream Sensor (stage)	West Nishnabotna River, HWY 44, at Harlan, Iowa, WNISH03	2010–Present
IFC Stream Sensor (stage)	West Nishnabotna River, County H12, near Henderson, Iowa, WNISH02	2010–Present
IFC Stream Sensor (stage)	Mud Creek, W of 350th St., near Henderson, Iowa, MDCRK01	2011–Present
IFC Stream Sensor (stage)	Indian Creek, County H34, at Emerson, Iowa, INDIAN01	2010–Present
IFC Stream Sensor (stage)	Indian Creek, A Ave., near Emerson, Iowa, INDIAN02	2013–Present
IFC Stream Sensor (stage)	Silver Creek, Dobney Ave., at Silver City, SLVRCR01	2010–Present
IFC Stream Sensor (stage)	West Nishnabotna River, County J46, near Riverton, Iowa, WNISH01	2016–Present
Precipitation Gauges (29)		
NOAA Daily Precip	Atlantic 2.2 NW, Iowa (GHCND:US1IACS0004)	2007–present
NOAA Daily Precip	Atlantic Municipal Airport, Iowa (GHCND:USW00014930)	1947–Present
NOAA Daily Precip	Audubon, Iowa (GHCND:USC00130385)	1892–Present
NOAA Daily Precip	Council Bluffs, Iowa (GHCND:US1IAPT0007)	2007–Present
NOAA Daily Precip	Denison, Iowa (GHCND:USC00132171)	1892–Present
NOAA Daily Precip	Elk Horn, Iowa (GHCND:US1IASH0003)	2016–Present
NOAA Daily Precip	Emerson 4.0 NNE, Iowa (GHCND:US1IAMY0002)	2017–Present
NOAA Daily Precip	Glenwood, Iowa (GHCND:USC00133288)	2008–Present
NOAA Daily Precip	Hancock, Iowa (GHCND:USC00133589)	1995–Present
NOAA Daily Precip	Hastings 4 NE, Iowa (GHCND:USC00133675)	2007–Present
NOAA Daily Precip	Manning 0.2 ESE, Iowa (GHCND:US1IACR0007)	2017–Present
NOAA Daily Precip	Oakland, Iowa (GHCND:USC00136151)	1918–Present

NOAA Daily Precip	Persia 2.0 S, Iowa (GHCND:US1IAHR0004)	2008-Present
NOAA Daily Precip	Randolph, Iowa (GHCND:USC00136891)	1953–Present
NOAA Daily Precip	Red Oak, Iowa (GHCND:USC00136940)	1897–Present
NOAA Daily Precip	Shenandoah, Iowa (GHCND:USC00137613)	1918–Present
NOAA Daily Precip	Sidney 1 SSE, Iowa (GHCND:USC00137669)	1895–Present
NOAA Daily Precip	Sidney 5.1 NNE, Iowa (GHCND:US1IAFM0001)	2014–Present
NOAA Daily Precip	Underwood, Iowa (GHCND:USC00138410)	2002–Present
NOAA Hourly Precip	Atlantic 1 NE, Iowa (COOP: 130364)	1950–Present
NOAA Hourly Precip	Boyer 4 SE, Iowa (COOP: 130853)	1950–Present
NOAA Hourly Precip	Carson 3 NNE, Iowa (COOP: 131245)	1950–Present
NOAA Hourly Precip	Irwin 3 ESE, Iowa (COOP: 134174)	1950–Present
NOAA Hourly Precip	Omaha Eppley Airfield, NE US (COOP: 256255)	1948–Present
NOAA Hourly Precip	Shelby, Iowa (COOP: 137582)	1950–Present
NOAA Hourly Precip	Shenandoah, Iowa (COOP: 137613)	2009–Present
NOAA Hourly Precip	Soldier, Iowa (COOP: 137774)	1948–Present
NOAA Hourly Precip	Wallin 1 NW, Iowa (COOP: 138646)	1948–Present
NOAA Hourly Precip	Woodbine 4 ENE, Iowa (COOP: 139165)	2012–Present

g. Baseflow and Runoff Historic Trends

We estimated annual precipitation volumes for each water year (October 1–September 30) using daily precipitation records near the northern portion of West Nishnabotna River Watershed upstream of Randolph, Iowa. Total annual discharge for each water year was also calculated at Randolph, using daily discharge observations from USGS gauging station 06808500. Using these historical precipitation and discharge records, it is possible to estimate partitioning of precipitation into baseflow and direct runoff on an annual basis. Using the local minimum method, we separated daily discharge into baseflow and runoff. Figure 2.9 shows plots of annual precipitation, streamflow, baseflow, and runoff. All datasets have a slight positive trend, with low correlation values. The positive trend in annual streamflow appears to be more attributable to baseflow than runoff.

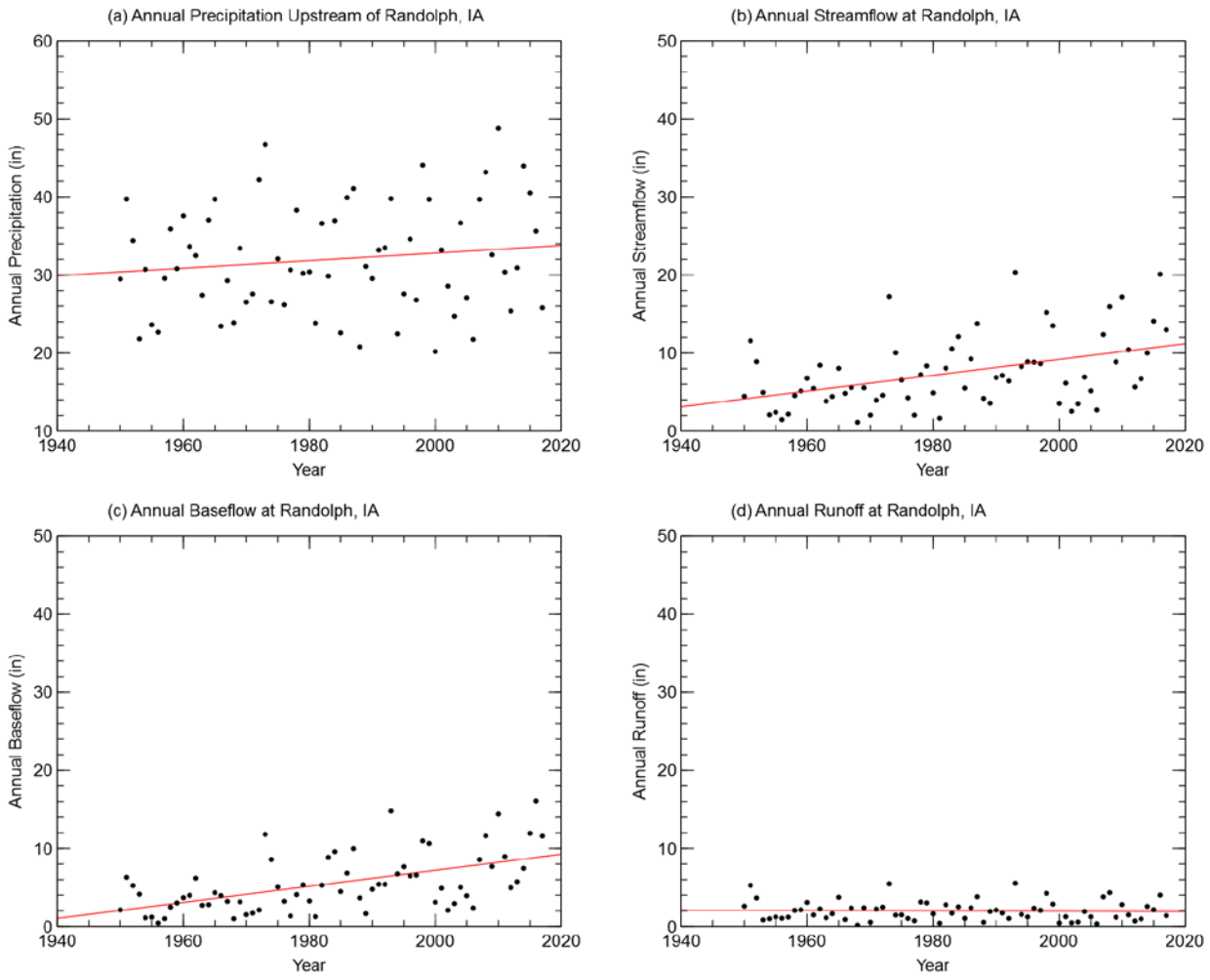

Figure 2.9. Annual totals for: (a) precipitation; (b) streamflow; (c) baseflow; and (d) runoff at Randolph, Iowa.

We developed cumulative mass curves to further visualize and investigate any historic trends associated with these data. Cumulative mass curves allow visualization of long-term discharge or precipitation trends, with changes in slope indicating possible historical change points. Cumulative mass curves were created for precipitation, streamflow, baseflow, and runoff by summing each consecutive annual total volume (inches), as shown in Figure 2.10. Cumulative annual precipitation closely follows a linear trend, with little deviation from the fitted trend line. This indicates no significant change in long-term total precipitation upstream of Randolph. Beginning in the 1980s, cumulative annual streamflow totals at Randolph indicate a departure from the historical trend, with the largest departures beginning in the mid-1990s and continuing to the present. This change appears to be a result of increased baseflow, which shows more noticeable departures from the historic trend than does cumulative annual runoff. It is worth noting that the 1993 water year appears to contribute to an abrupt departure from the historic trend.

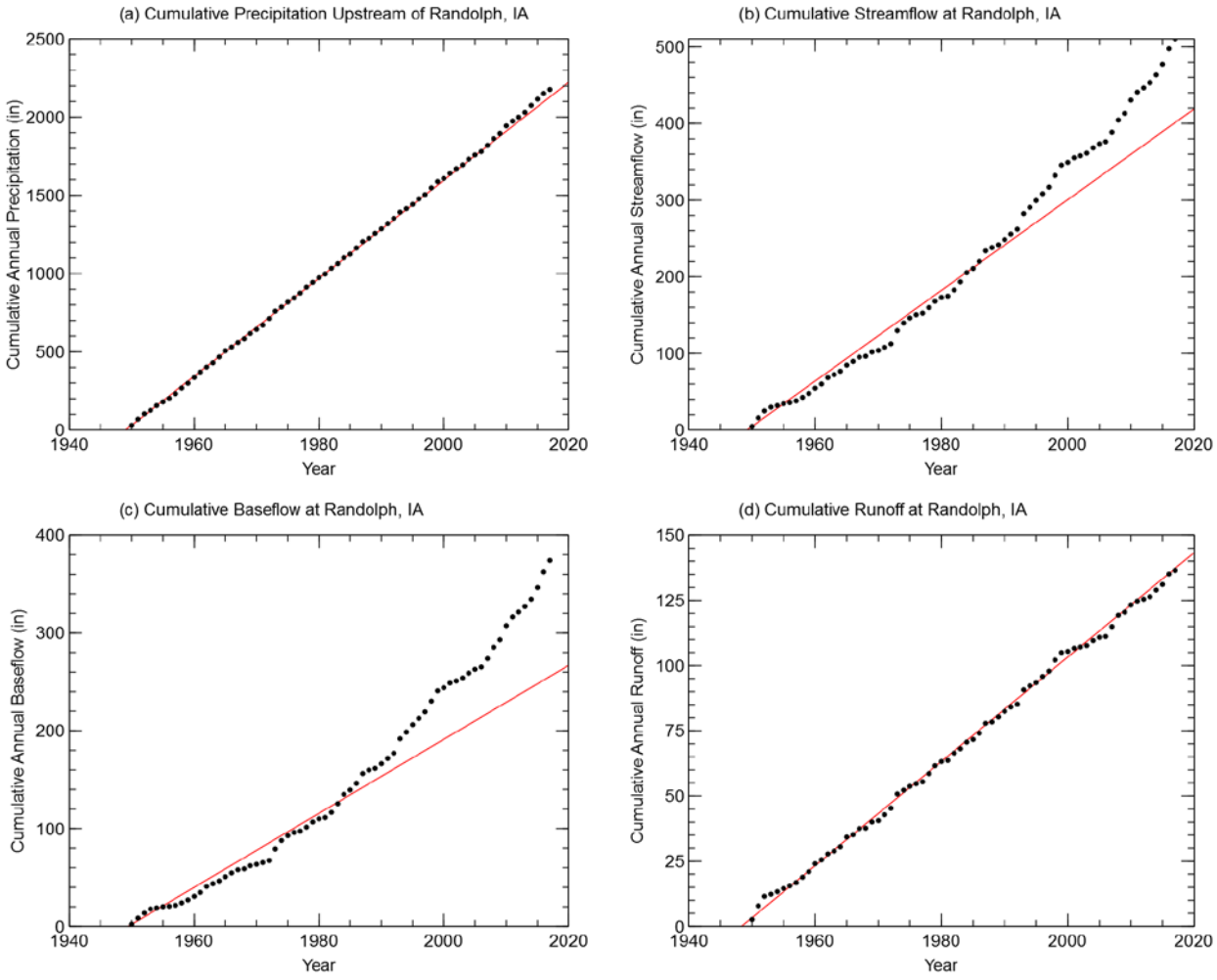

Figure 2.10. Cumulative annual totals for: (a) precipitation; (b) streamflow; (c) baseflow; and (d) runoff at Randolph, Iowa.

The influence of extremely wet years, such as 1993, on the linear trend can be accounted for using a double-mass curve. A double-mass curve based on a plot of two cumulative quantities during the same period will follow a straight line if the proportionality between the qualities remains unchanged (Gao et al. 2010). Figure 2.11 shows double mass curves of cumulative precipitation with cumulative streamflow, baseflow, and runoff. These plots indicate that changes in historic streamflow totals are likely a result of historic increases in baseflow beginning in the 1980s, with the largest changes occurring in the last two decades. The reason for changes in streamflow continues to be intensely investigated (Mora et al. 2013, Frans et al. 2013, Yiping et al. 2013); likely drivers include improved conservation practices promoting infiltration, greater artificial drainage, increasing row crop production, and channel incision (Schilling and Libra, 2003).

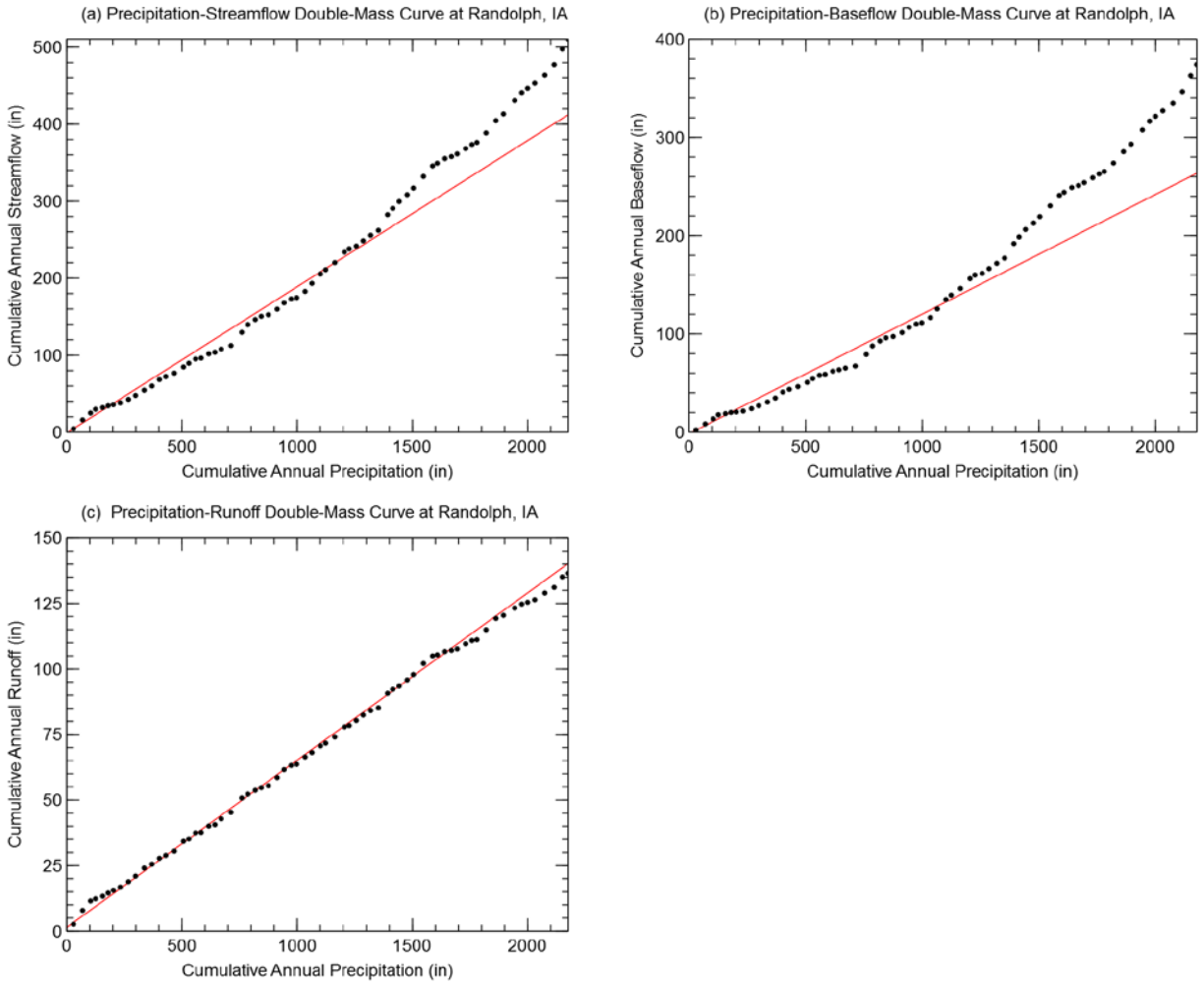

Figure 2.11. Double-mass curves using cumulative annual precipitation with cumulative annual (a) streamflow, (b) baseflow, and (c) runoff at Randolph, Iowa.

h. Monthly Water Cycle

Using historic USGS streamflow and precipitation records, we calculated the average monthly stream flow at Randolph and precipitation upstream of Randolph for the period 1950–2017. Precipitation amounts are lowest during the winter months. However, this precipitation is likely snowfall, which accumulates before melting in the warmer spring temperatures. A large increase in the average precipitation occurs in the spring months, before peaking in the months of May and June. Streamflow follows a similar trend; the largest monthly average streamflow occurs in May and June. Precipitation slowly decreases through late summer and early fall, while streamflow drops significantly after the summer months.

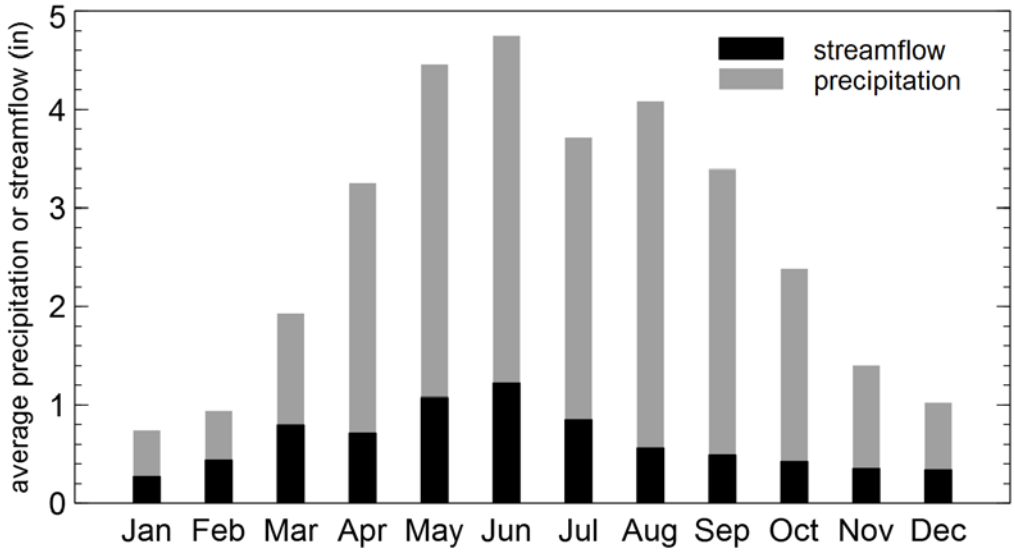

Figure 2.12. Monthly water cycle for the West Nishnabotna River Watershed. The plots show the average monthly precipitation (inches) and the average monthly streamflow (inches). The average monthly estimates for precipitation and streamflow are based on the period 1950–2017.

i. Floods of Record

Figure 2.13 shows the annual maximum peak discharges observed at the Randolph, Iowa, USGS gauging station 06808500. While these are annual maximum, many were not flood events. Calculating the mean annual peak discharge by averaging all annual peak observations can serve as a reasonable threshold for flooding occurrences. Of the 69 annual maximum peak discharges, 31 peaks were greater than the mean annual peak discharge.

Further analyses of these annual maximum peak discharges reveal the seasonal flood pattern for the West Nishnabotna Watershed. Figure 2.14 (left) shows the calendar day of occurrence for each of the annual maximum peak discharges, and Figure 2.14 (right) shows the number of flood occurrences for each calendar month. Most flooding events occur during the months of May and June. A secondary peak occurs in March, likely caused by snowmelt and spring rains. Late summer and early fall see a similar small increase in the occurrence of flood events.

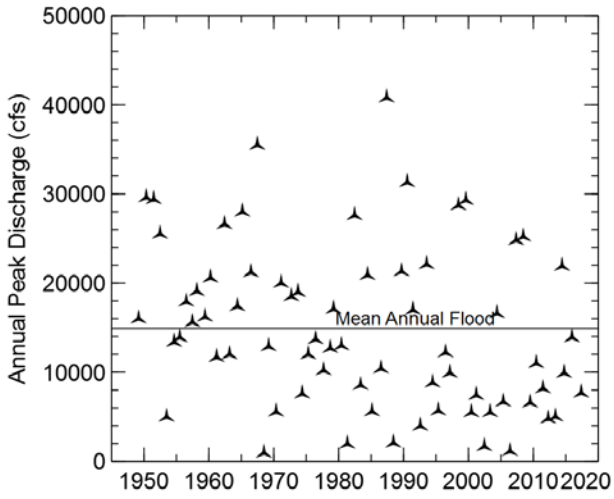

Figure 2.13. Annual maximum peak discharges observed at the Randolph USGS stream gauge station.

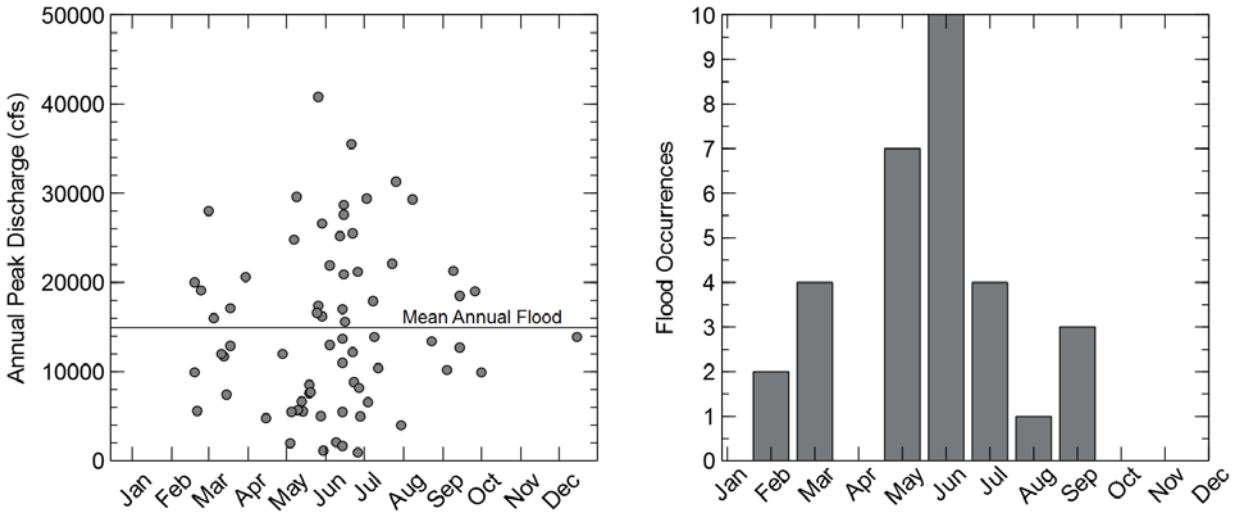

Figure 2.14. Annual maximum peak discharge and the calendar day of occurrence at Randolph, Iowa (left), and the flood occurrence frequency by month (right).

The five largest observed river discharges occurring at Hancock, Randolph, and Riverton USGS gauging stations do not have any events in common. Table 2.4 shows the dates and discharges associated with each flooding event at these three gauging stations. The Riverton gauging station has a limited period of record relative to the other sites. The absence of dates in common is likely due to the spatial variability of historic storm tracks and rainfall accumulations.

The flood of record at Hancock occurred on July 10, 1993, with a discharge of 30,100 cfs. This event was the result of an unusually wet spring that created saturated soil conditions prior to summer 1993. From late June through late July, an unusual weather pattern stationed over the Midwest brought rainfall amounts that exceeded historical Iowa rainfall records (Galloway 2010). The largest rainfall totals that produced this discharge record occurred mainly in the northern portion of the West Nishnabotna River Watershed.

The flood of record at Randolph occurred on May 26, 1987, with a discharge of 40,800 cfs. This event was the result of intense rainfall occurring primarily in the lower West Nishnabotna River Watershed (Eash and Heinitz, 1991). NOAA reported up to 10 inches of rainfall on May 26 in parts of Mills and Montgomery counties (NOAA 2017). Damages estimated at $5.5 million ($12 million adjusted for inflation) to farm terraces and levees, as well as severe soil erosion, were attributed to this event (Eash and Heinitz, 1991). Mills, Montgomery, Fremont, and Page counties were declared Presidential and State disaster areas (Eash and Heinitz 1991).

Table 2.4. Discharges from the five largest flooding events at USGS Gauging Stations in the West Nishnabotna River Watershed.

W. Nishnabotna at Hancock (1960–Present)	7/10/1993 30,100 cfs	9/13/1972 26,400 cfs	5/6/2007 19,800 cfs	3/18/1979 18,300 cfs	3/1/1965 18,000 cfs
W. Nishnabotna at Randolph (1947–Present)	5/26/1987 40,800 cfs	6/21/1967 35,500 cfs	7/26/1990 31,300 cfs	5/9/1950 29,600 cfs	7/3/1951 29,400 cfs
W. Nishnabotna at Riverton (2010–Present)	6/4/2014 23,500 cfs	6/14/2010 11,800 cfs	8/9/2015 10,700 cfs	6/27/2011 7,980 cfs	4/15/2012 6,990 cfs

3. West Nishnabotna River Watershed Hydrologic Model Development

This chapter summarizes the development of the model used in the Phase I Hydrologic Assessment for the West Nishnabotna River Watershed. Researchers used the U.S. Army Corps of Engineers' (USACE) Hydrologic Engineering Center's Hydrologic Modeling System (HEC-HMS), Version 4.0.

HEC-HMS is designed to simulate rainfall-runoff processes of a watershed. It is applicable in a wide range of geographic areas and for watersheds ranging in size from very small (a few acres) to very large (the size of the West Nishnabotna River Watershed or larger). Figure 3.1 reviews the water cycle and major hydrologic processes that occur in a watershed. The physical processes of the West Nishnabotna River Watershed explicitly modeled with HEC-HMS include the partitioning of precipitation into infiltrated and overland flow volumes, transformation of excess runoff to subbasin outflow, and flood wave routing. The model accounts for the cumulative effects of all other physical processes through antecedent conditions or general approximation.

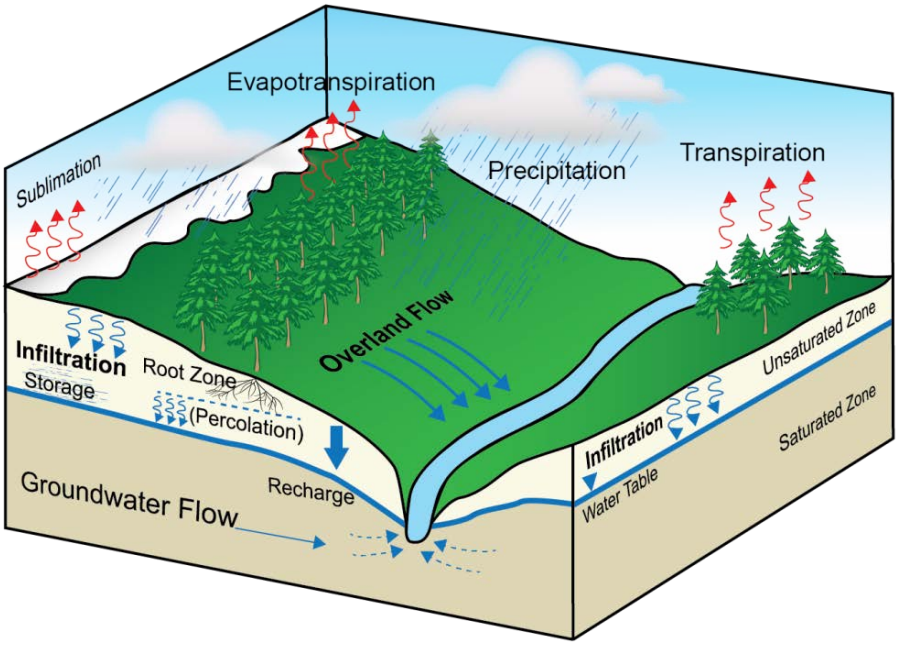

Figure 3.1. Hydrologic processes that occur in a watershed. Phase I modeling only considered the precipitation, infiltration, and overland components of the water cycle.

HMS is a mathematical, lumped parameter, uncoupled, surface water model. The authors of this report will briefly discuss each of these characteristics. HMS is a mathematical model, which implies that it represents the different hydrologic processes with mathematical expressions that are often empirically developed to best describe observations or controlled experiments. HMS is also a lumped parameter model, meaning physical characteristics of the watershed, such as land use and soil type, are "lumped" together into a single representative value for a given land area. Once HMS establishes these averaged values, they remain constant throughout the simulation,

rather than varying over time. HMS is an uncoupled model, meaning that it solves the different hydrologic processes independent of one another rather than jointly. In reality, surface and subsurface processes are dependent on one another and their governing equations should be solved simultaneously (Scharffenberg, 2013). Finally, HMS is a surface water model, meaning that it works best to simulate large storm events or when the ground is nearly saturated because overland flow is expected to dominate the partitioning of rainfall in both cases.

The two major components of the HMS hydrologic model are the basin model and the meteorologic model. The basin model defines the hydrologic connectivity of the watershed and how rainfall is converted to runoff, as well as how water is routed from one location to another. The meteorologic model stores the precipitation data that define when, where, and how much it rains over the watershed. Simulated hydrographs from HMS can be compared to discharge observations.

a. Model Development

The West Nishnabotna River Watershed modeled and described herein comprises approximately 1,650 square miles. For modeling, the research team divided the watershed into 614 smaller units, called subbasins in HMS. These have an average area of approximately 2.7 square miles but can be as large as 16.1 square miles. We delineated smaller subbasins, averaging 0.6 square miles, in HUC 12s selected for implementation of demonstration projects. Figure 3.2 illustrates subbasin delineation of the West Nishnabotna River Watershed as implemented in HMS.

We used ESRI ArcGIS and Arc Hydro tools for terrain preprocessing, creating flow direction and flow accumulation grids to define the stream network and delineate the subbasins. Channels draining at least 1.5 square miles defined the stream network; we defined a subbasin upstream of all stream confluences. GIS-defined subbasins were further manually split to create an outlet point at each USGS gauge location, as well as the discharge point of one incorporated structure (Prairie Rose Lake). In HMS, the model performs the averaging previously described for lumped parameter models within the boundary of each subbasin. Then we assign each subbasin a single value for the parameter being developed.

i. Incorporated Structures

We incorporated Prairie Rose Lake into the HMS model. Prairie Rose Lake is a 173-acre lake located in Shelby County southeast of Harlan, Iowa. Our research team obtained stage-storage-discharge relationship information from Iowa Department of Natural Resources' Office of Dam Safety in Des Moines, Iowa. The stage-storage-discharge rating curve used in the West Nishnabotna River Watershed HMS model is available in Appendix C. We included no existing farm ponds or other possible water storage structures in the HMS model.

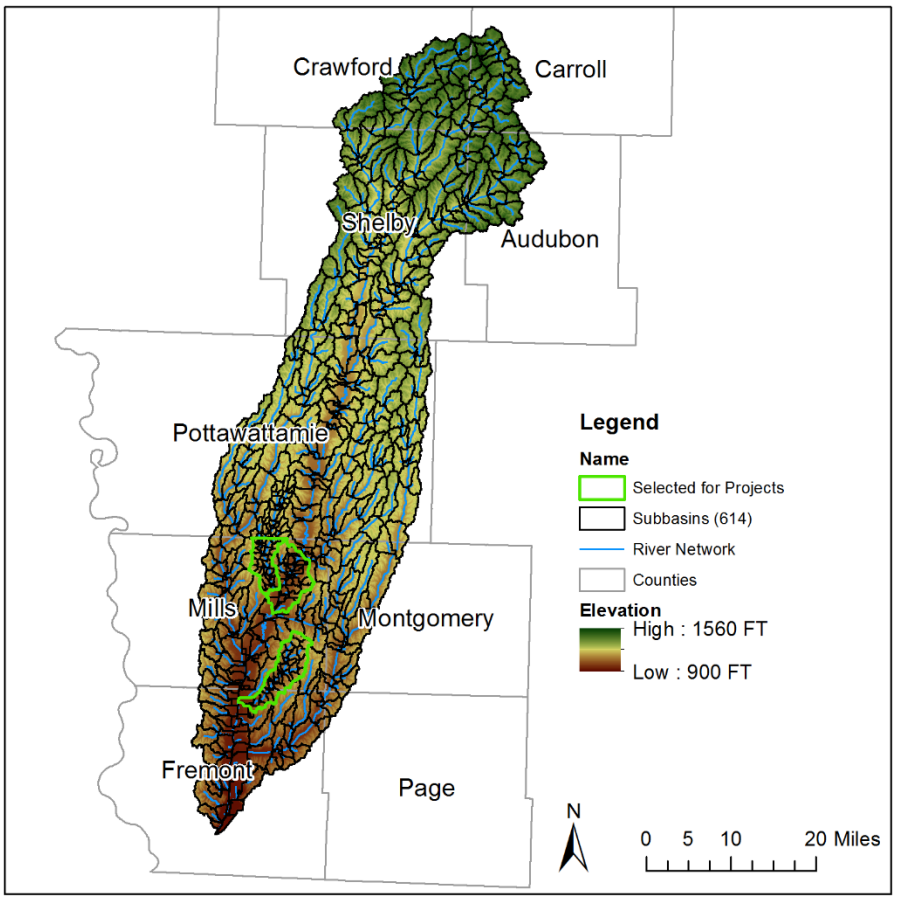

Figure 3.2. HMS model development of the West Nishnabotna River Watershed. The watershed was divided into 614 subbasins for modeling.

ii. Development of Model Inputs and Parameters

This section provides a brief overview of data inputs used and assumptions made to develop the HMS model. Appendix B of this report provides more detailed information on the hydrologic model development.

Rainfall (meteorological model)

We used Stage IV radar rainfall estimates (NCEP/EMC 4KM Gridded Data [GRIB] Stage IV Data) as the precipitation input to simulate actual rainfall events known to have occurred within the watershed. The National Center for Environmental Prediction (NCEP) produced the Stage IV data set by taking radar rainfall estimates produced by the 12 National Weather Service (NWS) River Forecast Centers across the continental United States and combining them into a nationwide 4 km x 4 km (2.5 mile x 2.5 mile) gridded hourly precipitation estimate data set. These data are available from Jan. 1, 2002–present.

Figure 3.3, developed using HEC-GridUtil 2.0, shows an example of the Stage IV radar rainfall estimates of cumulative rainfall during a one-hour period (May 05, 2007, 9–10 p.m.) in the West

Nishnabotna River Watershed. This figure demonstrates the gridded nature of the radar rainfall estimate data, as well as the distribution of rainfall in time and space during large storm events.

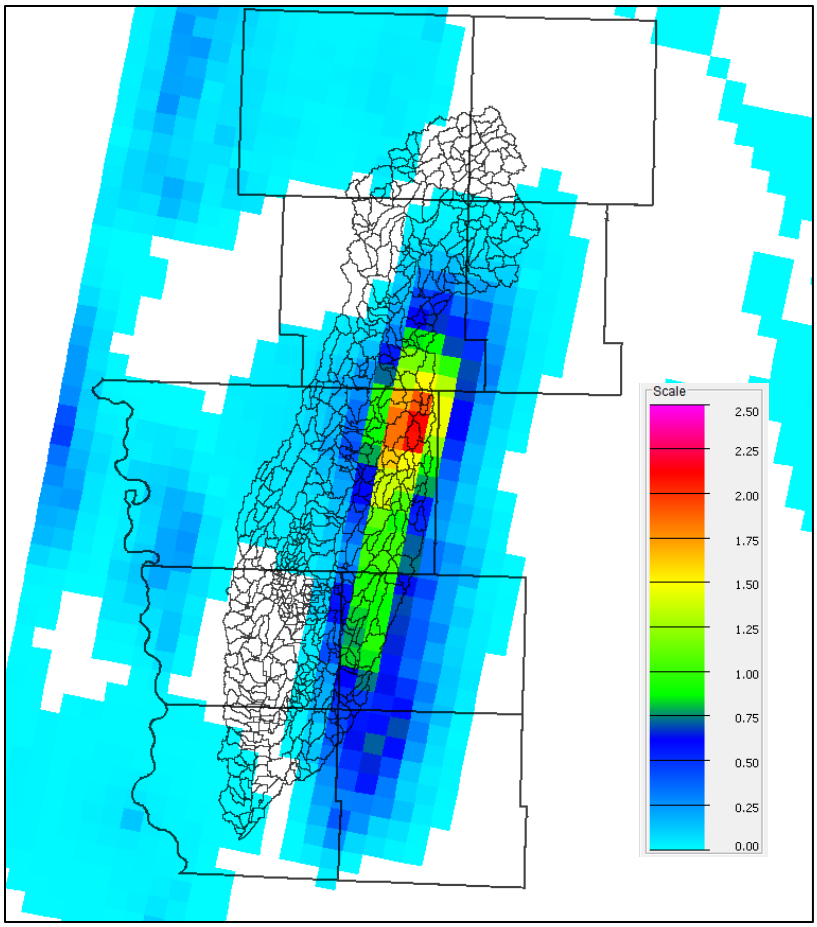

Figure 3.3. Example of the Stage IV rainfall product used as the precipitation input in the West Nishnabotna River Watershed HMS model. The Stage IV product provides hourly cumulative rainfall estimates for each 4 km x 4 km grid cell. The scale shown indicates the depth of rainfall (in inches) estimated for a one-hour period.

Radar rainfall provides increased accuracy in spatial and temporal distribution of precipitation over the watershed. In addition, Stage IV estimates provide a level of manual quality control (QC), performed by the NWS, which incorporates available rain gauge measurements into the rainfall estimates. Actual storms using Stage IV data provided the basis for model calibration and validation.

Our research team developed a hypothetical storm for comparative analyses, such as potential runoff generation, increased infiltration capacity, and increased distributed storage within the watershed. The hypothetical storm applies a uniform depth of six inches of rainfall across the entire watershed with the same timing everywhere. We used a Soil Conservation Service (SCS) Type-II distribution, 24-hour storm for the hypothetical storm. In reality, rainfall does not occur uniformly across the entire watershed. However, we can compare and analyze the hydrologic

response of subbasins more easily if all the subbasins are subject to the same rainfall depth and timing.

Watershed (basin model)

Iowa's statewide LiDAR dataset provided elevation data. The USGS has performed quality assurance testing on these LiDAR data, which have reported vertical positional accuracy of +/- 18 cm. The LiDAR product used had a resolution of 3-meters and was processed as a bare earth product, with structures and vegetation removed. Using ESRI ArcGIS, our team clipped the LiDAR data to the watershed boundary and mosaicked them into a seamless digital elevation model. We used the Universal Transverse Mercator (UTM) Zone 15 North geographic coordinate system, referencing the North American Datum of 1983 (NAD 83). All elevation values are in feet and are referenced to the North American Vertical Datum of 1988 (NAVD 88).

We used Soil Conservation Service (SCS) Curve Number (CN) methodology to determine the rainfall-runoff partitioning for the West Nishnabotna River Watershed HMS modeling. Curve number values range from 30–100, and as the CN becomes larger, less water infiltrates the ground and a higher percentage of runoff occurs. CN values are an estimated parameter based primarily on the intersection of a specific land use and the underlying soil type. General guidelines for developing curve numbers based on land use and soil type are available in technical references from the U.S. Department of Agriculture–Natural Resource Conservation Service (USDA-NRCS), previously known as the SCS. Table 3.1 shows the CNs assigned to each land use and soil type combination for the West Nishnabotna River HMS model. Dual hydrologic soil groups (e.g., A/D, B/D, C/D) are typically located in areas with water tables at a depth of 24 inches or less. For example, type A/D would behave like soil type A when drained and like soil type D when undrained. To be conservative, all dual hydrologic soil groups were treated like soil type D.

Table 3.1. Curve number assignment in the West Nishnabotna River Watershed based on land use and soil type. All dual hydrologic soil groups were treated as type D.

	Hydrologic Soil Group			
Land Cover Description	*A*	*B*	*C*	*D*
Water	100	100	100	100
Wetland	100	100	100	100
Shadow	100	100	100	100
Roads / Impervious	100	100	100	100
Structures	100	100	100	100
Barren / Fallow	98	98	98	98
Soybeans	67	78	85	89
Corn	67	78	85	89
Cut Hay	49	69	79	84
Grass 2	49	69	79	84
Grass 1	49	69	79	84
Deciduous Tall	32	58	72	79

Deciduous Medium	32	58	72	79
Deciduous Short	32	58	72	79
Coniferous Forest	32	58	72	79

Antecedent moisture conditions

Rainfall runoff partitioning for an area is also dependent on the antecedent soil moisture conditions (AMC) at the time rain falls on the land surface. In essence, the wetter the soil is, the less water can infiltrate, and thus more water is converted to runoff. Therefore, we developed a methodology to adjust the subbasin CNs to reflect the soil moisture conditions at the beginning of a storm simulation to better predict runoff volumes.

Existing NRCS methodology accounts for antecedent moisture conditions (AMC) by classifying CNs into one of three classes based on the seasonal five-day antecedent rainfall total. While this method provides a simple way to adjust CNs to reflect AMC based on the seasonal five-day antecedent rainfall total, it is oversimplified in several ways. The five-day antecedent rainfall totals defining each AMC class are universal; they have not been adjusted to reflect differences in geographic location or climate. Additionally, the five-day antecedent rainfall total applies equal weight to each of the five days preceding a storm to reflect the soil moisture conditions. Hence, rain that fell five days before or one day before the event being simulated is treated the same in determining the appropriate AMC CN class. In reality, the soil moisture conditions may differ significantly, depending on how close in time the rain fell prior to the event being simulated. Finally, existing NRCS methodology provides only three discrete classifications for CN; this can lead to drastic overestimations or underestimations of runoff volume with only a small change in the five-day antecedent rainfall total.

Runoff hydrographs

We used the Clark and ModClark Unit Hydrograph methods to convert excess precipitation into a direct runoff hydrograph for each subbasin. The ModClark method requires the same grid used for radar rainfall, so this method was used to simulate historical storms in calibration and validation steps, while the traditional Clark method was used for hypothetical design storm analysis. Both methods account for translation (delay) and attenuation (reduction) of the peak subbasin hydrograph discharge due to travel time of the excess precipitation to the subbasin outlet and temporary surface storage effects. The primary difference between the two methods is that the traditional Clark Unit Hydrograph method uses a pre-developed time-area histogram, while the ModClark method uses a grid-based travel time model to account for translation (lag) of the subbasin hydrograph. Both methods route the hydrograph through a linear reservoir to account for temporary storage effects.

Both the ModClark and Clark unit hydrograph methods require two inputs — time of concentration and a time storage coefficient. The time of concentration is the time required for water to travel from the hydraulically most remote point in the subbasin to the subbasin outlet. We estimated this at 5/3 times the lag time, where lag time is the time difference between the center of mass of the excess precipitation and the peak of the runoff hydrograph. This is a reasonable approximation, according to NRCS methodology (Woodward, 2010). Lag time is a

function of land slope, longest flow path, and soil retention (represented through CN); we estimated these parameters for each subbasin using ArcGIS tools. While time of concentration is a measure of lag due to travel time effects as water moves through the watershed, the time storage coefficient is a measure of lag due to natural storage effects in the subbasin (Kull and Feldman, 1998). Based on the literature, we can estimate it as a function of basin parameters (Sabol, 1988):

$$\frac{T_c}{R} = 1.46 - 0.0867\frac{L^2}{A}$$

Where R is the time storage coefficient, T_c is the time of concentration, A is the drainage area, and L is the longest flow path for each subbasin.

Figure 3.4 illustrates the NRCS methodologies for runoff depth estimation and how this runoff depth is converted to discharge (using one of the Clark unit hydrograph methods).

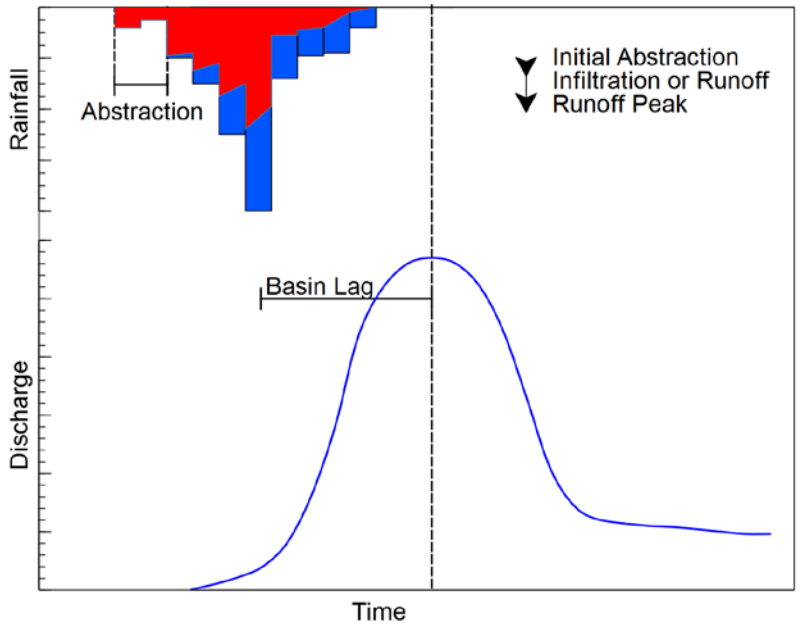

Figure 3.4. Subbasin runoff hydrograph conceptual model. Rainfall is partitioned into a runoff depth using the NRCS Curve Number methodology, which is then converted to discharge using either the ModClark or Clark unit hydrograph method.

ArcGIS to HEC-HMS

Upon completion of GIS processing to prepare the basin topography data, establish the stream network, delineate the subbasins, and develop and assign the necessary parameters to describe the rainfall-runoff partitioning for each subbasin, we used HEC-GeoHMS tools to intersect the subbasins with the appropriate grid system (HRAP) to allow use of the Stage IV radar rainfall estimates. Lastly, from ArcGIS, we used HEC-GeoHMS tools to create a new HMS project and export all the data developed in ArcGIS to the appropriate format such that the model setup was mostly complete upon opening HMS for the first time. Once in the HEC-HMS user interface, we

performed quality checks to ensure the connectivity of the subbasins and stream network of the watershed.

Parameters Assigned in HEC-HMS

Baseflow

We approximated baseflow using a first order exponential decay relationship for all historical storms. The USGS stage/discharge gauges for the West Nishnabotna River near Hancock and Randolph were used to develop discharge-drainage area (cfs/mi^2) relationships to set initial conditions for streamflow prior to each historical storm event simulation. Initial baseflow conditions were applied to the appropriate subbasins in HMS for each historical storm event simulation. We also specified a baseflow recession constant describing the rate of decay of baseflow per day and a threshold indicating when baseflow should be reactivated. No baseflow was modeled for the hypothetical design storms, as these analyses are more concerned with the effects of how much direct runoff is produced. We assumed the contribution of baseflow during these analyses to be relatively small compared to the amount of runoff produced.

Flood Wave Routing

We accomplished conveyance of runoff through the river network, or flood wave routing, using Muskingum-Cunge routing methods for major streams and Muskingum routing methods for smaller tributaries. The Muskingum-Cunge routing model uses an eight-point cross-section configuration and quasi-physical parameters to route channel and floodplain flow. Each routing reach requires specification of a reach length, roughness coefficients (channel, left and right overbanks), and energy grade. We adjusted roughness coefficients as part of the calibration process to best reproduce observations.

Two inputs are required to use the Muskingum routing model in HMS — the flood wave travel time in a reach (K) and a weighting factor that describes storage within the reach as the flood wave passes through (X). The allowable range for the X parameter is 0–0.5; values of 0.1–0.3 are generally applicable to natural streams. A value of 0.2 is frequently used in engineering practice and was used in this modeling analysis. Great accuracy in determining X may not be necessary because the results are relatively insensitive to the value of this parameter (Chow et al., 1988). The flood wave travel time, K, is much more important and can be estimated by dividing the reach length by a reasonable travel velocity (1–6 feet per second, in general) as a starting point, but is generally best obtained by adjustment in the model calibration process using measured discharge records, if available. For this modeling analysis, we used a flood wave travel velocity of 5.9 feet per second for all Muskingum routing reaches. We assumed that all reservoirs or ponds incorporated into the model were filled to the normal pool level at the beginning of each simulation.

b. Calibration

To calibrate a model, we usually take an initial set of parameters developed for a hydrologic model through GIS and other means to adjust them so the model's simulated results match an observed time series as closely as possible. Typically, this is stream discharge at a gauging station. However, modelers should not make extreme adjustments to parameters just to manipulate the end results to match the observed time series. If this is necessary, the model does not reasonably represent the watershed, and it is requisite upon the modeler to change methods used within the model or find out which parameter(s) might be needed to better represent the watershed's hydrologic response. We calibrated the West Nishnabotna River Watershed HMS model to three storm events between April 2007 and June 2014. We selected the storms based on their range of antecedent conditions, magnitude, time of year, and availability of Stage IV radar rainfall estimates and USGS discharge estimates. We selected large, high runoff storms that occurred between late April and September so the impacts of snow, rain on frozen grounds, and freeze-thaw effects were minimized. We made global adjustments to the runoff (CN) and timing (river routing and unit hydrograph) parameters to best match the simulated response to the observed discharge time series at each USGS discharge gauge location. Appendix B provides more details on calibration and validation.

c. Validation

For model validation, researchers use the model parameters developed during calibration to simulate other events and evaluate how well the model can replicate observed stream flows. Because we had already selected several of the largest storms for calibration (others occurred before Stage IV radar rainfall estimates became available, January 2002), we selected the next best available storms. Four storms were considered for model validation.

As with calibration, HMS model validation results are not perfect. Appendix B shows validation simulation plots. However, the general runoff volume, hydrograph shape, and peak flow timing are very similar to the observed streamflow hydrographs. The model consistently under-predicts the duration and volume produced during the falling limb of observed hydrographs. This mainly occurs during the transition from overland to baseflow dominated streamflow. Because HMS is a surface water model, it struggles to simulate conditions in which overland flow does not dominate the partitioning of rainfall.

It is important to note that many historic storm events resulted in spatially- and temporally-varied precipitation totals. The API curve used to assign CNs assumes antecedent conditions are consistent across the entire watershed before the event. For example, if the majority of antecedent rainfall occurred in the northern portion of the basin, the CNs should be relatively higher in those areas only, rather than watershed-wide. In addition, most of the storms occurred in or near the peak of the growing season when precipitation losses from evapotranspiration and plant root uptake are highest. While this HMS model did not explicitly model evapotranspiration losses, the API method did use a parameter that decreased the influence of prior rainfall.

4. Analysis of Watershed Scenarios

We used the HEC-HMS model of the West Nishnabotna River Watershed to identify areas in the watershed with high runoff potential and run simulations to help understand the potential impact of alternative flood mitigation strategies in the watershed. We focused the scenarios on understanding the impacts of: (1) increasing infiltration in the watershed; and (2) implementing a system of distributed storage projects (ponds) across the landscape. There are many BMP practices not investigated in this report that could potentially increase infiltration or runoff storage at the watershed scale. However, our analysis was limited by the resolution and capability of the HEC-HMS model to simulate effects of BMP practices aggregated across subbasin areas of several square miles. Therefore, we limited our investigations to distributed storage provided by ponds, which are relatively large BMP structures, and broad-scale land cover changes. Simulation of other much smaller BMP structures like terracing or WASCOBS, while demonstrably effective in this watershed, would require considering many more individual structures to make any impact at the watershed scale, and a much higher degree of model resolution to reliably quantify impacts.

a. High Runoff Potential Areas

Identifying areas of the watershed with higher runoff potential is the first step in selecting mitigation project sites. High runoff areas offer the greatest opportunity to retain more water from large rainstorms on the landscape and to reduce downstream flood peaks.

In the HMS model of the West Nishnabotna River Watershed, the runoff potential for each subbasin is defined by the SCS Curve Number (CN). The runoff CN assigned to a subbasin depends on its land use and the underlying soils. The fraction of rainfall converted to runoff — also known as the runoff coefficient — is a convenient way to illustrate runoff potential. Areas with higher runoff coefficients have higher runoff potential. To evaluate the runoff coefficient, the HMS model simulates runoff from each subbasin area for the same rainstorm; we chose a rainstorm with a total accumulation of 6.0 inches in 24 hours (approximately 25-year average recurrence interval) (National Oceanic and Atmospheric Administration, 2013). The timing of the rainfall and example infiltration is shown in Figure 4.1. This design storm corresponds to approximately the 25-year return interval at small scales, similar to the size of model subbasins. Applying this design storm across the entire West Nishnabotna Watershed results in unrealistic peak discharge values at many locations with moderate drainage area. However, subjecting each model subbasin to the same storm allows for direct comparison among them.

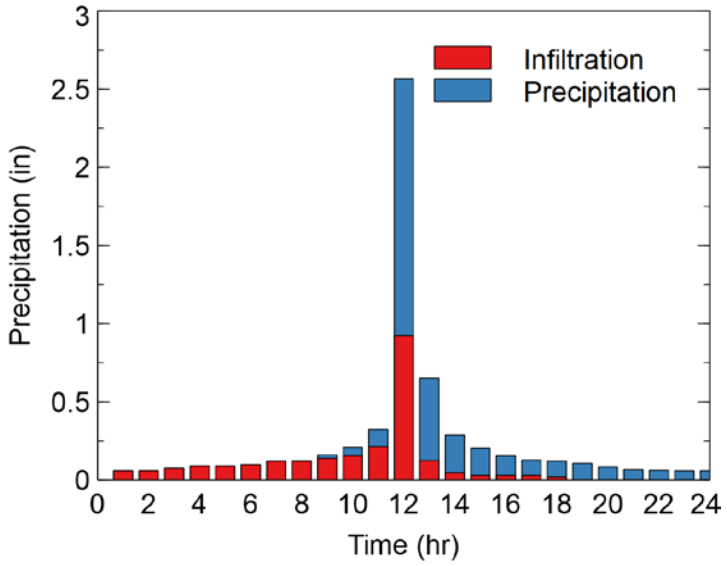

Figure 4.1. SCS design storm hyetograph, showing the timing of the rainfall and example infiltration for a given subbasin area.

Figure 4.2 shows the runoff coefficient as a percentage (from 0% for no runoff to 100% when all rainfall is converted to runoff). Since the subbasin areas shown were defined for numerical modeling purposes, the results were also aggregated to more commonly used subbasin areas — namely, hydrologic units defined by the USGS. The smallest hydrologic units, known as HUC 12 watersheds, are also shown in Figure 4.2. We determined area-weighted average runoff coefficients for each of the 44 HUC 12 watersheds in the West Nishnabotna River Watershed. Areas in the basin with the highest runoff potential are primarily located in the north and areas along the south reach of the West Nishnabotna River. Runoff coefficients exceed 50% in many areas. Agricultural land use dominates these counties (and the watershed in general). However, these areas have moderate to poorly drained soils, which are characteristic of the Southern Drift Plain geographic landform. From a hydrologic perspective, flood mitigation projects that can reduce runoff from these high runoff areas should be a priority.

Still, high runoff potential is only one factor in selecting locations for potential projects. Taken alone, it has limitations. The watershed's high degree of subbasin slope and topographic relief can generate numerous sites favorable for flood mitigation ponds. Of course, there are many factors to consider in site selection. Landowner willingness to participate is essential. Also, existing conservation practices may be in place, and areas such as timber should not be disturbed. Stakeholder knowledge of places with repetitive loss of crops or roads/road structures is also valuable in selecting locations.

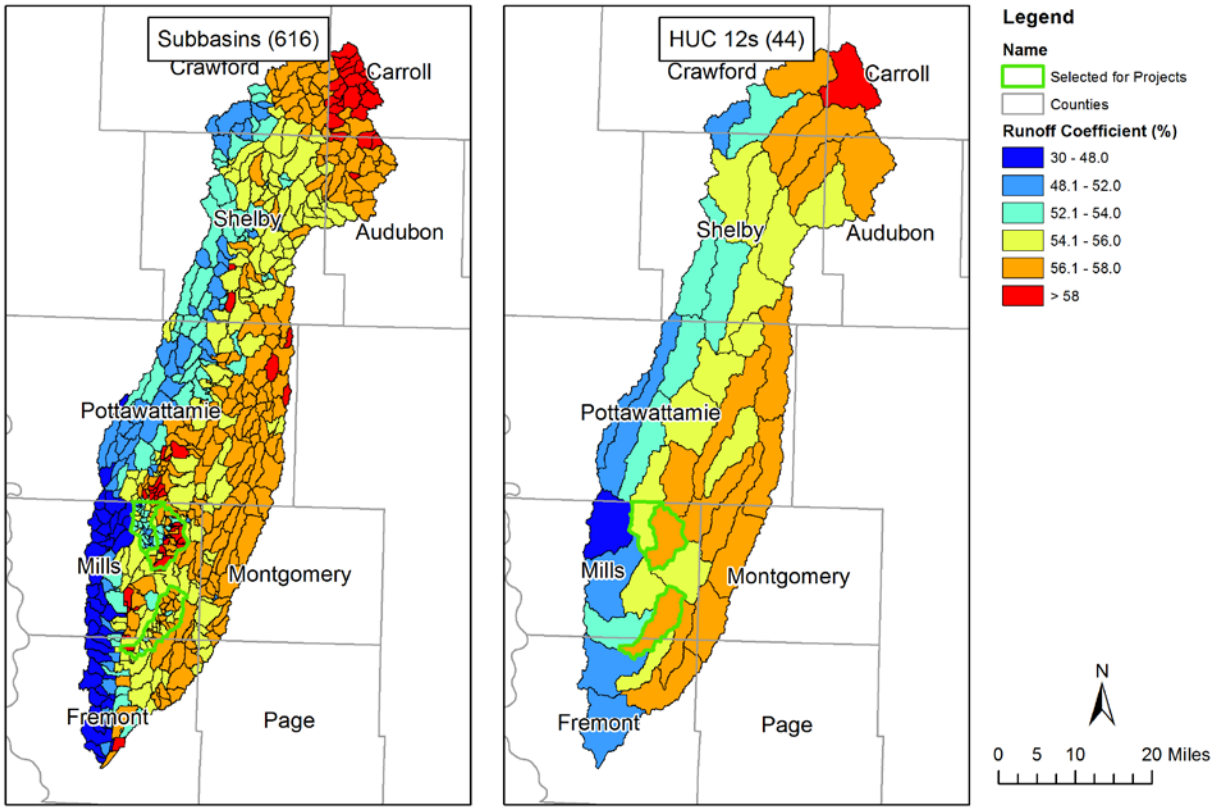

Figure 4.2. Runoff potential in the West Nishnabotna River Watershed. Runoff coefficients computed for each subbasin (left) and HUC 12 watershed (right) for a 6-inch, 24-hour design storm are shown. Higher runoff coefficients are shown in red.

b. Mitigating the Effects of High Runoff with Increased Infiltration

We can reduce runoff from areas with high runoff potential by increasing how much rainfall infiltrates into the ground. Changes that result in higher infiltration reduce the volume of water that drains off the landscape during and immediately after the storm. The extra water that soaks into the ground may later evaporate or transpire. Or it may slowly travel through the soil, either seeping deeper into the groundwater storage or traveling beneath the surface to a stream. Increasing infiltration has several benefits. Even if the infiltrated water reaches a stream, it arrives much later (long after the storm has ended and flooding has subsided). Also, its late arrival keeps rivers running during long periods without rain.

In this section, we examine several different alternatives to reduce runoff through either land use changes or soil quality improvements. One hypothetical land use change would be the conversion of row crop agriculture back to native tall-grass prairie. Another possible land use change would be improvements to agricultural conditions that would result from planting cover crops during the dormant season. These are hypothetical examples; they are meant to illustrate the potential effects on flood reduction. The examples are also not project proposals; they would neither be recommended nor practically feasible. Still, the hypothetical examples do provide valuable

benchmarks on the limits of flood reduction that are physically possible with broad-scale land cover changes.

It is also worth noting the existing BMPs, shown in Appendix A, include a high concentration of terracing and ponds. These BMPs have likely increased infiltration and caused a subsequent increase in baseflow in the West Nishnabotna Watershed.

i. Conversion of Row Crop Agriculture to Tall-Grass Prairie

Much has been documented about the historical water cycle of the native tall-grass prairie of the Midwest. Prior to the transformation to agricultural landscape, tall-grass prairies dominated the landscape. This ecosystem infiltrated, transpired, and stored extremely large volumes of water throughout the entire year (Mutel, 2010; Hernandez-Santana et al., 2013). The deep, loosely packed organic soils and the deep root systems of the prairie plants (Jackson et al., 1996) allowed a high volume of the rainfall to infiltrate into the ground (Bharati et al., 2002). The soils retained the water instead of allowing it to travel rapidly to a nearby stream as surface flow. Once in the soils, much of the water was actually taken up by the root systems of the prairie grasses (Brye et al., 2000).

We performed an analysis to quantify the impact of human-induced land use changes on the flood hydrology of the West Nishnabotna River Watershed. In this example, all current agricultural land use is converted to native tall-grass prairie with its much higher infiltration characteristics. Obviously, returning to this pre-settlement condition is unlikely to occur. Still, this scenario is an important benchmark to compare with any watershed improvement project considered.

To simulate the conversion to native tall-grass prairie with the HMS model, we adjusted the model parameters affecting runoff potential across the landscape to reflect the tall-grass prairie condition. Specifically, existing agricultural land use, which accounts for 76% of the watershed area, was redefined as tall-grass prairie. We assigned new CNs, reflecting the lower runoff potential of prairie, to each subbasin as shown in Table 4.1. It is important to note that other parameters estimated from CNs — such as the water flow travel time through the subbasin — were not adjusted. Thus, this scenario only considers the runoff reduction resulting from the much-improved infiltration characteristics of the native prairie and not the additional attenuation and delay in the timing of the peak discharge that would be expected due to a higher surface roughness. Following new assignment of subbasin CNs, we ran the model for the design storm with total accumulation of 6.0 inches in 24 hours.

Six-Inch, 24-Hour SCS Design Storm

As expected, improving the infiltration of 76% of the watershed area by converting row crop agriculture to native tall-grass prairie has a significant effect on the flood hydrology. For the 6-inch design storm, the simulated tall-grass prairie infiltrates 0.9 inches more rainfall into the ground than does the current agricultural landscape. Figure 4.3 shows reductions in subbasin and junction peak discharges. Most of the watershed experienced greater than a 20% reduction in subbasin peak discharge. Application of this design storm across the entire watershed produces

unrealistic peak discharges at junction locations with relatively large drainage area, therefore, results are not shown at junctions with drainage area greater than 100 mi^2.

Table 4.1. Curve Numbers used to define the tall-grass prairie and cover crop land use conditions.

	Hydrologic Soil Group			
Land Use	A	B	C	D
Row Crops	67	78	85	89
Tall-Grass Prairie	30	58	71	78
Row Crops after Planting Cover Crops	64	74	81	85

Note: Curve number combinations derived from the *Urban Hydrology for Small Watersheds (TR-55)*, Table 2-2, June 1986

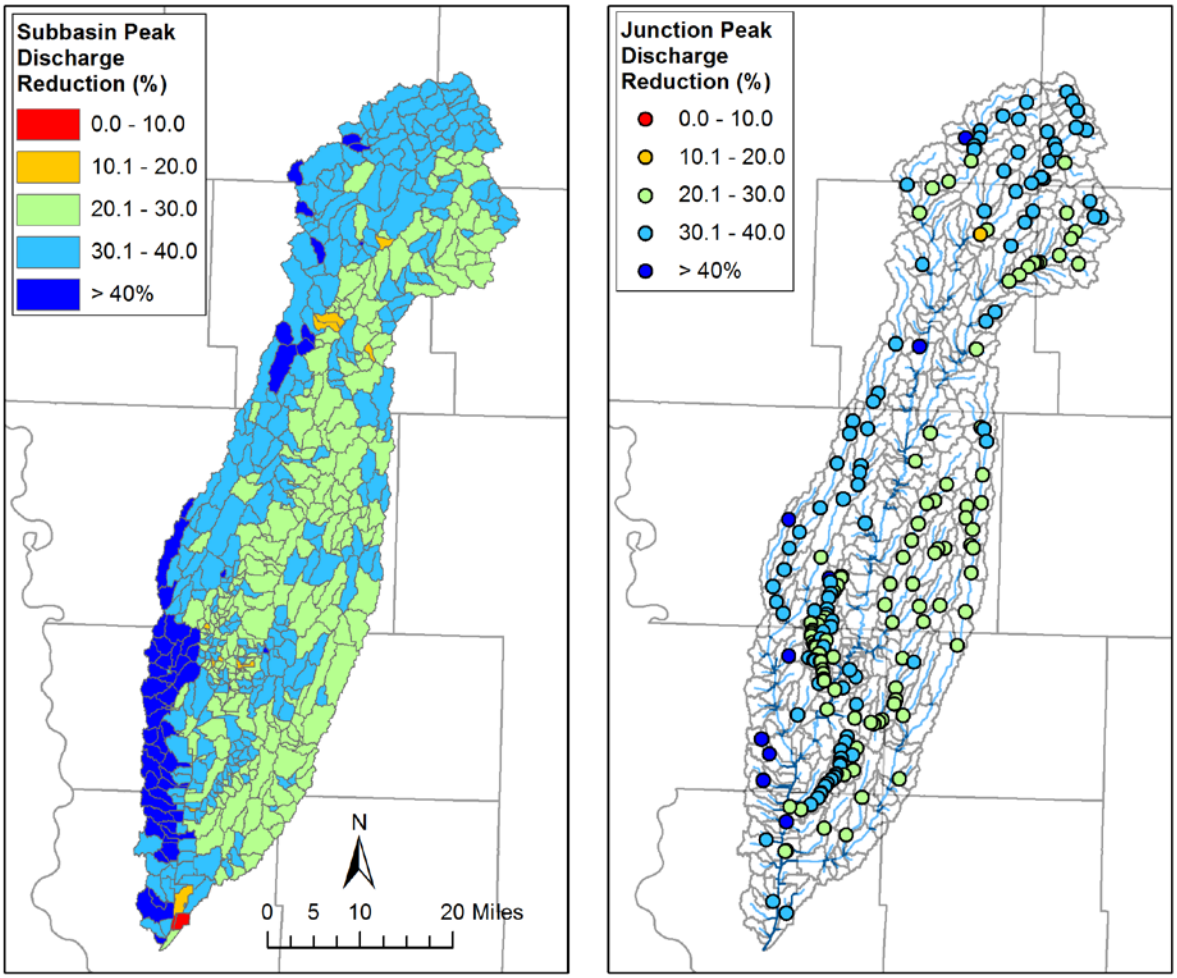

Figure 4.3. Peak discharge reductions for subbasins (left) and junctions (right) for conversion of row crop agriculture to native prairie for a 6-inch, 24-hour design storm. Simulation results at junctions with large drainage area are not realistic for this design storm event, therefore, results are not shown at junctions with drainage area greater than 100 mi^2.

ii. Improved Agricultural Conditions from Planting Cover Crops

Cover crops can be an effective farming conservation practice that also enhances infiltration. Farmers typically plant cover crops after the harvest of either corn or soybeans and "cover" the ground through the winter until the next growing season begins. The cover crop can be killed off in the spring by rolling it or grazing it with livestock; afterwards, row crops can be planted directly into the remaining cover crop residue. Cover crops provide a variety of benefits, including improved soil quality and fertility, increased organic matter content, increased infiltration and percolation, reduced soil compaction, and reduced erosion and soil loss. Cover crops also retain soil moisture and enhance biodiversity (Mutch, 2010). One source suggests that for every one percent increase in soil organic matter (e.g., from 2% to 3%), the soil can retain an additional 17,000–25,000 gallons of water per acre (Archuleta, 2014). Examples of cover crops include clovers, annual and cereal ryegrasses, winter wheat, and oilseed radish (Mutch, 2010).

The purpose of this hypothetical example is to investigate the impact improved agricultural management practices could have on reducing flood peak discharges throughout the watershed. We hypothesize that planting cover crops across all agricultural areas in the watershed during the dormant (winter) season would lower the runoff potential of these same areas during the growing season (spring and summer) because of increased soil health and fertility. To be clear, this scenario does not represent the conversion of the existing agricultural landscape (primarily row crops) to cover crops. Rather, the existing agricultural landscape is still mostly intact, but its runoff potential during the growing season has been slightly reduced by planting cover crops during the dormant season. Similar to the tall-grass prairie scenario, Table 4.1 shows the new runoff CNs we assigned to each subbasin, reflecting the landscape's lower runoff potential from improved agricultural management practices. Comparisons were made between current and cover crop simulations for the 6-inch, 24-hour SCS design storm.

Six-Inch, 24-Hour SCS Design Storm

Improved agricultural management practices, represented by planting cover crops during the dormant season, result in less reduction of runoff and peak discharges than the native tall-grass prairie simulation. On average for the basin, planting cover crops increases infiltration by 0.25 inches for the 6-inch, 24-hour SCS Design Storm. Figure 4.4 shows the peak discharge reductions for each subbasin resulting from improved agricultural conditions due to cover crops for the 6-inch, 24-hour design storm. Peak discharge reductions of 7–10% are common at the subbasin scale. Application of this design storm across the entire watershed produces unrealistic peak discharges at junction locations with relatively large drainage area, therefore, results are not shown at junctions with drainage area greater than 100 mi^2.

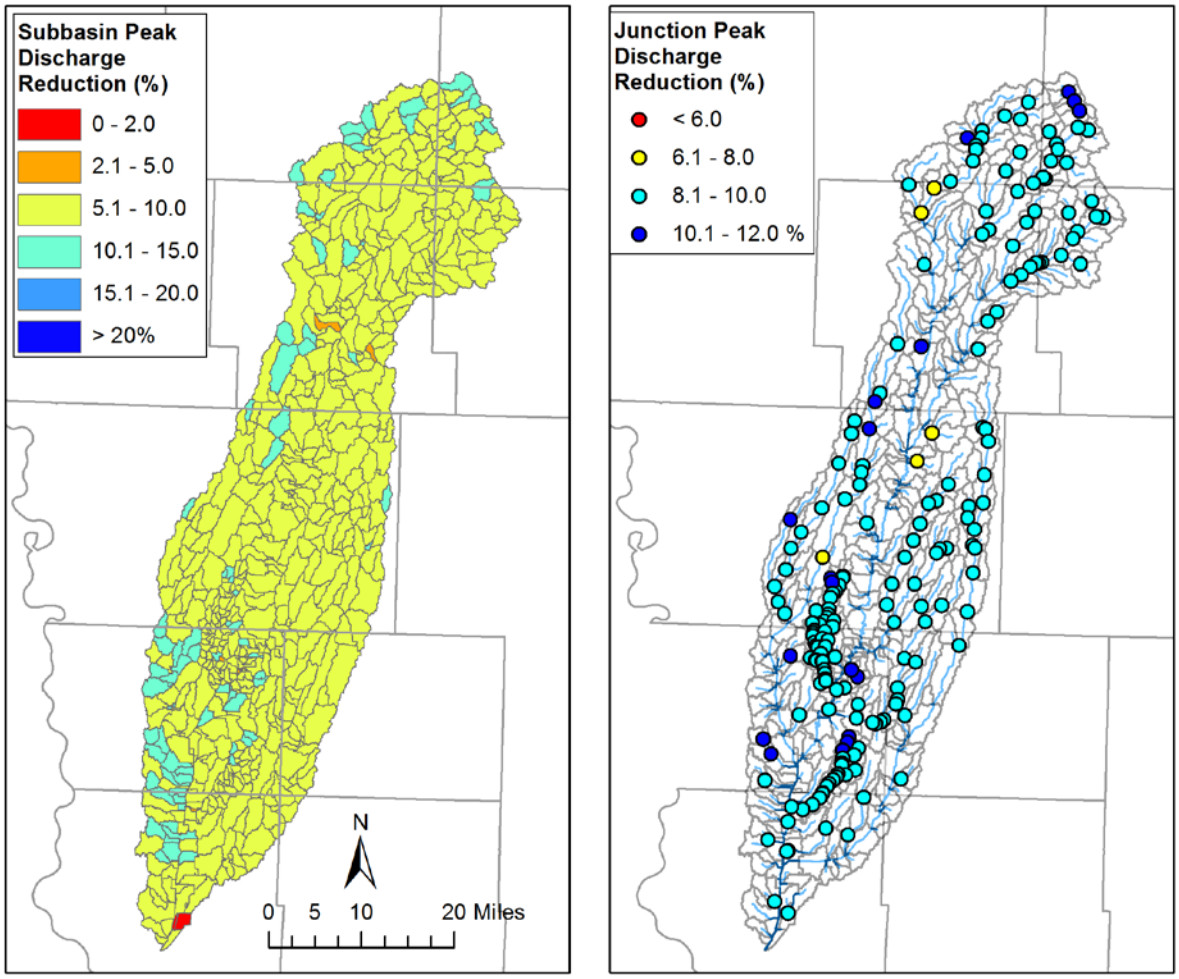

Figure 4.4. Peak discharge reductions for subbasins (left) and junctions (right) for the 6-inch, 24-hour design storm with improved soil infiltration after many years of using cover crops during the dormant season for all row crop agriculture. Simulation results at junctions with large drainage area are not realistic for this design storm event, therefore, results are not shown at junctions with drainage area greater than 100 mi^2.

c. Mitigating the Effects of High Runoff with Distributed Storage

In general, a system providing distributed storage does not change the volume of water that runs off the landscape. Instead, storage ponds (Figure 4.5) hold floodwater temporarily and release it at a slower rate. Therefore, the peak flood discharge downstream of the storage pond is lowered. The effectiveness of any one storage pond depends on its size (storage volume) and how quickly water is released. By adjusting the size and the pond outlets, storage ponds can be engineered to efficiently use available storage for large floods.

Generally, these ponds have a permanent storage area that holds water all the time. This is achieved by constructing an earthen embankment across a stream and setting an outlet (usually a pipe called the principal spillway) at some elevation above the floor of the pond. When a storm event occurs, runoff enters the pond. Once the elevation of the water surface is higher than the

pipe inlet, water will pass through the pipe, leaving the pond at a controlled rate. Additionally, the earthen dam is built higher than the pipe, allowing for more storage capacity within the pond. An auxiliary or emergency spillway that can discharge water at a much faster rate than the pipe does is set at an elevation higher than the pipe. This auxiliary spillway is designed to release rapidly rising waters in the pond, so they do not damage the earthen embankment. The volume of water stored between the principal spillway and the emergency spillway is called flood storage.

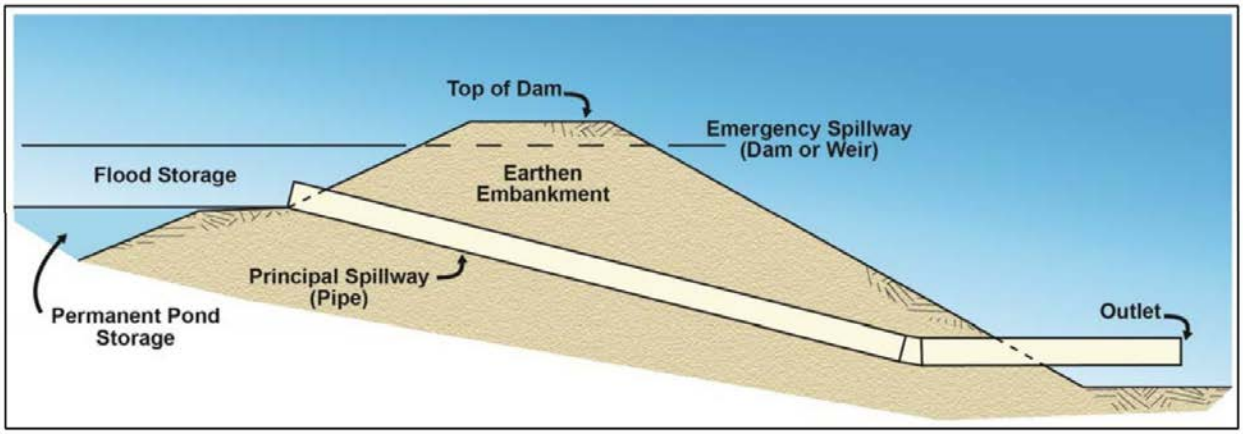

Figure 4.5. Schematic of a pond constructed to provide flood storage.

We based the hypothetical distributed storage analysis performed using the West Nishnabotna River HMS model on the flood control concept developed by the Soap Creek Watershed. The Soap Creek Watershed Board formed in the 1980s when landowners banded together to reduce flood damage and erosion within their watershed. They adopted a plan to identify potential locations for 154 distributed storage structures (mainly ponds) that could be built within the watershed. As of 2018, 135 of these structures have been built (Stolze, 2018).

The Soap Creek Watershed drains approximately 250 square miles, equaling an average density of 1 built pond for every 1.9 square miles of drainage area. Further analysis of the Soap Creek structures shows that most are constructed in the headwater areas of the watershed, which allows for smaller structures, rather than large, high-hazard class structures on the main rivers. The average pond density in the headwater areas where most of the ponds are sited is approximately 1 pond per 1.4 square miles of drainage area.

i. Siting of Ponds in the West Nishnabotna River Watershed

Figure 4.6 shows the 1153 locations in the West Nishnabotna Watershed identified as potential locations for nutrient reduction wetlands using the ACPF toolbox. With these ACPF data, we can design a pond for each specific nutrient reduction wetland location. With detailed information about the pond site and drainage area, we ran the NRCS Water Resources Site Analysis Computer program (SITES) to design the principal and auxiliary (emergency) spillway of each pond.

SITES requires a time-of-concentration (TOC) estimate at each NRW location. We estimated TOC using the Watershed Lag method from the National Engineering Handbook (NEH) Part 630,

Chapter 15 (National Resources Conservation Service, 2010). The flow length (l) is found using Equation 4.1,

$$l = 209A^{0.6} \quad 4.1$$

where A is the drainage area in acres and l is in feet.

We then use the flow length to compute the TOC using Equation 4.2,

$$Tc = \frac{l^{0.8}(S+1)^{0.7}}{1140Y^{0.5}} \quad 4.2$$

where Y is the average watershed land slope in percentage, and S is the maximum potential retention inches calculated by $\frac{1000}{CN} - 10$.

The SITES analysis makes the following assumptions for each ACPF NRW location:

- The principal spillway is an open-top drop inlet riser with a 10-inch minimum pipe diameter;
- The principal spillway elevation is the NRW permanent pool elevation reported by ACPF;
- The auxiliary spillway has a 12-foot width;
- The auxiliary spillway elevation is the NRW buffer elevation reported by ACPF, 4.9 feet above the principal spillway elevation; and
- The principal spillway is sized such that a 25-year NRCS Type II design rainfall event does not activate the auxiliary spillway.

We ran the SITES program iteratively for each pond until the designed principal spillway pipe diameter was large enough so that the auxiliary spillway was not activated for the 25-year design storm. We then developed storage-discharge relationships for each of the 1153 pond locations.

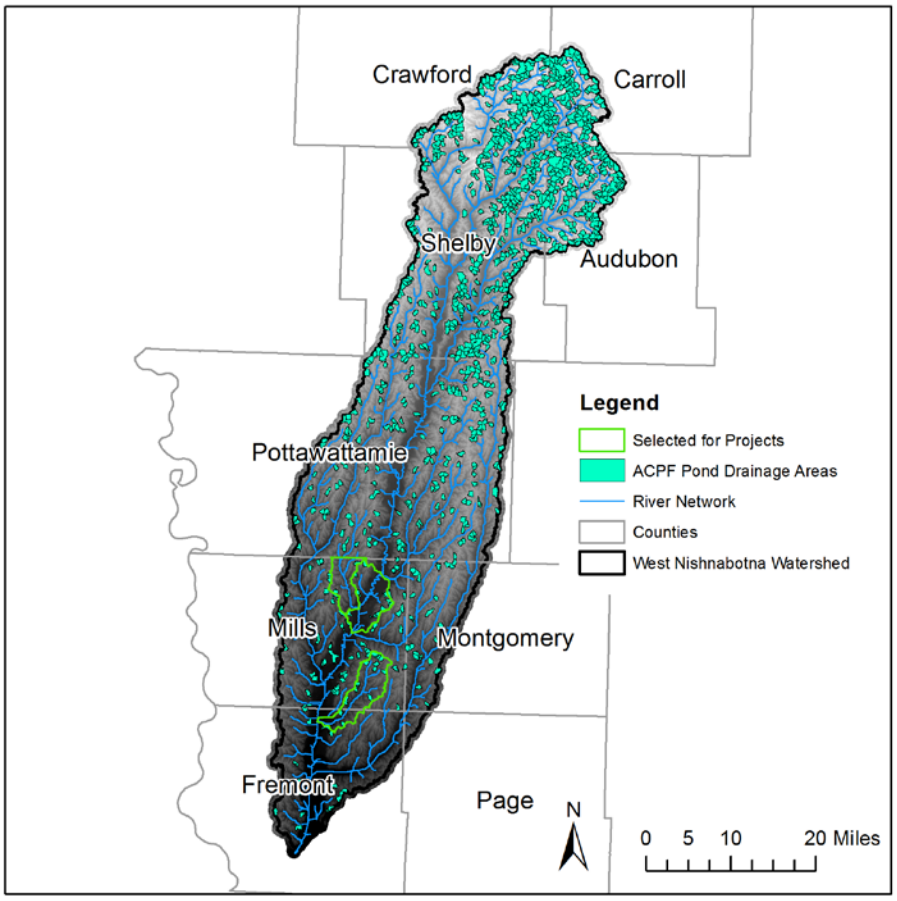

Figure 4.6. Areas draining to nutrient reduction wetlands (NRWs), identified by the Agricultural Conservation Planning Framework (ACPF) toolbox. NRW ponds were used to develop storage-discharge relationships for corresponding subbasins.

Numerous HEC-HMS model subbasins contained more than one pond within the subbasin area. This required aggregation of the ponds to simulate their cumulative impact. We treated all the ponds as if they were in a parallel configuration. We summed the abscissae and ordinates of the storage-discharge curves for a given group of ponds within a subbasin. We inserted a single pond HMS model element within each HMS model subbasin containing ponds and applied the aggregated storage-discharge relationship. The cumulative subbasin drainage area intercepted by the ACPF ponds was used to divert the appropriate percentage of subbasin runoff to the aggregated pond or allowed to bypass to the downstream subbasin outlet. For example, if a single subbasin contained three ponds, we summed the storage and outflow curves and diverted the corresponding drainage area to the ponds, with the remaining drainage area allowed to bypass to the downstream junction. Overlapping pond drainage areas for those in a series configuration were dissolved to prevent over-estimating intercepted drainage area. Figure 4.7 depicts the treatment of multiple ponds within a subbasin and the aggregation process. The number of ponds aggregated within each subbasin is shown in Figure 4.8. The variable storage available for runoff

provided by aggregated ACPF ponds and these hypothetical ponds for each subbasin is shown in Figure 4.9.

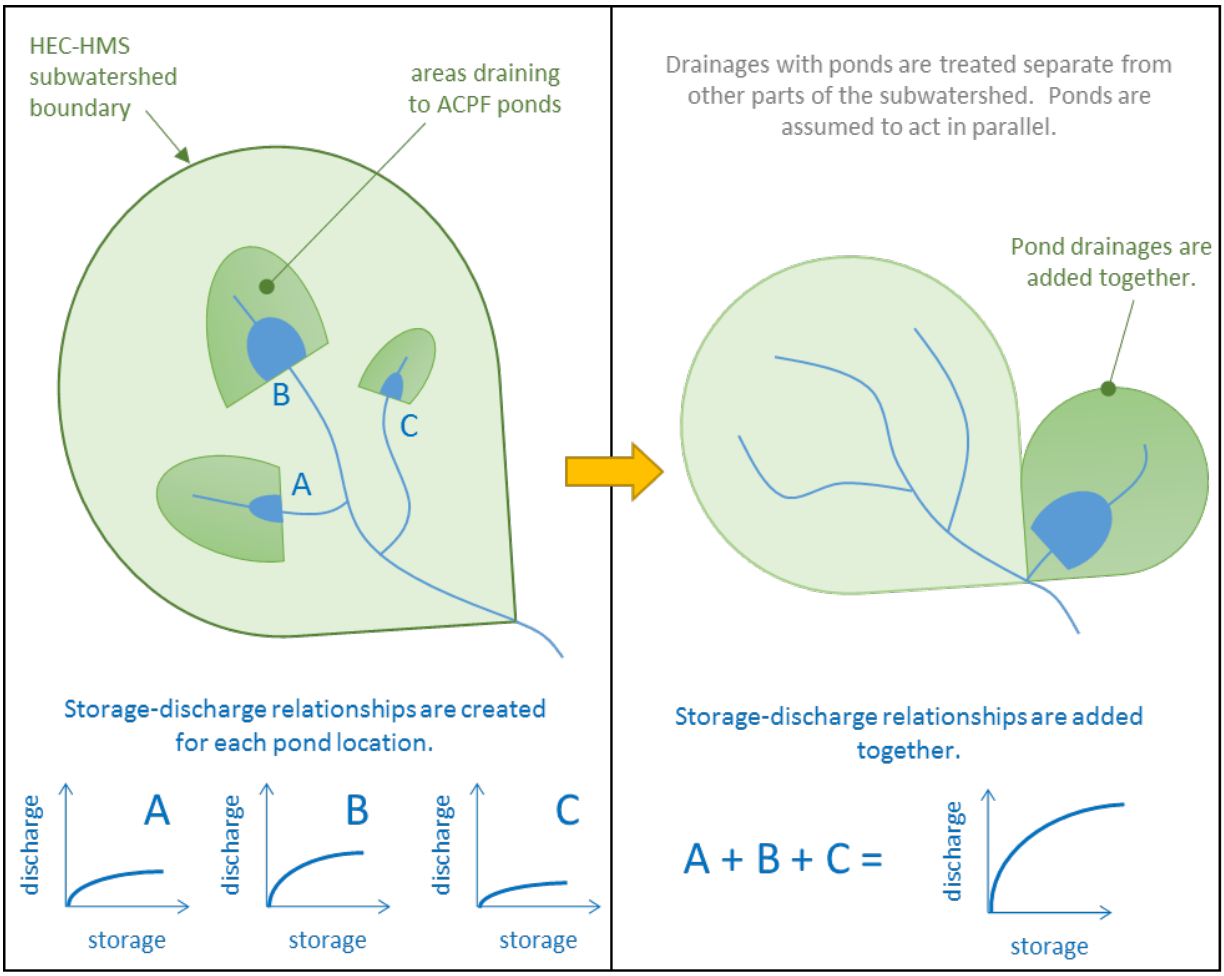

Figure 4.7. Aggregation of pond storage-discharge curves and drainage areas within an HMS model subbasin. Overlapping drainage areas of ponds in a series configuration were dissolved.

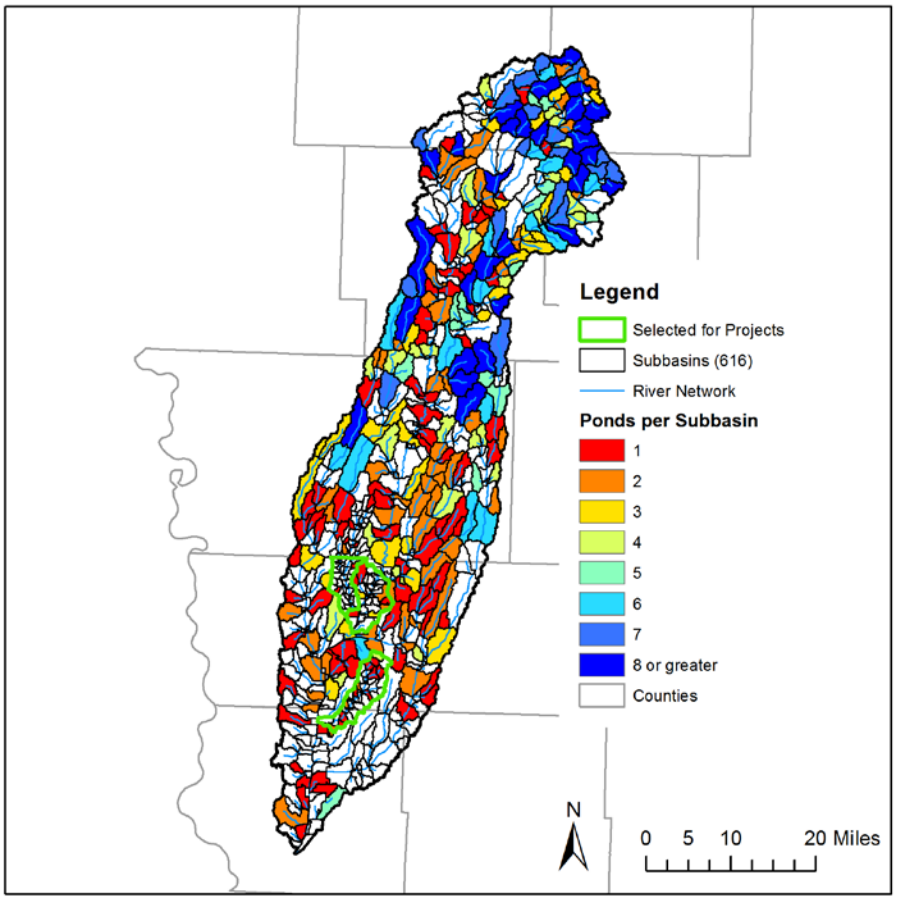

Figure 4.8. Number of potential NRW sites identified by ACPF tool within each HEC-HMS model subbasin.

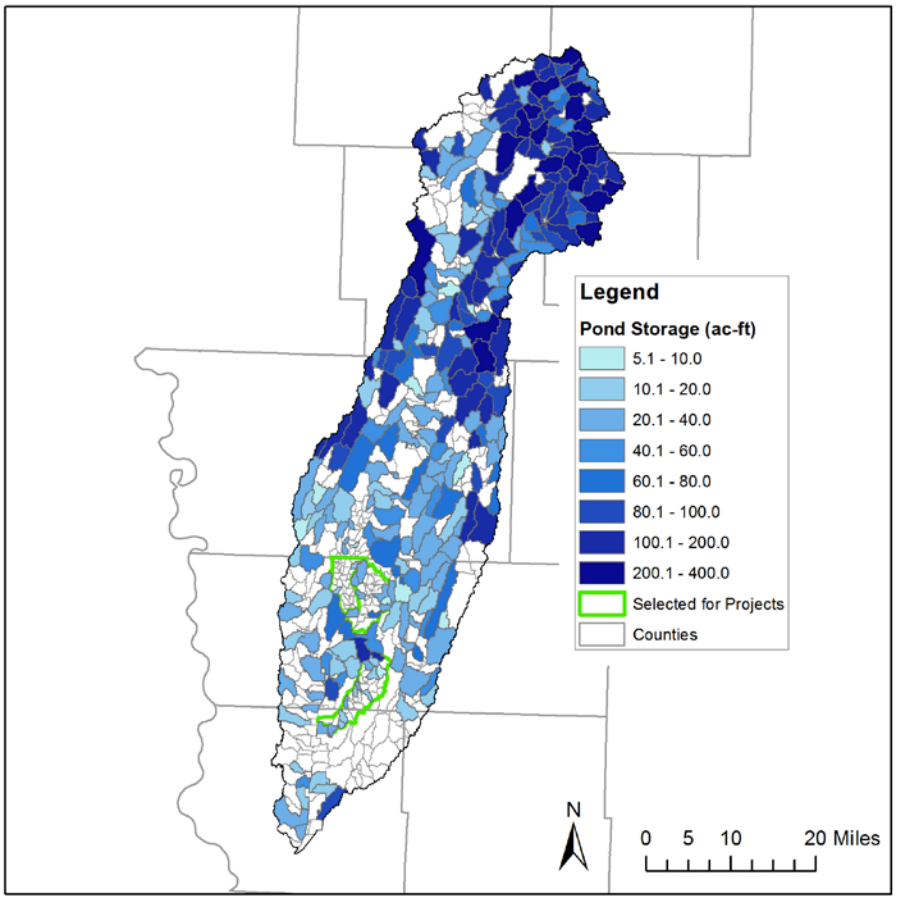

Figure 4.9. Flood storage (acre-feet) provided by ponds in each subbasin.

We selected discrete model index points (shown in Figure 4.10) throughout the watershed to compare upstream drainage area and pond characteristics. Index points were selected at head water locations along the main stem of the West Nishnabotna River, and HUC 12s were selected for project implementation at the outlets of Mud and Deer Creeks. Index points are introduced here to simplify comparison of upstream drainage area and pond characteristics, and are also referenced in historic storm event simulation results at the end this chapter. Table 4.2 details the drainage area, number of upstream ACPF ponds, number of upstream aggregated ponds, and the upstream drainage area intercepted by ponds for each model index point. The potential pond locations are concentrated in the northern portion of the watershed, likely due to differences in topographic relief and number of suitable locations. As a result, the drainage area intercepted by ponds decreases as total drainage area increases. However, the percent of drainage area intercepted by ponds along main stem of the West Nishnabotna River remains near 20%. This is likely due to the watershed shape, terrain, and spatial distribution of pond storage. The direct relationship between drainage area intercepted by ponds and reductions in peak discharge is evident in the following simulations.

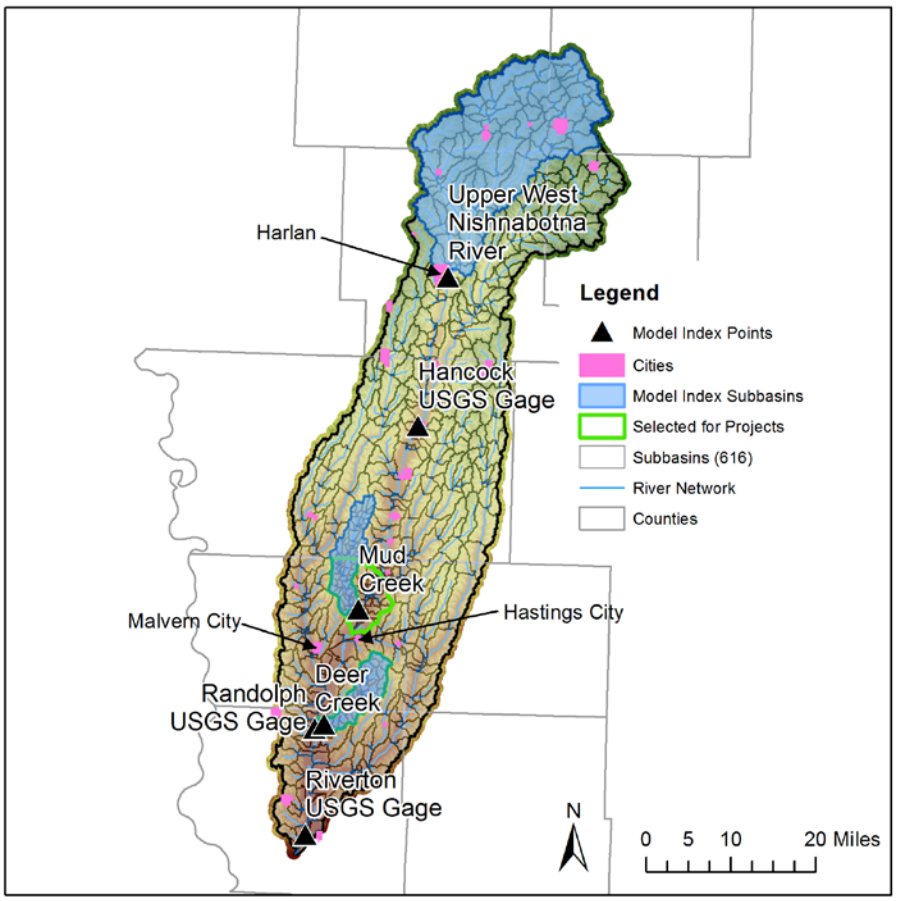

Figure 4.10. Model index locations selected for comparisons of hypothetical flood mitigation scenarios to current conditions.

Table 4.2. The flood storage available upstream of the model index locations. In general, the smaller the upland drainage area, the larger the percentage of drainage area is controlled by ponds, and the more flood storage is available.

Location	*Drainage Area (mi^2)*	*ACPF Ponds Upstream*	*Aggregated Ponds Upstream*	*Drainage Area intercepted by Ponds (mi^2)*	*Upstream Pond Flood Storage (ac-ft)*	*Upstream Pond Flood Storage Equivalent Depth(in)*
Outlet of Deer Creek	29	16	12	4.0 (14%)	308.5	0.20
Outlet of Mud Creek	36	8	7	2.4 (6.6%)	138.3	0.07
Outlet of Upper West Nishnabotna River	313	382	68	112.8 (36%)	9431	0.56
West Nishnabotna River at Hancock	610	759	140	212.9 (35%)	17399	0.53
West Nishnabotna River at Randolph	1328	1063	269	288.7 (22%)	23017	0.32
West Nishnabotna River at Riverton	1645	1153	299	312.1 (19%)	24930	0.28

Six-Inch, 24-Hour SCS Design Storm

We ran the HMS model with ponds to simulate the effects of flood storage on peak discharges. Each simulation started with all pond water levels at the primary spillway elevation; this assumes that the permanent storage is full as the storm begins. We then compared this to the simulated discharges without ponds in place (the existing baseline condition).

Figure 4.11 shows the percent reduction in peak discharge at model junction locations for the 6-inch, 24-hour SCS Design Storm. Application of this design storm assumes that a 6-inch rainfall occurs everywhere within the watershed simultaneously and produces unrealistic peak discharges at junction locations with relatively large drainage area, therefore, results are not shown at junctions with drainage area greater than 100 mi^2. In general, upland sites with more drainage area intercepted by ponds had the greatest reductions in peak discharge. This coincides with the intercepted drainage area percentages shown in Table 4.2. The most northerly portion of the watershed had the largest peak discharge reductions, approximately 5–10% or greater.

Ponds can effectively reduce flood peaks immediately downstream of their headwater sites. This is evident in Figure 4.11. At junctions farther downstream, floodwaters originating from locations throughout the watershed arrive at vastly different times; some areas have ponds, others do not. The result is that the storage effect from ponded areas is spread out over time, instead of being concentrated at the time of highest flows. Hence, for larger drainage areas downstream in the watershed, the flood peak reduction of storage ponds diminishes.

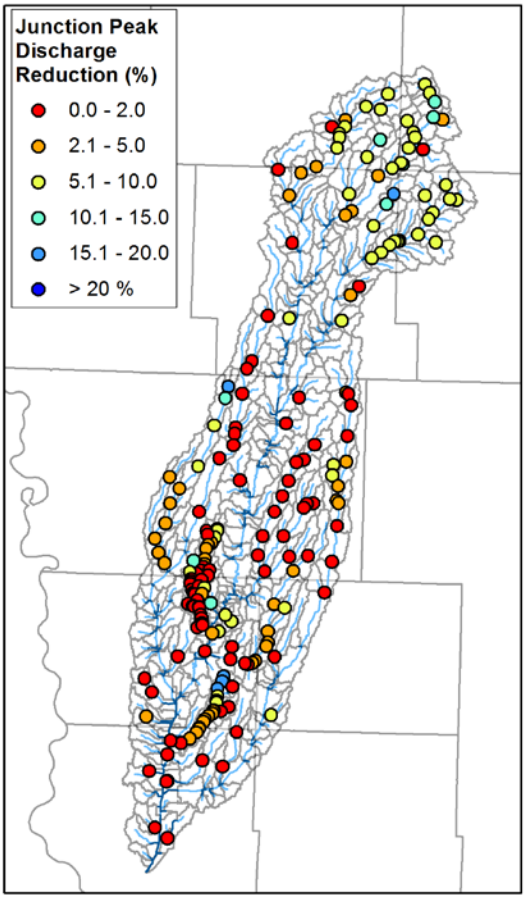

Figure 4.11. Junction (with drainage area less than 100 mi^2) peak discharge reductions with ACPF ponds in place for a 6-inch, 24-hour SCS Design Storm. Simulation results at junctions with large drainage area are not realistic for this design storm event, therefore, results are not shown at junctions with drainage area greater than 100 mi^2.

d. Mitigating the Effects of High Runoff with Distributed Storage and Increased Infiltration

Implementation of actual flood reduction practices in the watershed will likely rely on a mixture of enhanced infiltration and distributed flood storage projects. The use of cover crops enhanced infiltration in this scenario, but to a lesser extent than the previous cover crop scenario or the tall-grass prairie scenario. We assumed an average implementation of cover crops on 50% of the agricultural land, rather than 100%. This is a more realistic expectation for broad implementation of this practice, but it is still extremely ambitious. As with the previous cover crop scenario, this agricultural management practice would involve planting cover crops during the dormant season in an effort to improve soil quality and infiltration during the growing season. Changes in soil infiltration properties would take many years to be fully realized.

We achieved implementation of cover crops in the HMS model by modifying the CN using values provided in Table 4.1. To represent cover crops on 50% of the agricultural land, we assigned each subbasin a CN corresponding to the average of the CNs from the baseline simulation (existing agricultural landscape) and the cover crop simulation of section 4b (all agricultural area improved because of cover crops).

Implementation of distributed flood storage projects remained the same as in section 4c, with all aggregated potential ACPF NRW sites included in the model.

Six-Inch, 24-Hour SCS Design Storm

We ran the HMS model with ponds and implementation of cover crops on 50% of agricultural areas to simulate the effects of enhanced filtration and flood storage on peak discharges. Each simulation started with all pond water levels at the primary spillway elevation; this assumes that the permanent storage is full as the storm begins. Comparisons were then made for the simulated discharges without improvements in place (the existing baseline condition).

Figure 4.12 (left) shows the percent reduction in subbasin peak discharge with cover crops and ponds in place for the 6-inch, 24-hour SCS Design Storm. Reductions in subbasin peak discharges were 4–6% across the whole watershed, with an additional basin-averaged 0.13 inches of rainfall infiltrated as a result of cover crop utilization. Figure 4.12 (right) shows the percent reduction in peak discharge at model junction locations. Application of this design storm assumes that a 6-inch rainfall occurs everywhere within the watershed simultaneously and produces unrealistic peak discharges at junction locations with relatively large drainage area, therefore, results are not shown at junctions with drainage area greater than 100 mi^2.

Like the ponds-only simulation, upland locations with more drainage area intercepted by ponds had the greatest reductions in peak discharge.

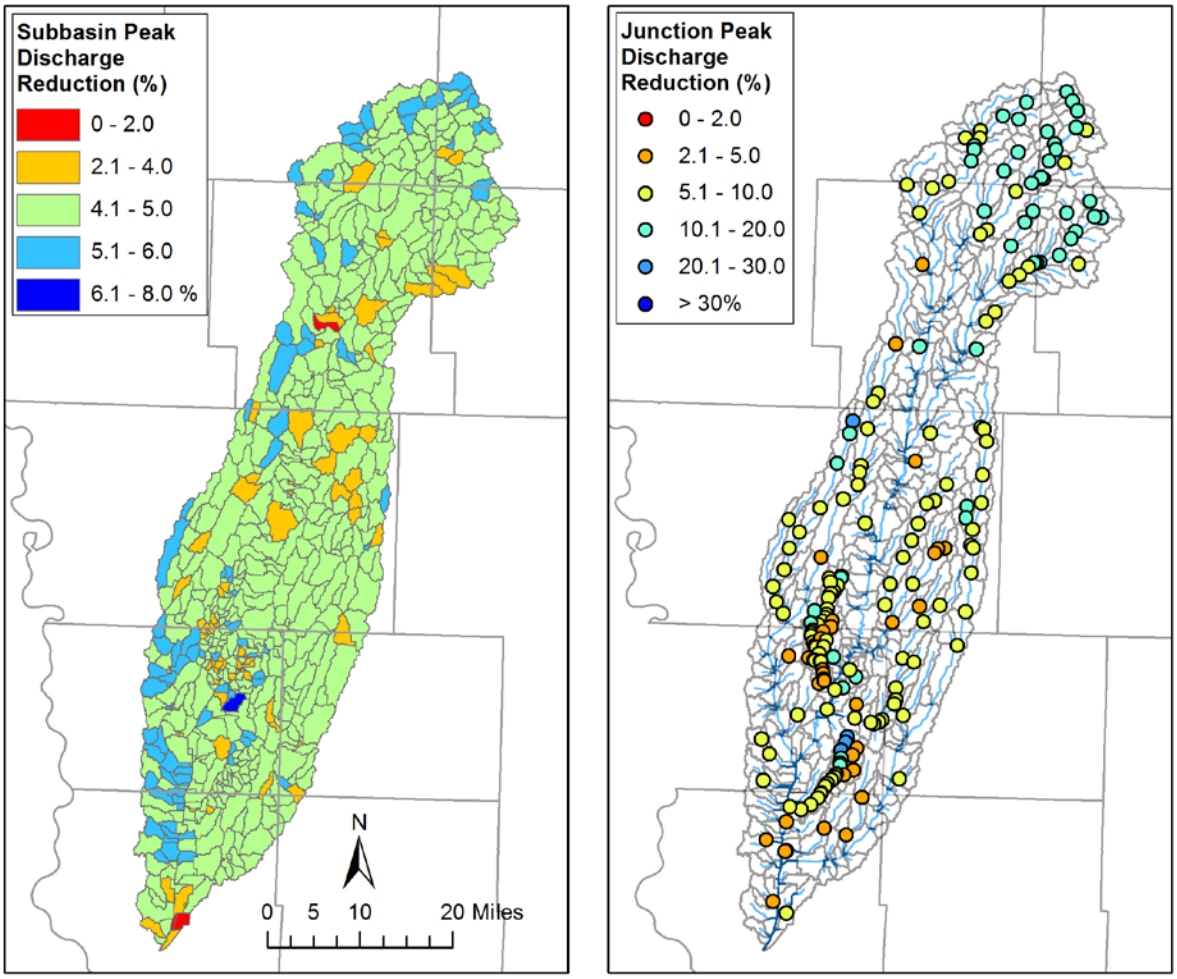

Figure 4.12. Peak discharge reductions for subbasins (left) and junctions (right) with ACPF ponds in place and improved soil infiltration following many years of 50% utilization of cover crops for a 6-inch, 24-hour SCS Design Storm. Simulation results at junctions with large drainage area are not realistic for this design storm event, therefore, results are not shown at junctions with drainage area greater than 100 mi^2.

e. Comparison of Watershed Scenarios for Historic Storm Events

In addition to the design storm event, we compared watershed scenarios through simulation of several historic storm events. Simulations of these historic events are more relevant to people than a design storm, and many likely remember the consequences of some of these events. In this section, we describe the differences in simulation results at the model index locations, shown in Figure 4.10.

May 4–10, 2007, Storm Event

Figure 4.13 (top left) shows the cumulative rainfall from May 4 to May 10, 2007. The largest cumulative rainfall, totaling more than 6 inches, occurred primarily along the east and western portions of the watershed. Figure 4.13 (top right) shows the peak discharge reductions at model junction points with improved soil infiltration following many years of 100% utilization of cover crops during the dormant season for all row crop agriculture. As expected, cover crops result in large, broad-scale reductions in peak discharge. An additional basin-averaged 0.3 inches of rainfall infiltrated as a result of cover crop use. The largest discharge reductions occurred in the northeastern portion of the watershed. Peak discharge reductions along the main stem of the West Nishnabotna River were approximately 5–10%.

Figure 4.13 (bottom left) shows peak discharge reductions at model junctions with distributed storage ponds in place. Similar to the design storm, the largest peak discharge reductions of 5–10% occur in the northern portion of the watershed. While this area has the highest concentration of ponds, there was also relatively less rainfall in the northern half of the watershed. Reductions decrease as the drainage area ratio controlled by storage ponds decreases. This is evident along the main stem of the West Nishnabotna River near Randolph and Riverton, where reductions were less than 2%.

Figure 4.13 (bottom right) shows peak discharge reductions at model junctions with 50% utilization of cover crops and all distributed storage ponds in place. As expected, improving soil infiltration on 50% of agricultural land using cover cops provides broad benefits. An additional basin-averaged 0.15 inches of rainfall infiltrated as a result of cover crop use. Peak discharge reductions ranged from 5–20% throughout much of the watershed. The lowest discharge reductions ranged from 2–5% along the main stem of the West Nishnabotna River near Randolph and Riverton.

Figure 4.14 shows a time series of simulated discharge at each of the model index locations. Percent reductions in peak discharge at model index locations are shown in Figure 4.15. Reductions in peak discharge were converted to stage reductions using rating curves provided by USGS and Iowa's Statewide Floodplain Mapping Project. Stage reductions at each location are shown in Figure 4.16. Some locations may have a large reduction in peak discharge but negligible stage reduction due to simulated low flow conditions or the particular relationship between depth and flow at the location.

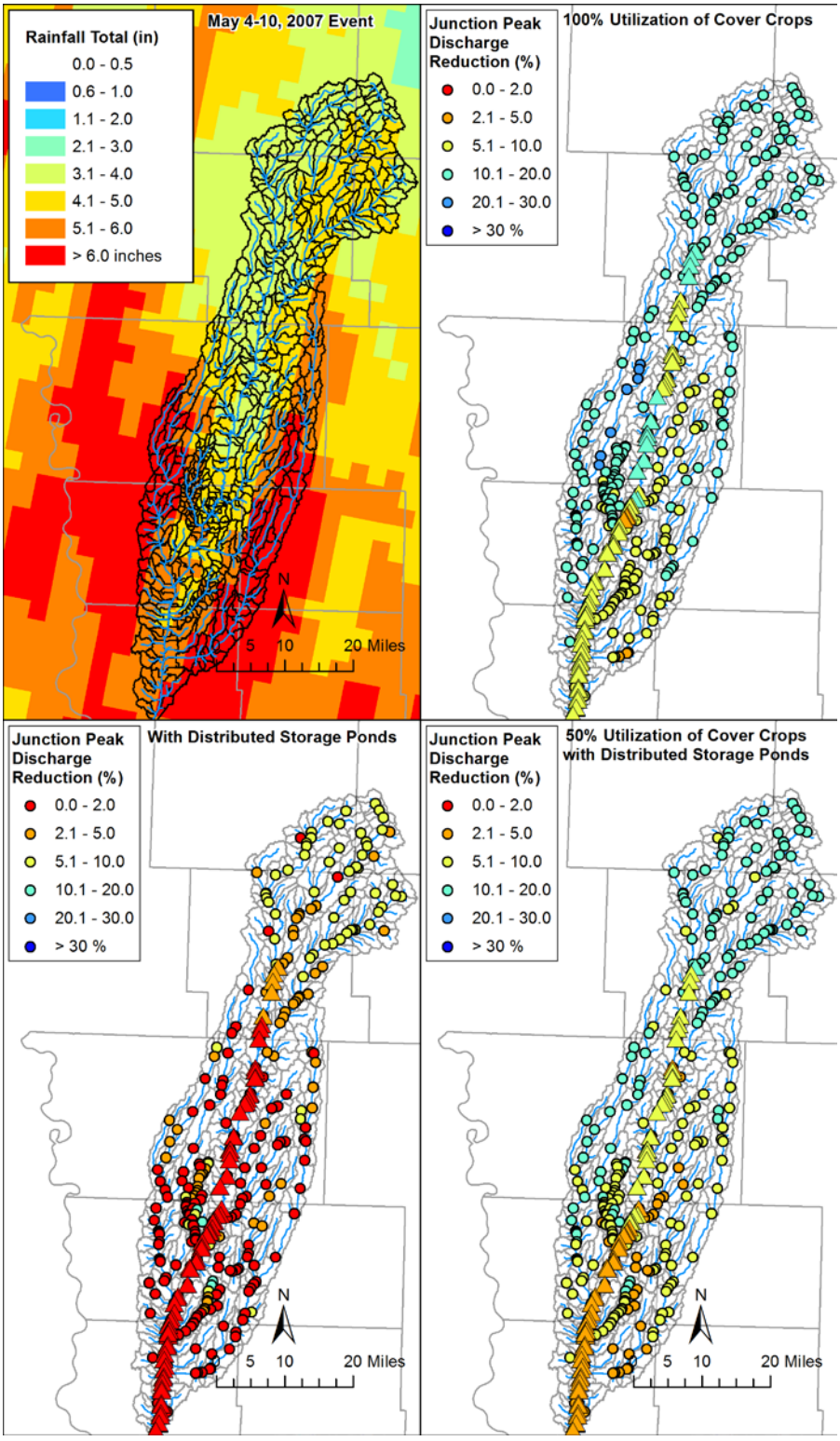

Figure 4.13. Rainfall totals for the period May 4–10, 2007 (top left), and junction peak discharge reductions (top right) with 100% utilization of cover crops, (bottom left) ACPF ponds in place, and (bottom right) 50% use of cover crops with ACPF ponds in place for the May 2007 event. Junction points along the main stream are denoted by triangles.

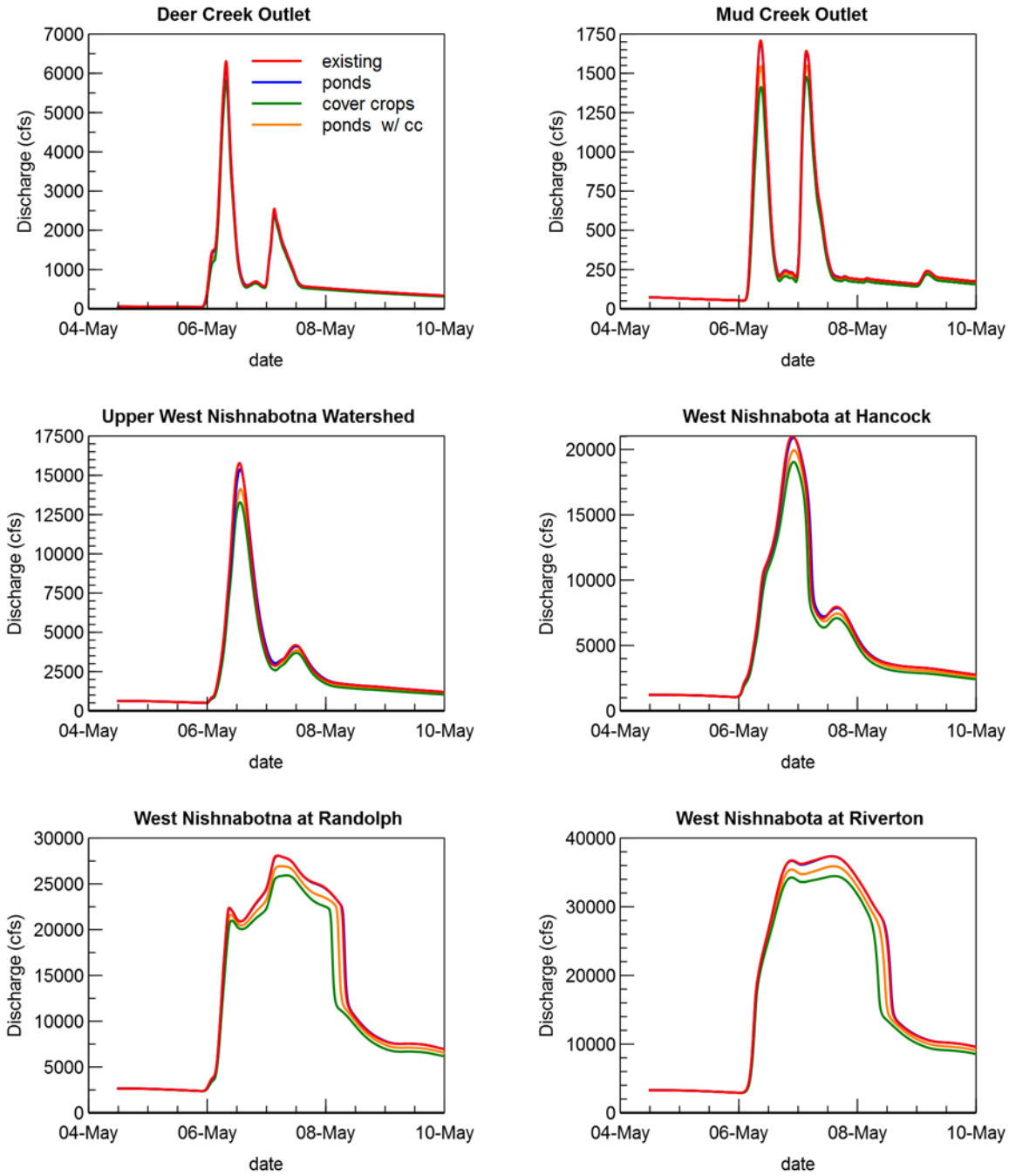

Figure 4.14. Hydrograph comparisons – with ACPF ponds, with 100% utilization of cover crops, and a combination of ACPF ponds and 50% utilization of cover crops for the May 2007 event.

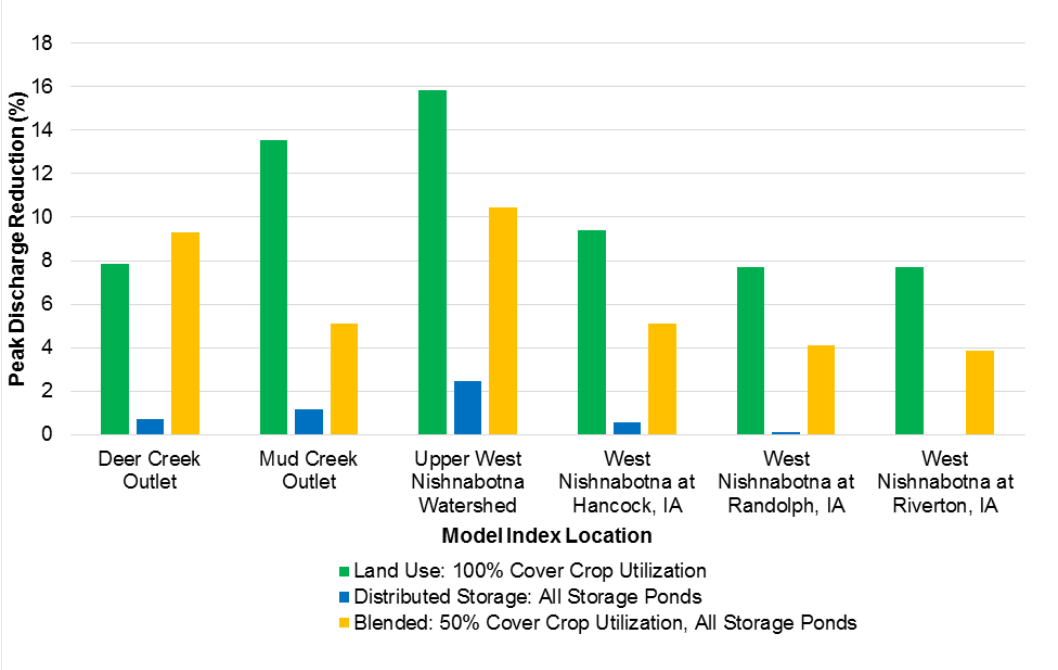

Figure 4.15. Percent reduction in peak discharge at model index locations with implementation of each watershed scenario for the May 2007 event.

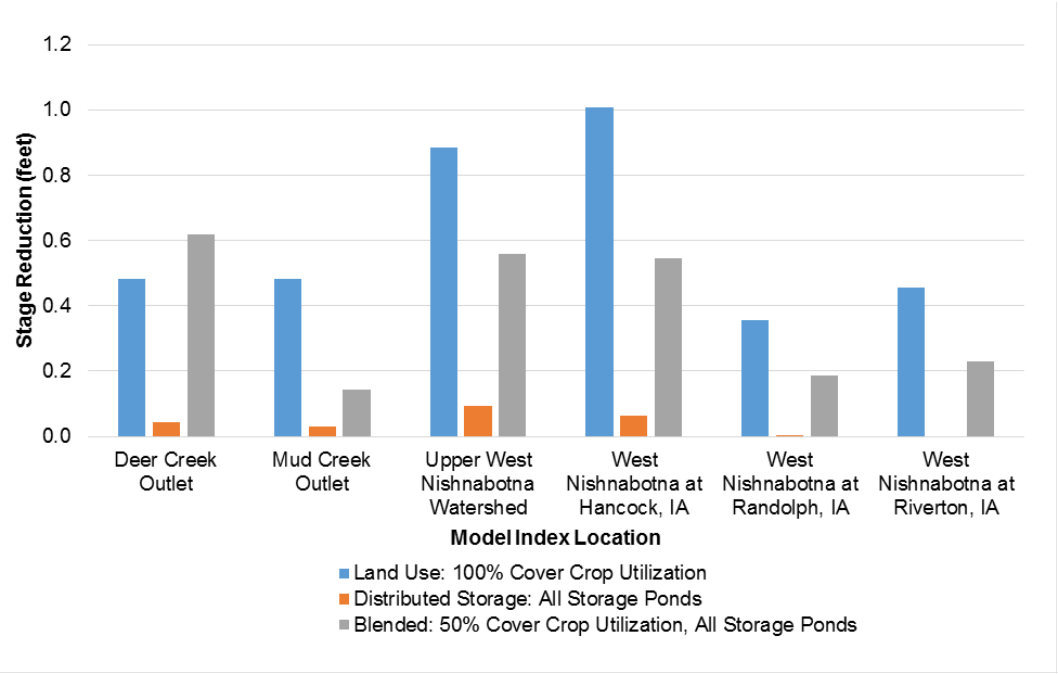

Figure 4.16. Reduction in stage at model index locations with implementation of each watershed scenario for the May 2007 event.

June 10–14, 2008, Storm Event

Figure 4.16 (top left) shows the cumulative rainfall from June 10 to June 14, 2008. This particular rainfall occurred when the soil was already saturated. The largest cumulative rainfall, totaling 3–5 inches, occurred in the center of the watershed. Figure 4.16 (top right) shows the peak discharge reductions at model junction points with improved soil infiltration following many years of 100% utilization of cover crops during the dormant season for all row crop agriculture. An additional basin-averaged 0.23 inches of rainfall infiltrated as a result of cover crop use. Once again, cover crops resulted in large, broad-scale reductions in peak discharge. The largest discharge reductions occurred in the northern portion of the watershed. Peak discharge reductions along the main stem of the West Nishnabotna River were approximately 5–20%.

Figure 4.16 (bottom left) shows peak discharge reductions at model junctions with distributed storage ponds in place. The largest peak discharge reductions of 5–20% occur in the northern portion of the watershed, where pond density is highest, and more storage is available to intercept drainage area and store excess runoff. Similar to previous simulations, reductions decrease as the drainage area ratio controlled by storage ponds decreases. Flow reductions along the lower reach of the West Nishnabotna River (i.e., Randolph and Riverton) were less than 2%. Some junction locations in the watershed experienced an increase in peak discharges due to timing effects of the ponds.

Figure 4.16 (bottom right) shows peak discharge reductions at model junctions with 50% utilization of cover crops and all distributed storage ponds in place. An additional basin-averaged 0.1 inches of rainfall infiltrated as a result of cover crop use. Broad-scale reductions in peak discharge are the result of cover crop utilization. Peak discharge reductions ranged from 5–30% throughout the entire watershed. The lowest discharge reductions ranged from 2–10% along the main stem of the West Nishnabotna River near Randolph and Riverton.

Figure 4.17 shows a time series of simulated discharge at each of the model index locations. Percent reductions in peak discharge at model index locations are shown in Figure 4.18. Stage reductions at each location are shown in Figure 4.20.

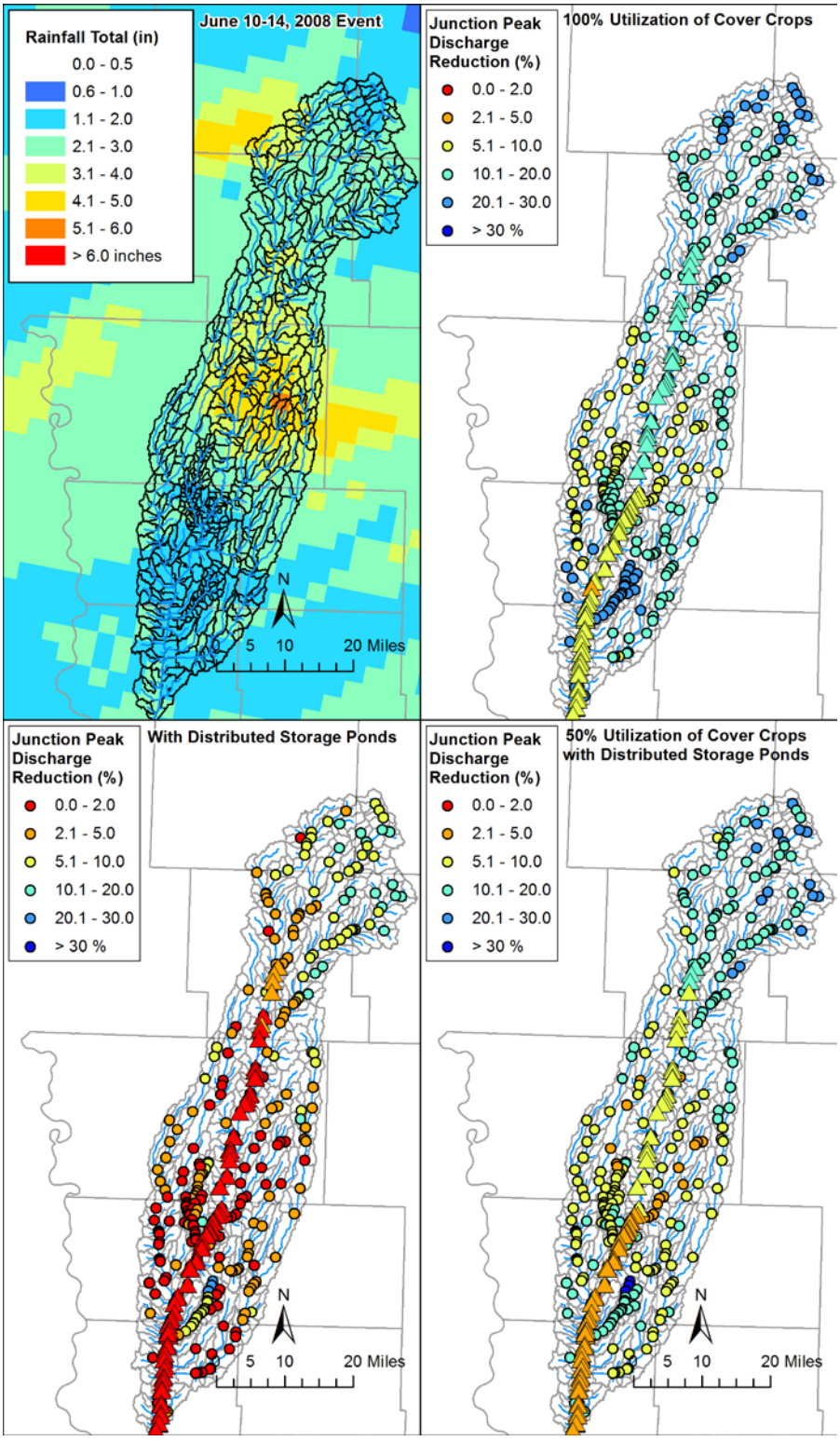

Figure 4.17. Rainfall totals for the period June 10–14, 2008 (top left), and junction peak discharge reductions (top right) with 100% utilization of cover crops, (bottom left) ACPF ponds in place, and (bottom right) 50% utilization of cover crops with ACPF ponds in place for the May 2007 event. Junction points along the main stream are denoted by triangles.

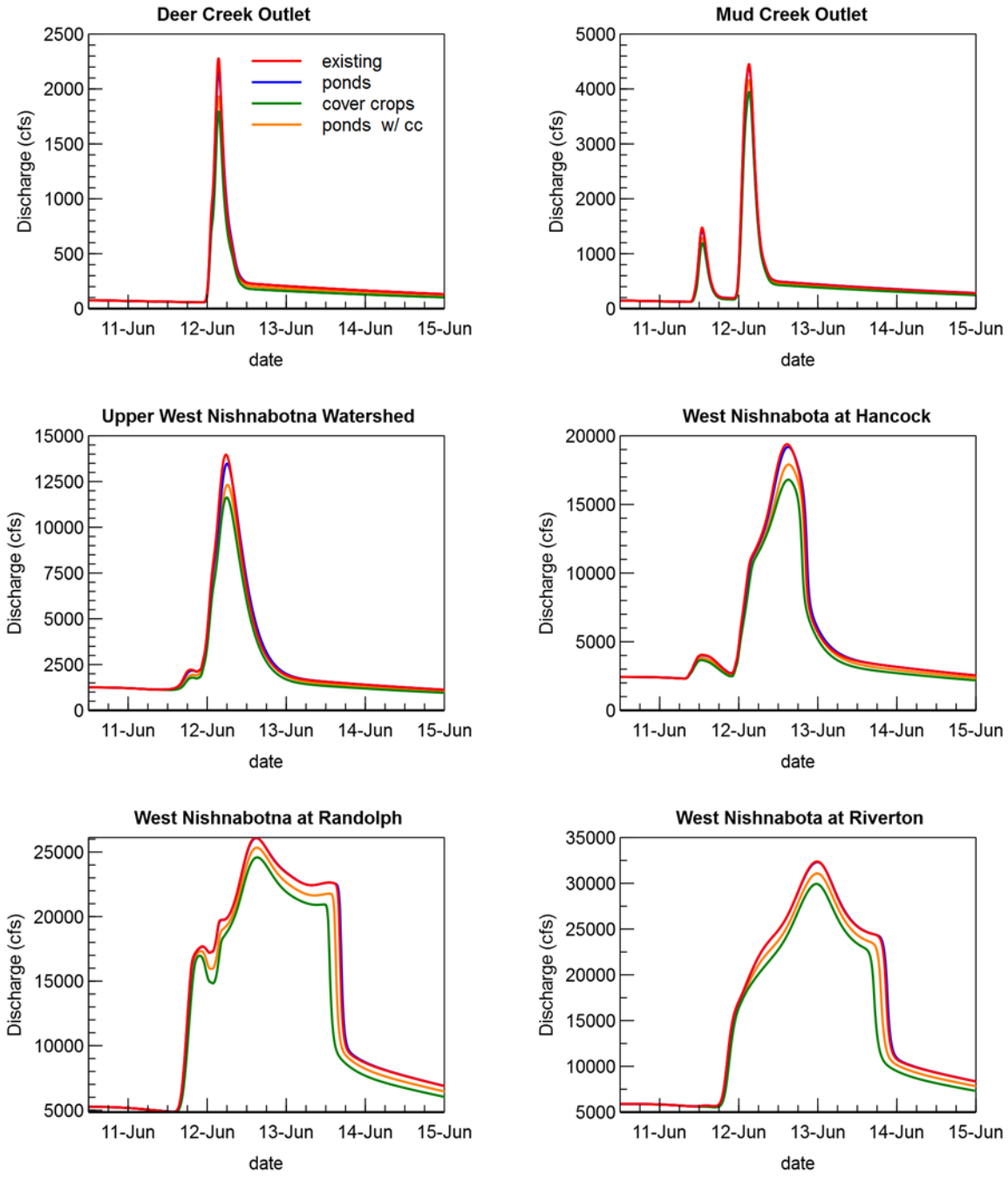

Figure 4.18. Hydrograph comparisons – with ACPF ponds, with 100% utilization of cover crops, and a combination of ACPF ponds and 50% use of cover crops for the June 2008 event.

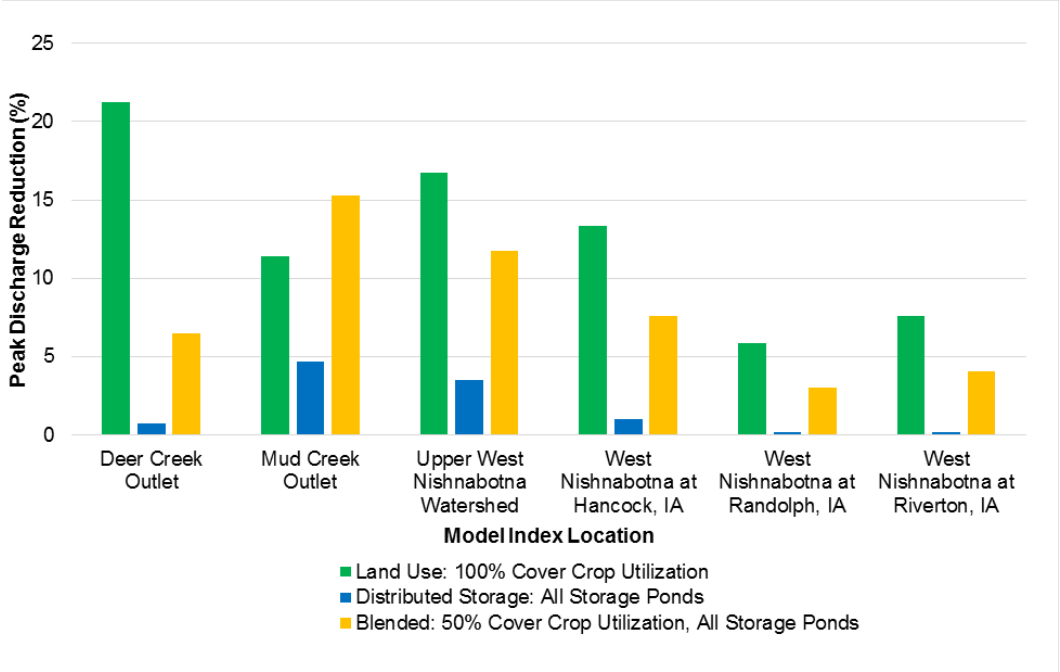

Figure 4.19. Percent reduction in peak discharge at model index locations with implementation of each watershed scenario for the June 2008 event.

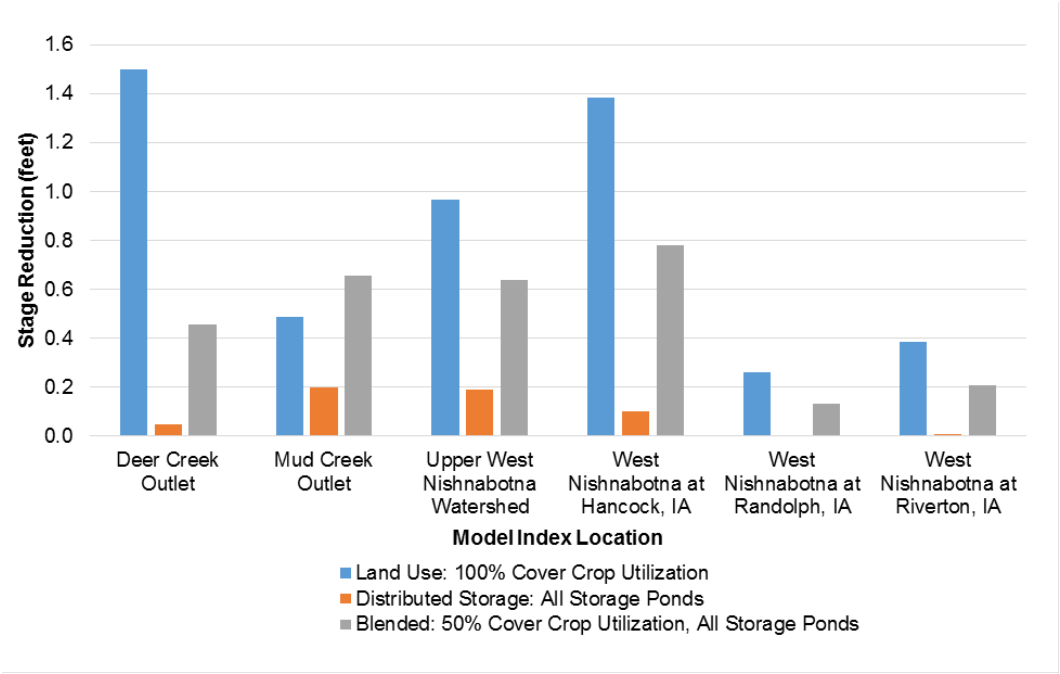

Figure 4.20. Reduction in stage at model index locations with implementation of each watershed scenario for the June 2008 event.

June 3–5, 2014, Storm Event

Figure 4.19 (top left) shows the cumulative rainfall from June 3 to June 5, 2014. Most of the watershed experienced cumulative rainfall totals of 2–3 inches, occurring primarily in the southern half of the watershed. The northernmost portion of the watershed received 1–2 inches of rain and generated little runoff. Figure 4.19 (top right) shows the peak discharge reductions at model junction points with improved soil infiltration following many years of 100% utilization of cover crops during the dormant season for all row crop agriculture. An additional basin-averaged 0.1 inches of rainfall infiltrated as a result of cover crop use. Once again, cover crops result in large, broad-scale reductions in peak discharge. The largest discharge reductions of around 50% occurred in the northernmost portion of the watershed, likely due to the small rainfall totals. Peak discharge reductions along the main stem of the West Nishnabotna River were approximately 10–20%.

Figure 4.19 (bottom left) shows peak discharge reductions at model junctions with distributed storage ponds in place. The largest peak discharge reductions of 5–20% occur in the northern portion of the watershed, where pond density is highest, and more storage is available to intercept drainage area and store excess runoff. The magnitude of the peak discharge reductions in this area were likely also a result of the small rainfall totals. Similar to previous simulations, reductions decrease as the drainage area ratio controlled by storage ponds decreases. Flow reductions along the lower reach of the West Nishnabotna River were less than 2%.

Figure 4.19 (bottom right) shows peak discharge reductions at model junctions with 50% utilization of cover crops and all distributed storage ponds in place. An additional basin-averaged 0.05 inches of rainfall infiltrated as a result of cover crop use. Broad-scale reductions in peak discharge are the result of cover crop utilization. The largest discharge reductions of around 50% occurred in the northernmost portion of the watershed, likely due to the small rainfall totals. The lowest discharge reductions ranged from 5–10% along the main stem of the West Nishnabotna River near Randolph and Riverton.

Figure 4.20 shows a time series of simulated discharge at each of the model index locations. Percent reductions in peak discharge at model index locations are shown in Figure 4.21. Stage reductions at each location are shown in Figure 4.24.

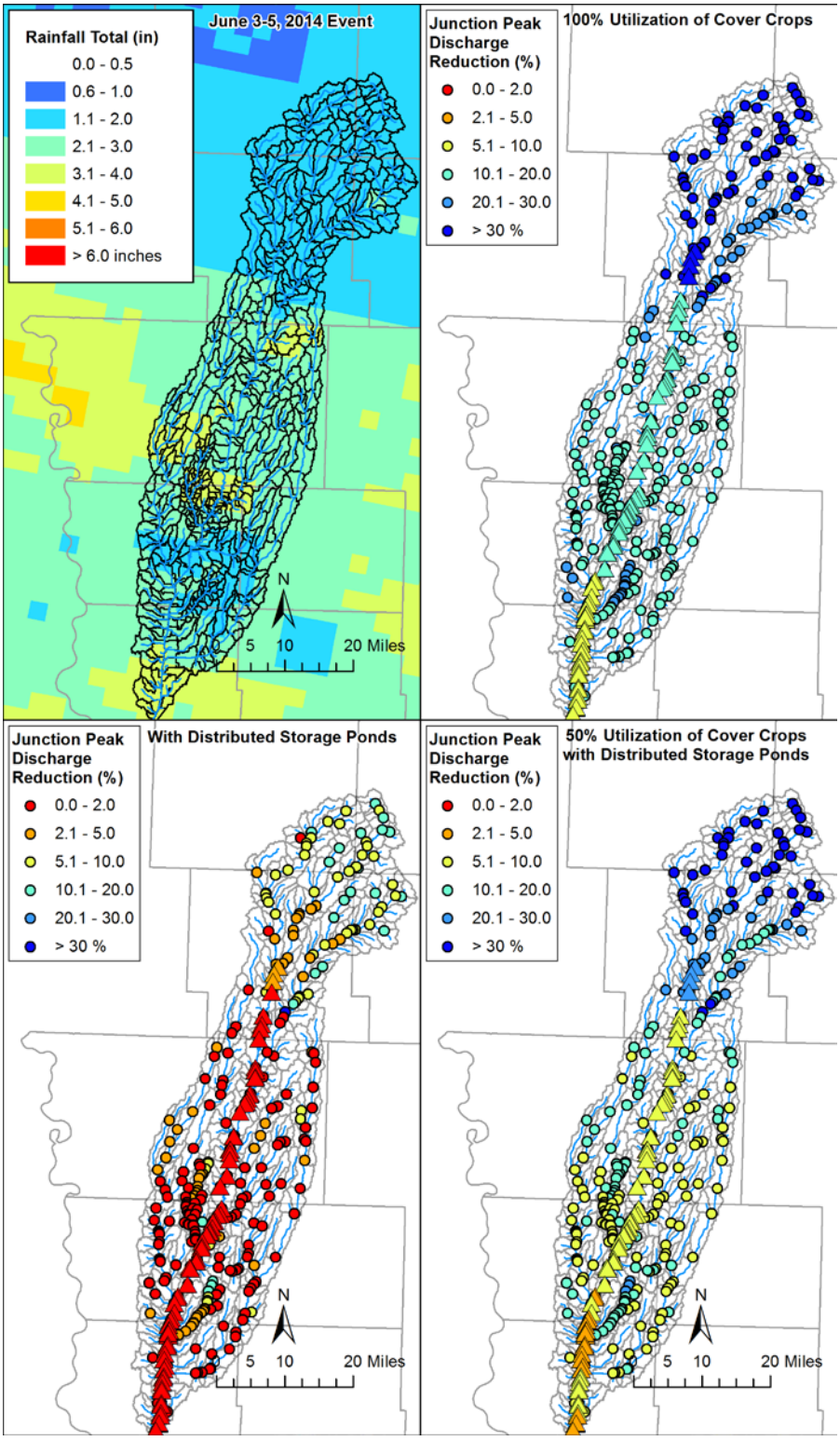

Figure 4.21. Rainfall totals for the period June 29–30, 2014 (top left), and junction peak discharge reductions with 100% utilization of cover crops (top right), ACPF ponds in place (bottom left), and 50% use of cover crops with ACPF ponds in place (bottom right) for the June 2014 event. Junctions with zero flow in the base condition are not displayed. Junction points along the main stream are denoted by triangles.

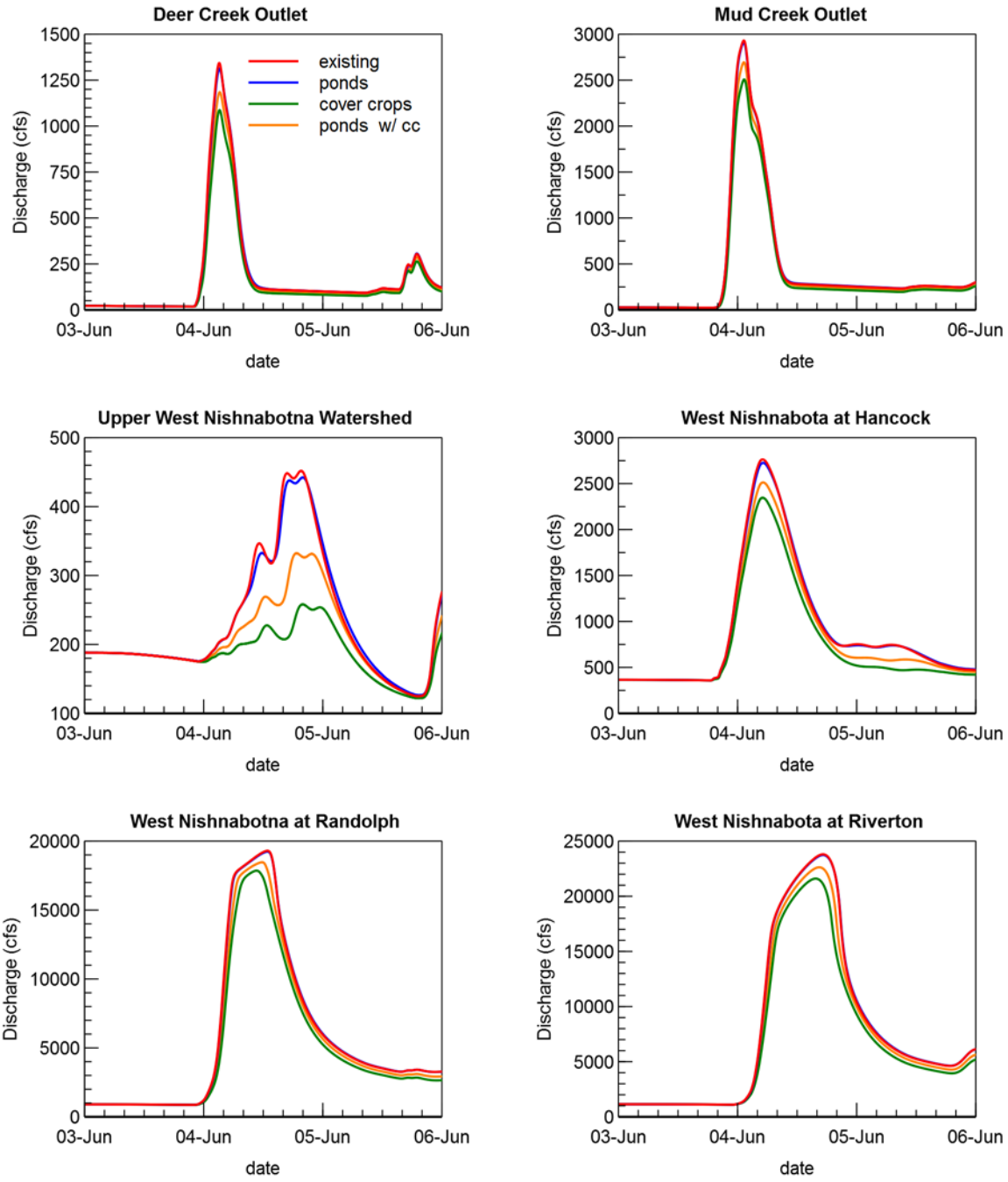

Figure 4.22. Hydrograph comparisons – with ACPF ponds, with 100% utilization of cover crops, and a combination of ACPF ponds and 50% use of cover crops for the June 2014 event.

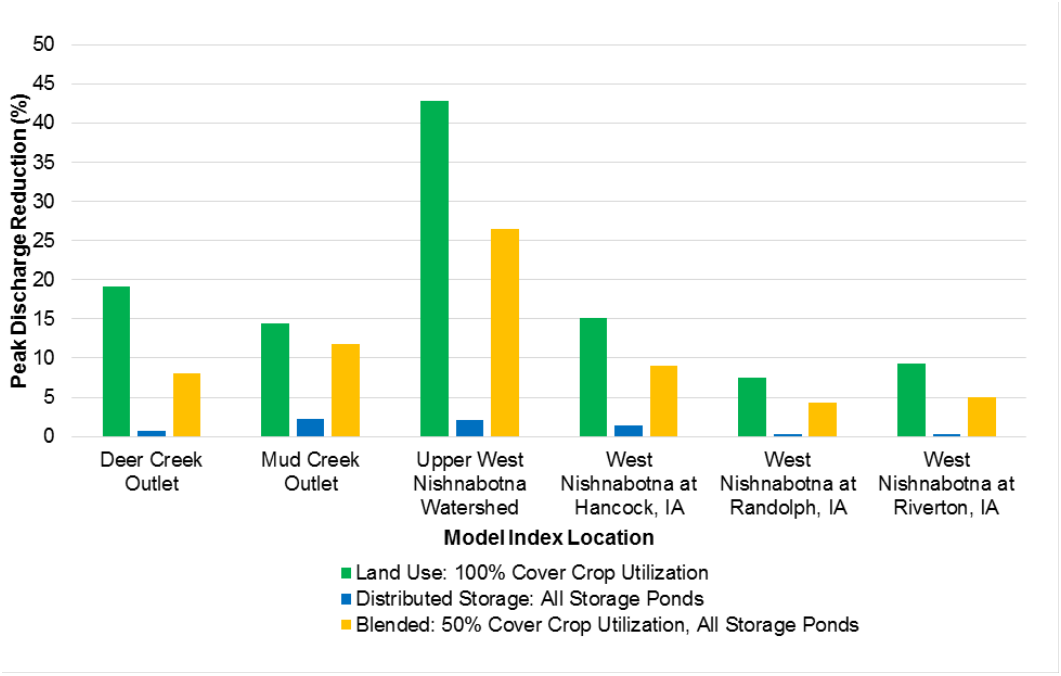

Figure 4.23. Percent reduction in peak discharge at model index locations with implementation of each watershed scenario for the June 2014 event.

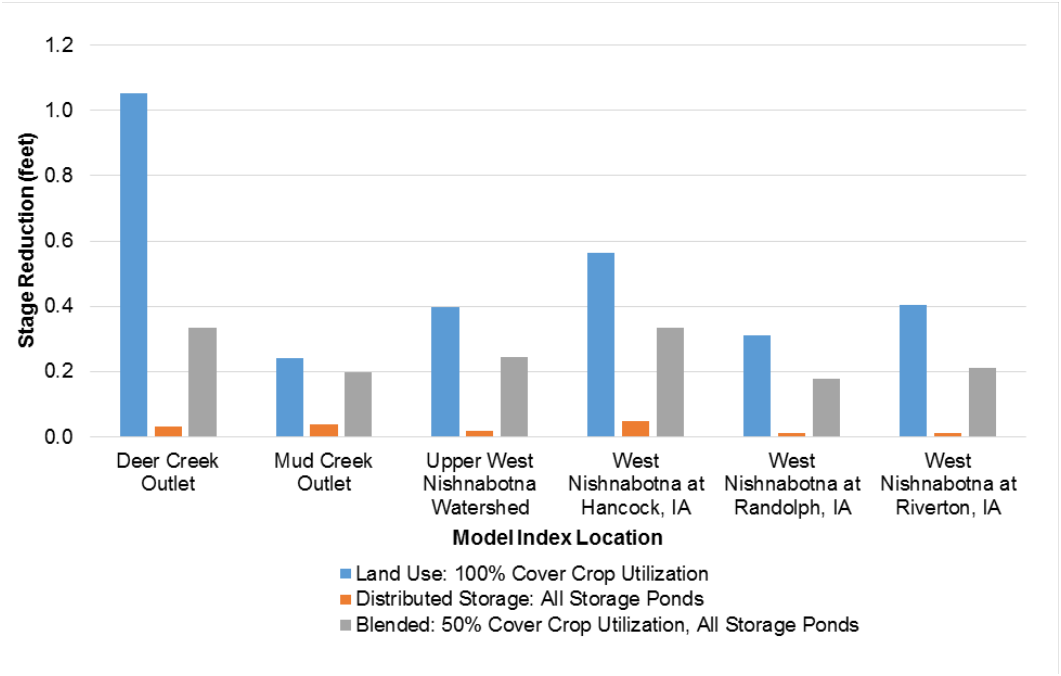

Figure 4.24. Reduction in stage at model index locations with implementation of each watershed scenario for the June 2014 event.

June 14, 2018, Ames, Iowa, Storm Event

Ames, Iowa, experienced significant flash flooding resulting from an intense rainfall event in the early hours of June 14, 2018. Rainfall totaling approximately 4–5 inches occurred over a very short period. This simulation translated the same rainfall event to the central portion of the West Nishnabotna Watershed. Initial conditions for this hypothetical storm event were the same as those used for the SCS design storm.

Figure 4.22 (top left) shows the cumulative rainfall that occurred on June 14, 2018, over Ames, Iowa, translated to the West Nishnabotna Watershed. The largest cumulative rainfall, totaling 4–5 inches, occurred primarily in the middle of the watershed. Subbasins in the northern and southernmost portions of the watershed received little rainfall, 0.5–1.0 inches, during this hypothetical event. Figure 4.22 (top right) shows the peak discharge reductions at model junction points with improved soil infiltration following many years of 100% use of cover crops during the dormant season for all row crop agriculture. An additional basin-averaged 0.15 inches of rainfall infiltrated in areas receiving greater than 0.5 inches as a result of cover crop utilization. Once again, cover crops result in large, broad-scale reductions in peak discharge. The largest discharge reductions occurred in the northern and southernmost portions of the watershed, likely due to the small rainfall totals. The middle of the watershed area, which received greater rainfall, experienced reductions of 10–20%. Peak discharge reductions along the main stem of the West Nishnabotna River were approximately 5–20%.

Figure 4.22 (bottom left) shows peak discharge reductions at model junctions with distributed storage ponds in place. The largest peak discharge reductions of 5–20% occur in the northern portion of the watershed, where pond density is highest, and rainfall totals were smallest. Similar to previous simulations, reductions decrease as the drainage area ratio controlled by storage ponds decreases. Flow reductions along the lower reach of the West Nishnabotna River near Randolph and Riverton were less than 2%.

Figure 4.22 (bottom right) shows peak discharge reductions at model junctions with 50% utilization of cover crops and all distributed storage ponds in place. An additional basin-averaged 0.1 inches of rainfall infiltrated in areas receiving greater than 0.5 inches as a result of cover crop use. Broad-scale reductions in peak discharge are the result of cover crop utilization. The largest discharge reductions of around 50% occurred in the northernmost portion of the watershed, likely due to the small rainfall totals. Peak discharge reductions along the main stem of the West Nishnabotna River were approximately 2–10%.

Figure 4.23 shows a time series of simulated discharge at each of the model index locations. Figure 4.24 shows percent reductions in peak discharge at model index locations. Stage reductions at each location are shown in Figure 4.28.

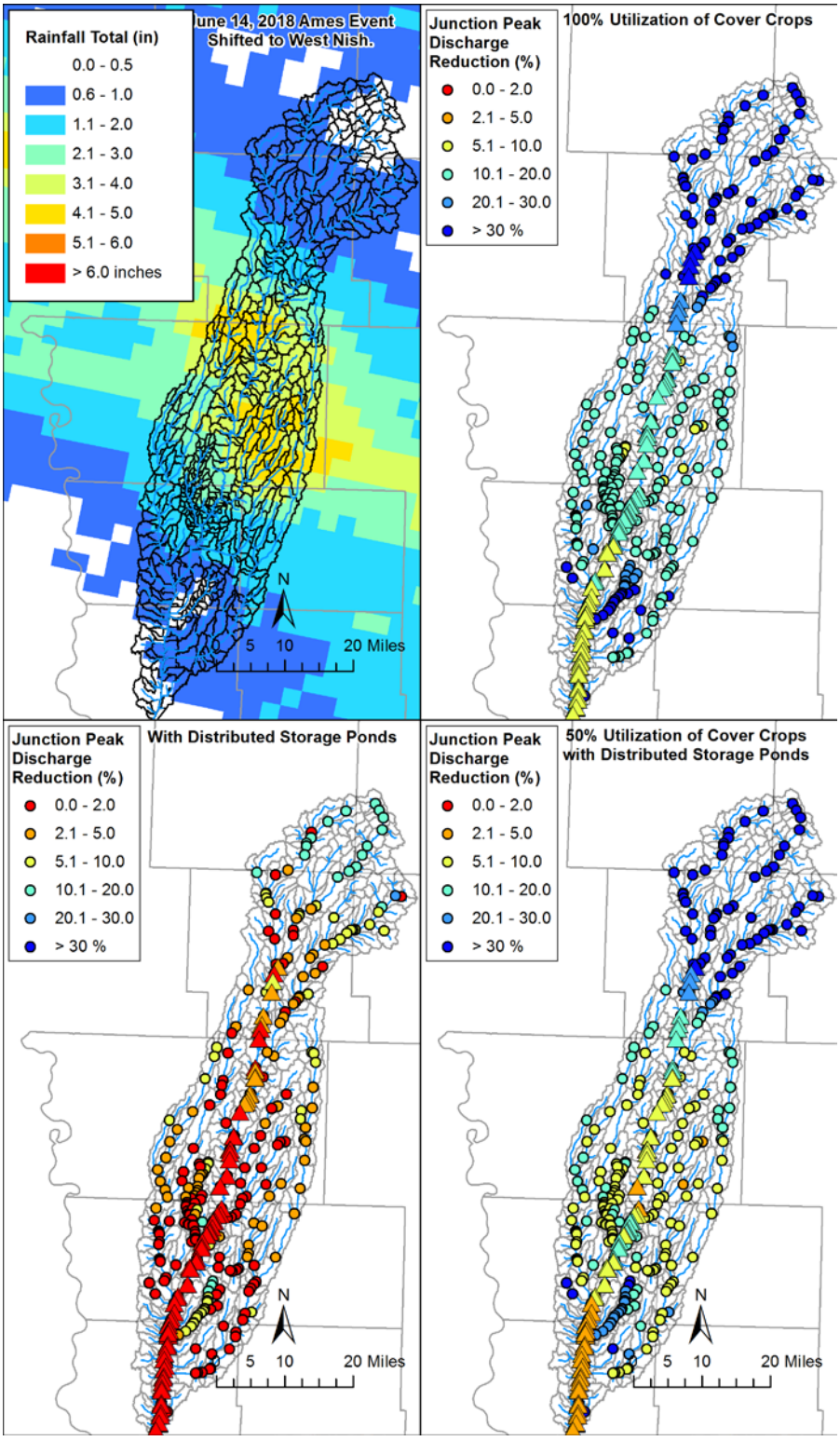

Figure 4.25. Rainfall totals for the translated Ames, Iowa, June 14, 2018, event (top left), and junction peak discharge reductions with 100% utilization of cover crops (top right), ACPF ponds in place (bottom left), and 50% utilization of cover crops with ACPF ponds in place (bottom right) for the Ames, Iowa, June 2018 event. Junctions with zero flow in the base condition are not displayed. Junction points along the main stream are denoted by triangles.

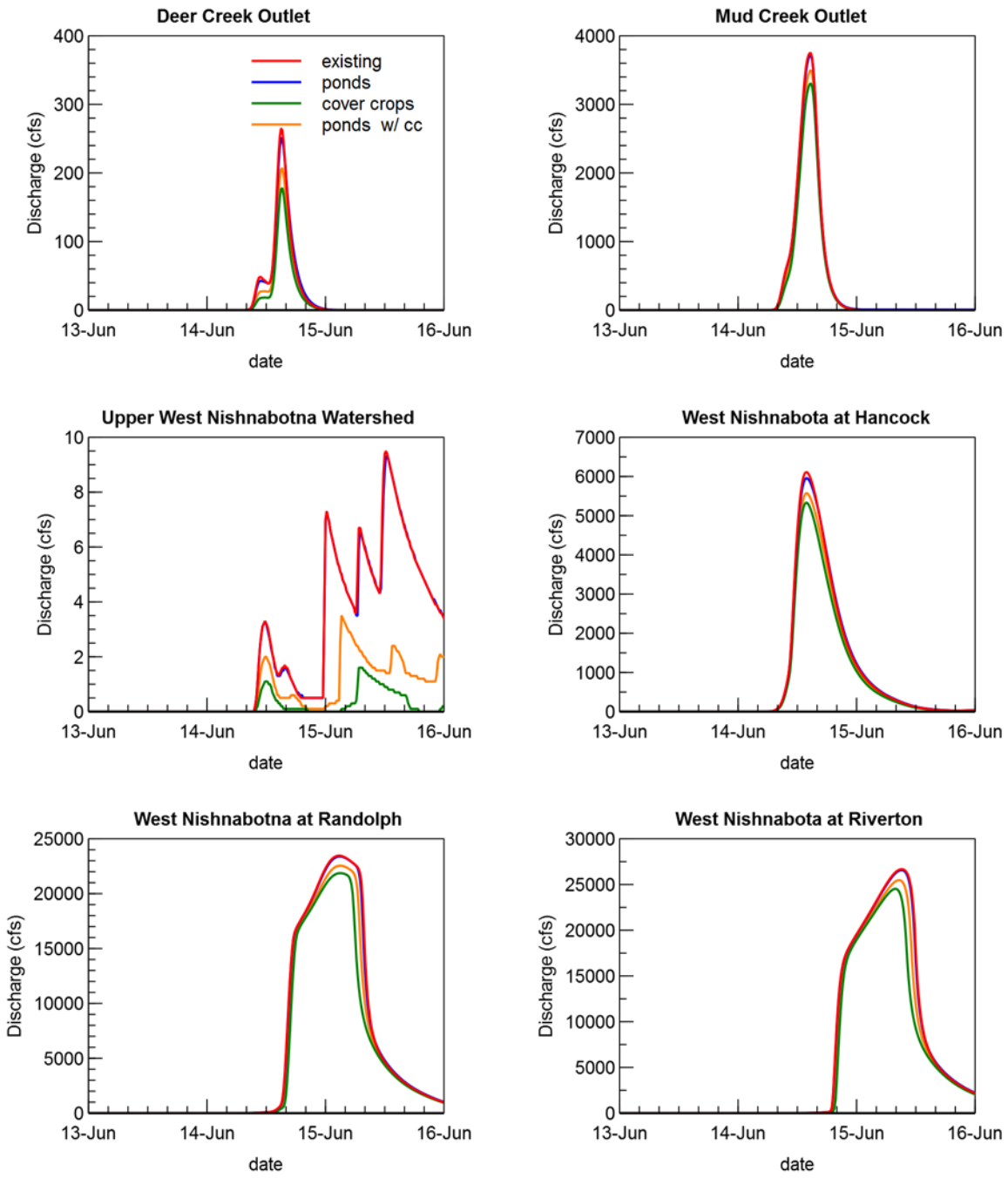

Figure 4.26. Hydrograph comparisons – with ACPF ponds, with 100% utilization of cover crops, and a combination of ACPF ponds and 50% utilization of cover crops for the translated Ames, Iowa, June 2018 event.

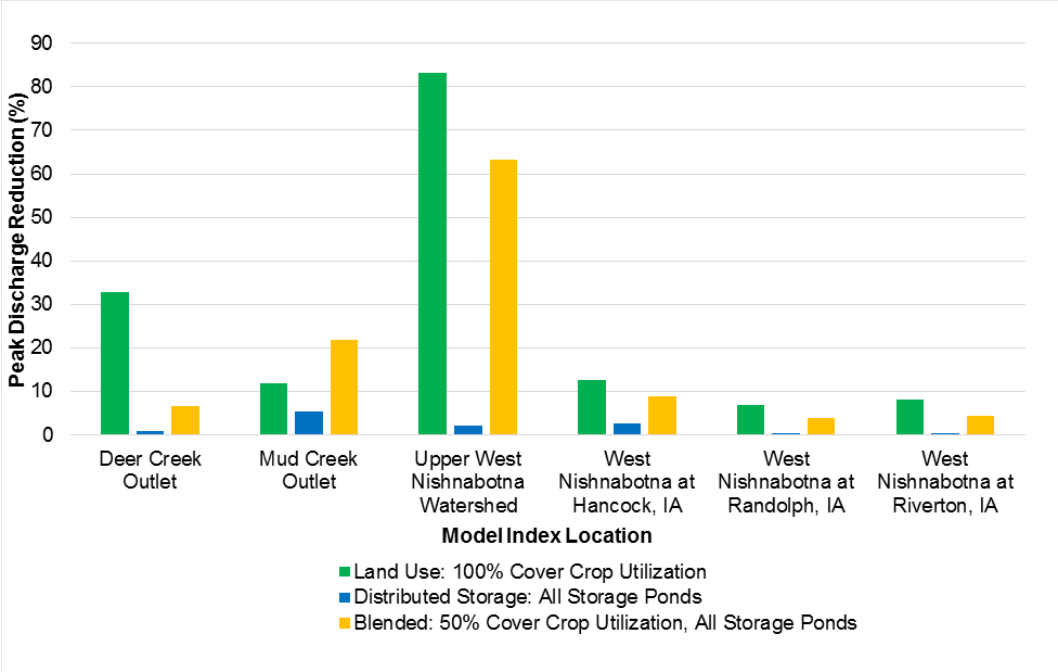

Figure 4.27. Percent reduction in peak discharge at model index locations with implementation of each watershed scenario for the translated Ames, Iowa, June 2018 event.

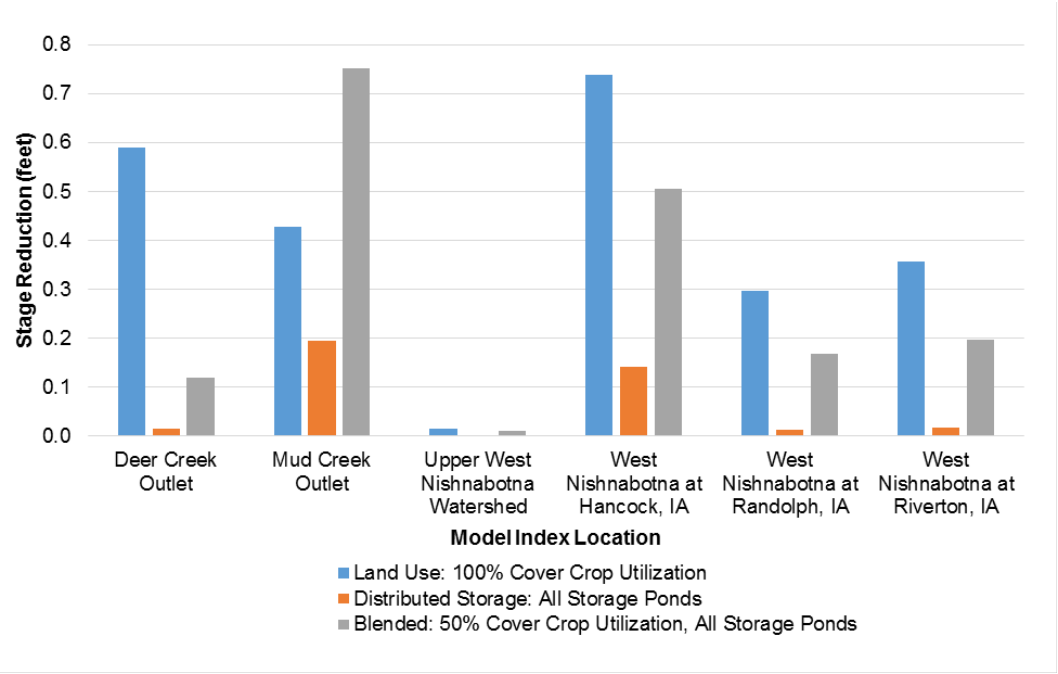

Figure 4.28. Reduction in stage at model index locations with implementation of each watershed scenario for the translated Ames, Iowa, June 2018 event.

A summary of the typical median, low, and high range of peak discharge reductions across all locations and historical events for each scenario is shown in Figure 4.29.

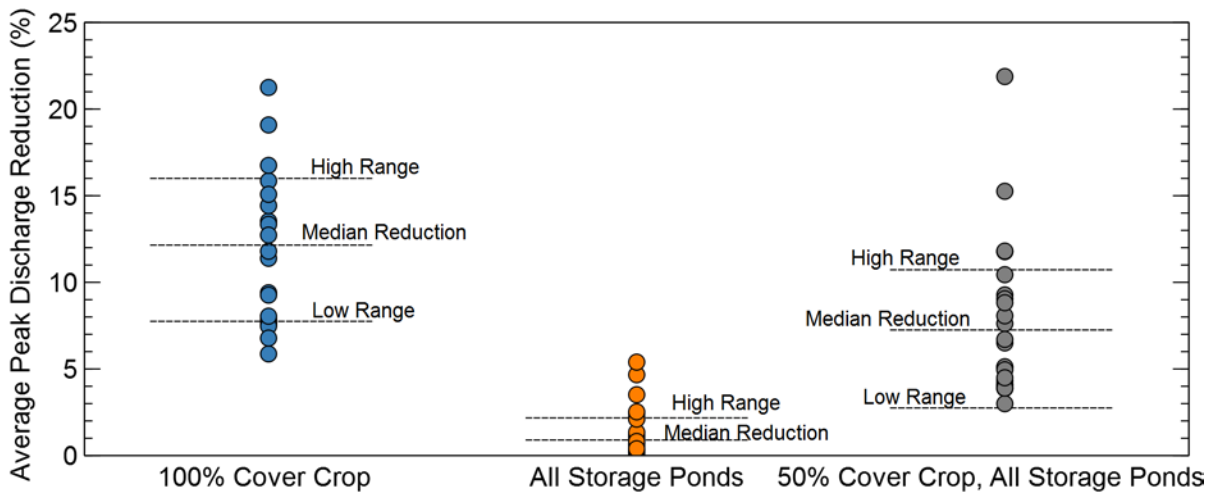

Figure 4.29. Summary of peak discharge reductions across all model index locations and historical events for each scenario.

5. Summary and Conclusions

The West Nishnabotna River Watershed is one of nine distinct Iowa watersheds participating in the IWA program. The program will accomplish six specific goals in each watershed: (1) reduce flood risk; (2) improve water quality; (3) increase flood resilience; (4) engage stakeholders through collaboration and outreach/education; (5) improve quality of life and health, especially for susceptible populations; and (6) develop a program that is scalable and replicable throughout the Midwest and the United States. The purpose of this hydrologic assessment is to provide an understanding of the watershed hydrology in the West Nishnabotna basin and the potential of various hypothetical flood mitigation strategies that may be leveraged to accomplish goals of the IWA.

a. West Nishnabotna River Water Cycle and Watershed Conditions

We examined the water cycle of the West Nishnabotna River Watershed using historical precipitation and streamflow records. The average annual precipitation for the West Nishnabotna River Watershed is 34.0 inches. Of this precipitation amount, 79% (27.0 inches) evaporates back into the atmosphere and the remaining 21% (7.0 inches) runs off the landscape into the streams and rivers. Most of the runoff amount is baseflow (70%, or 5.0 inches), and the rest is surface flow (30%, or 2.0 inches). Average monthly streamflow peaks in June and decreases slowly through the summer growing season. In most years, the largest discharge observed during the year occurs in May or June, associated with heavy spring/summer rainfall events.

The water cycle has changed because of land use and climate changes. The largest change occurred in the late 1800s when the landscape was transformed from low-runoff prairie and forest to higher-runoff farmland. Since the 1970s, Iowa precipitation has increased in quantity, while intense rain events have changed in timing and frequency. Streamflow records in Iowa (including those for the West Nishnabotna River) suggest that average flows, low flows, and perhaps high flows have all increased and become more variable since the late 1960s or 1970s; however, the relative contributions of land use and climate changes are difficult to sort out.

The majority of the West Nishnabotna River Watershed lies in the Southern Iowa Drift Plain landform region and has well developed drainage divides. Much of the watershed has soils with moderately high runoff potential. The terrain is characterized by numerous steeply rolling hills and valleys. Typical land slopes are between 0.4 and 8.0% (25th and 75th percentiles), with the steepest areas occurring in uplands in the northern portion of the watershed. The land use is predominantly row crop agriculture, accounting for 77% of the area. Storms in recent decades have produced record flood levels at stream gauges in May 1987, July 1993, and June 2014.

b. West Nishnabotna River Hydrologic Model

We used the U.S. Army Corps of Engineers' (USACE) Hydrologic Engineering Center's Hydrologic Modeling System (HEC-HMS) to develop a flood prediction model for the West Nishnabotna River Watershed. First, we divided the watershed into 614 smaller units, called subbasins, with an average area of 2.7 square miles. For model calibration and validation with actual (historical) rainfall events, we used radar rainfall estimates as the precipitation input for each simulation. For

the analysis of watershed scenarios, a 24-hour duration SCS Design Storm with rainfall accumulations approximately equal to the 25-year return period was used to drive the watershed response. We used several historical storm events to evaluate the relative difference between watershed scenario simulations.

The NRCS Curve Number (CN) methodology was used to determine rainfall-runoff partitioning in the West Nishnabotna River Watershed HMS model. The CN methodology accounts for precipitation losses due to initial abstractions and infiltration during the rainstorm. CN value estimates are based on land use and the underlying soil type, and the area-weighted average CN was assigned to each subbasin as an initial parameter estimate. We used the Clark and ModClark Unit Hydrograph methods to convert excess precipitation to a direct runoff hydrograph for each subbasin. Baseflow was simulated for model calibration and validation with actual (historical) rainfall events but was not simulated during the design storm. We accomplished conveyance of runoff through the river network, or flood wave routing, using Muskingum-Cunge routing methods for major streams and Muskingum routing methods for smaller tributaries. Flow routing through Lake Anita was executed using level pool routing.

Model calibration adjusts the initial set of model parameters, so the simulated results more closely match observed discharges at gauging stations for historical events. We calibrated the West Nishnabotna River Watershed HEC-HMS model with three storm events that occurred in April 2007, June 2008, and June 2014 (significant events for which radar rainfall estimates were available). After calibration of model parameters, model validation assesses the predictive capability of the model to simulate discharge for other storm events (not used in calibration). We considered five storms for model validation. The model generated runoff volume, hydrograph shape, and peak flow timing very similar to the observed streamflow hydrographs for validation events.

c. Watershed Scenarios for the West Nishnabotna River

The HEC-HMS model was used to better understand the flood hydrology of the West Nishnabotna River watershed and to evaluate potential flood mitigation strategies. We first assessed the runoff potential throughout the watershed using the HMS model's representation of storm runoff generated from a design storm. Agricultural lands and moderately to poorly drained soils had the highest runoff potential. Reducing runoff for these high runoff potential areas should be a priority and would likely have the greatest benefit-to-cost ratio. It is worth noting that other land uses – particularly urban development – likely have the highest runoff potential. However, the footprint of these areas is small compared to the agricultural areas that dominate the watershed. In urban areas, local drainage issues could be improved by more effectively capturing and storing storm water (e.g., storm water detention and low-impact development practices).

We used the HEC-HMS model to quantify potential effects of flood mitigation strategies applied throughout the West Nishnabotna River Watershed. Several flood mitigation strategies were considered — enhancing local infiltration through changes in land use (from agricultural to native tall-grass prairie), enhancing local infiltration through improvements in soil quality through the

use of cover crops, and storing floodwaters temporarily in ponds throughout the watershed to reduce downstream discharges. We also considered a blended scenario using cover crops and storage ponds. The effects of these strategies were simulated for a 6-inch, 24-hour SCS Design Storm, occurring simultaneously over the entire watershed, and also for several historical rainfall events. We compared the results of these strategies to simulations of flows for the existing watershed condition. Although each scenario simulated is hypothetical and simplified, the results provide valuable insights on the relative performance of each strategy for flood mitigation planning.

There are many BMP practices not investigated in this report that could potentially increase infiltration or runoff storage at the watershed scale. However, our analysis was limited by the resolution and capability of the HEC-HMS model to simulate effects of BMP practices aggregated across subbasin areas of several square miles. Therefore, we limited our investigations to distributed storage provided by ponds, which are relatively large BMP structures, and broad-scale land cover changes. Simulation of other much smaller BMP structures like terracing or WASCOBS, while demonstrably effective in this watershed, would require considering many more individual structures to make any impact at the watershed scale, and a much higher degree of model resolution to reliably quantify impacts.

i. Increased Infiltration in the Watershed

Simulation results indicate that enhancements to local infiltration through changes in land use have the most significant impact on runoff. Converting current agricultural areas from row crop to native tall-grass prairie would increase rainfall infiltration by 0.9 inches during large rainfall events. This hypothetical scenario illustrates the dramatic reductions in stream flow as a result of land use change. However, converting the entire agricultural landscape back to pre-settlement tall-grass prairie is not a practical or economically desirable strategy. This scenario provides support for targeted land use changes that could be an effective part of a watershed's flood mitigation efforts.

Agricultural management practices could increase the infiltration of rain water without significantly decreasing agricultural production through the use of cover crops. Cover crop plantings during the dormant season can produce long-lasting improvements in soil quality. From the simulation results, we know that enhancement of local infiltration through soil quality improvement resulting from cover crops has a small but significant effect. The model predicts that adopting cover crop management practices would increase infiltration during large storms by 0.25 inches (for the 6-inch, 24-hour design storm), which is much less infiltration than we see on a tall-grass prairie landscape, but significant nonetheless. Reductions in peak discharge throughout the watershed ranged from 5–20%, depending on the storm event. Given the widespread agricultural land use in the West Nishnabotna Watershed and the growing interest in the use of cover crops as a part of Iowa's nutrient management strategy, cover crops could play an important role as a watershed-wide flood mitigation strategy.

ii. Increased Storage on the Landscape

In some ways, using ponds to temporarily store floodwaters is an attempt to replace the loss of water that was once stored in soils (in the pre-agricultural landscape). In the hypothetical scenarios involving pond storage, 24930 acre-feet of storage was added to the West Nishnabotna River Watershed utilizing 1153 potential ACPF nutrient reduction wetland locations. For the upstream areas draining to ponds, this is equivalent to an added storage depth of 1.5 inches for runoff. However, for the West Nishnabotna River Watershed as a whole (not just the area with ponds), the added storage depth is approximately 0.28 inches. Compared to the extra water that was stored by infiltration in the previous simulated scenarios, the amount of storage replaced by ponds is quite small. As a result, the overall flood peak reduction with storage ponds is less than predicted for the other scenarios. Since there is no additional infiltration, the overall volume of runoff in the watershed is higher than the enhanced filtration scenarios. Still, compared to the other scenarios, the flood storage scenario is realistically more achievable. Ponds can effectively reduce flood peaks immediately downstream of their headwater sites. Reductions in peak discharge throughout the watershed ranged from 0–20%, depending on the storm event. Reductions in peak discharge along the main stem of the West Nishnabotna River were approximately 0-5%. At junctions farther downstream, floodwaters originating from locations throughout the watershed arrive at vastly different times; some areas have ponds, others do not. The result is that the storage effect from ponded areas is spread out over time, instead of being concentrated at the time of highest flows. Hence, at larger drainage areas downstream in the watershed, the flood peak reduction of storage ponds diminishes.

The flood storage ponds were concentrated in the northern portion of the watershed. Siting of these ponds was driven by nutrient reduction criteria, rather than flood control. If flood control was the siting criteria, additional suitable locations could be identified, particularly in the southern portion of the watershed.

iii. Increased Infiltration and Increased Storage: A Blend of Cover Crops and Flood Storage Ponds

Future projects in the West Nishnabotna Watershed will likely use both enhanced infiltration practices and flood storage. We developed a blended scenario using agricultural management with cover crops and flood storage ponds to evaluate the flood mitigation benefits of multiple mitigation strategies. The watershed scenario assumes 50% of agricultural lands would use cover crops to improve soil infiltration. All the flood storage ponds considered in the previous scenario were incorporated. Converting current agricultural areas from row crop to native tall-grass prairie would increase rainfall infiltration by 0.13 inches during large rainfall events. Reductions in peak discharge throughout the watershed ranged from 2–20%, depending on the storm event. Reductions in peak discharge along the main stem of the West Nishnabotna River were approximately 2-10%. Simulation results of the design storm and historical events indicate the use of cover crops would provide much broader benefits than ponds alone and further enhance the ability of ponds to store excess runoff. While this blended scenario is more realistic in the use of multiple mitigation strategies, implementation of cover crops and ponds at this scale would be extremely ambitious and expensive. In addition, improvements in soil infiltration properties would take many years to be fully realized.

d. Concluding Remarks

It is important to recognize that these modeling scenarios evaluate the hydrologic effectiveness of the flood mitigation strategies and not their effectiveness in other ways. For instance, while certain strategies are more effective in terms of hydrology, they may not be as effective economically. As part of the flood mitigation planning process, other factors should be considered in addition to the hydrology, such as the cost and benefits of alternatives, landowner willingness to participate, and more.

Appendix A – Maps

Appendix B – Calibration and Validation

Calibration

This appendix details calibration and validation efforts for the West Nishnabotna River Watershed model. It includes the major calibration measures taken, a summary of the final calibrated model parameters, and results for the calibration and validation historical storms. The research team performed the modeling using the U.S. Army Corps of Engineers' (USACE) Hydrologic Engineering Center's Hydrologic Modeling System (HEC-HMS), Version 4.0.

i. Calibration Measures

We calibrated the West Nishnabotna River Watershed HMS model to three storm events that occurred in late April 2007, June 2008, and June 2014. Researchers selected the storms based on their range of antecedent conditions, magnitude, the time of year, and the availability of Stage IV radar rainfall estimates and United States Geological Survey (USGS) discharge estimates. We selected large, high-runoff storms occurring between late April and September to minimize the impacts of snow, rain on frozen grounds, and freeze-thaw effects that can happen during late fall to early spring. Our team made global adjustments to the model parameters described in Chapter 3 to best match simulated hydrographs to observed discharge time series at each USGS stage/discharge gauge location. We evaluated model performance based on how well several variables resembled the observed hydrograph at a particular USGS gauge location: simulated hydrograph peak discharge, time of peak discharge, total runoff volume, and general shape.

Antecedent Moisture Conditions

Rainfall-runoff partitioning for an area is dependent on the antecedent soil moisture conditions (how wet the soil is) at the time rain falls on the land surface. Wetter soil allows less water to infiltrate into the ground while more rain converts to runoff. Therefore, we needed a methodology to adjust subbasin Curve Numbers (CNs) to reflect the initial soil moisture conditions at the beginning of a storm simulation and to better predict runoff volumes.

Existing NRCS methodology accounts for antecedent soil moisture conditions by classifying CNs into one of three classes: AMC I (dry), AMC II (average or normal), or AMC III (wet), which are statistically defined as the 10th, 50th, and 90th percentiles of runoff depth, respectively (Hjelmfelt, 1982). Equations exist to adjust CNs from the base AMC II condition to either the AMC I or III condition, based on the seasonal five-day antecedent rainfall total prior to the event being simulated. Table B.1 shows the five-day antecedent rainfall totals defining the three AMC CN classes for the growing season developed by the NRCS.

While the NRCS method provides a simple way to adjust CNs to reflect antecedent moisture conditions based on the five-day antecedent rainfall total, it is oversimplified. The five-day antecedent rainfall totals listed in Table B.1 define the AMC classes everywhere, regardless of geographic location or climate. Additionally, the five-day antecedent rainfall total applies equal weight to each of the five days preceding a storm to reflect the soil moisture conditions. Hence, this method treats rain that fell five days before or one day before the event being simulated the

same in determining the appropriate AMC CN class. In reality, the soil moisture conditions may be significantly different, depending on how close in time the rain fell before the event being simulated. Finally, existing NRCS methodology provides only three discrete classes for CNs based on AMC. Substantial changes in CN can occur for only small differences in the five-day antecedent rainfall total (e.g., 2.09 inches (AMC II) versus 2.11 inches (AMC III)), which could result in dramatic overestimations or underestimations of runoff volume.

Table B.1. Five-day antecedent rainfall totals defining the AMC I, II, and III Curve Number classes developed by the NRCS for the growing season.

AMC Class	*Runoff Depth Percentile*	*Growing Season 5-Day Antecedent Rainfall Total (inches)*	*Curve Number Adjustment*
I (dry)	10^{th}	< 1.4	$CN(I) = \frac{4.2CN(II)}{10 - 0.58CN(II)}$
II (normal)	50^{th}	1.4-2.1	–
III (wet)	90^{th}	>2.1	$CN(III) = \frac{23CN(II)}{10 + 0.13CN(II)}$

Using records from 11 NOAA daily precipitation stations listed in Table 2.3 and shown in Figure 2.8, we computed basin average daily precipitation for the West Nishnabotna River Watershed over a 68-year period (1950–2017) using Thiessen Polygons. Because HMS simulated historical storms that occurred primarily during the growing season (May–September), it considered only precipitation that fell in this period; precipitation between Oct 1–April 30 of each year was not considered. Using the basin average daily precipitation calculated for the 68-year period, we developed and compared the five-day rainfall total cumulative distribution function (CDF) to existing NRCS AMC definitions for the growing season (Table B.1). Figure B.1 shows the basin average, five-day rainfall total CDF developed for the West Nishnabotna River Watershed.

Figure B.1 illustrates that using existing NRCS definitions to describe AMC classes (Table B.1) would place the West Nishnabotna River Watershed in the AMC I (dry) class most of the time, as 86% of the five-day, basin average rainfall totals are less than 1.4 inches. “Normal” conditions for the watershed, defined by five-day antecedent rainfall totals between 1.4 and 2.1 inches (AMC II), would only occur approximately 8% of the time. “Wet” conditions (AMC III) would occur rarely (6% of the time). In other words, the existing NRCS five-day rainfall totals that define the three AMC classes are not well-suited to the West Nishnabotna River Watershed. Applying the statistical definitions of the three AMC classes to the West Nishnabotna River Watershed, the AMC I class would be defined by five-day rainfall totals between 0–0.01 inches (0–10th percentiles), the AMC II class by five-day rainfall totals between 0.01–1.65 (10th–90th percentiles), and the AMC III class by five-day rainfall totals greater than 1.65 inches (90th–100th percentiles). The five-day rainfall total in the West Nishnabotna River Watershed over the 68-year period was zero for 6% of the records.

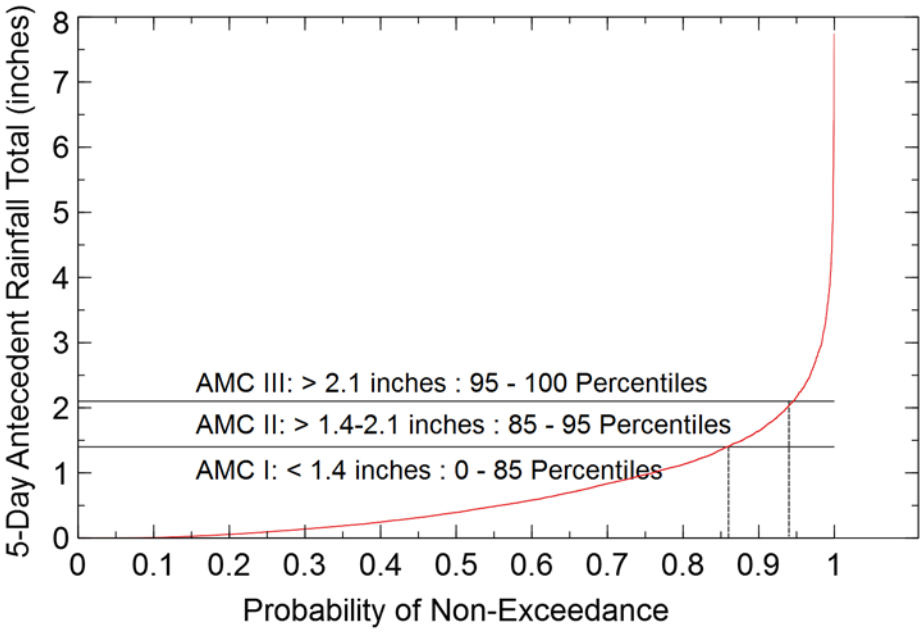

Figure B.1. Five-day rainfall total cumulative distribution function (CDF) for the West Nishnabotna River Watershed. We computed the CDF using the daily basin average precipitation computed between May and September of each year over a 68-year period (1950–2017).

To better account for AMC at the beginning of an HMS model simulation, we used a soil moisture proxy known as the antecedent precipitation index (API) instead of the five-day antecedent rainfall total. The API can be calculated over a longer period and uses a temporal decay constant (k) that accounts for soil moisture losses and allows us to apply more or less weight to precipitation that fell closer in time to the event of interest. The API on day t is calculated as:

$$API_k(t) = kAPI_k(t-1) + P(t)$$

Where P is the gauged, basin average precipitation. As with the five-day antecedent rainfall total, a greater API reflects a wetter initial condition and greater runoff potential.

The goal of this analysis was to relate CN to API, so we could make appropriate CN adjustments in the HMS model to reflect soil moisture conditions at the beginning of a simulation. Rather than have only three discrete AMC classes for CN classification, we developed a continuous function, so a unique CN change could be applied for all AMC. We calculated the basin average AMC I, II, and III CNs so we could compute the percent change from the AMC II CN for the AMC I and III classes. Then, our team performed linear interpolation between the percent changes for the basin average AMC I, II, and III CNs and their statistical definitions (10th, 50th, and 90th percentiles, respectively). In this way, we could determine a global CN adjustment (applied to all subbasin CNs) for any API percentile.

To apply a CN adjustment based on a given API percentile, we performed an analysis to determine the optimal value of k to use to compute the API. The literature reports that the decay constant (k) varies between 0.8 and 0.98 (Beck et al., 2009). Our team assumed various values of k in this range and computed the CDF for each API alternative using the basin average daily precipitation

records. For each k considered, we simulated the three calibration storms using the appropriate CN adjustment predicted from the percentile corresponding to the API for the day before the historical event simulation. The optimal k yielded the results most similar to the observed hydrographs at the USGS stage/discharge gauge locations, considering all three calibration storms; thus, researchers selected a value of 0.8 for k. For comparison, considering a five-day period and assuming equal precipitation on each day, we computed the five-day antecedent rainfall total assuming equal weight (20%) for each day. We computed API (k = 0.8) by applying a weight of nearly 30% to the precipitation that fell one day before the event and a weight of 12% to precipitation that fell five days before the event.

Figure B.2 shows the AMC methodology derived for the West Nishnabotna River Watershed. For each historical storm event, we calculated the API for the day before the start of the simulation and its percentile referenced from the CDF; we then used this percentile to determine the percent adjustment in CN to apply to all subbasin CNs in the HMS model. Our research team also performed a separate analysis in which we determined the optimal subbasin CN adjustment for each calibration storm through trial and error (independent of API). The crosses in Figure B.2 illustrate these results, which we used to adjust the initial CN-API curve (coarser dashed line) to better fit the simulated results. Because the original curve tended to lie above the best fit calibration events (crosses), we shifted the 50th percentile point down by the average percent difference between the CN adjustments predicted by the original curve and the CN adjustments determined through trial and error. This resulted in approximately a 20% reduction of the base AMC II CN.

Our team calculated new basin average AMC I, II, and III CNs, and the percent change of the AMC I and AMC III CNs from the AMC II CN defined the endpoints of the curve. The solid blue line in Figure B.2 shows the final curve used to adjust CNs to reflect the AMC prior to a historical storm. The finer dashed line illustrates how CNs would be defined into one of three classes if the NRCS methodology (Table B.1) were being used (same piecewise curve shown in Figure B.1).

The initial CN estimates resulted in a basin area-weighted average CN of 83. The 20% reduction in CN determined through calibration would result in a basin area-weighted average CN of 67. This adjusted curve number is significantly lower but reflects the aggregation of the effects of rainfall partitioning, surface storage, and soil characteristics within the watershed. Existing BMPs, particularly intensive terracing in this watershed, likely increase soil infiltration, requiring a significant reduction in model CN to replicate observed runoff volumes.

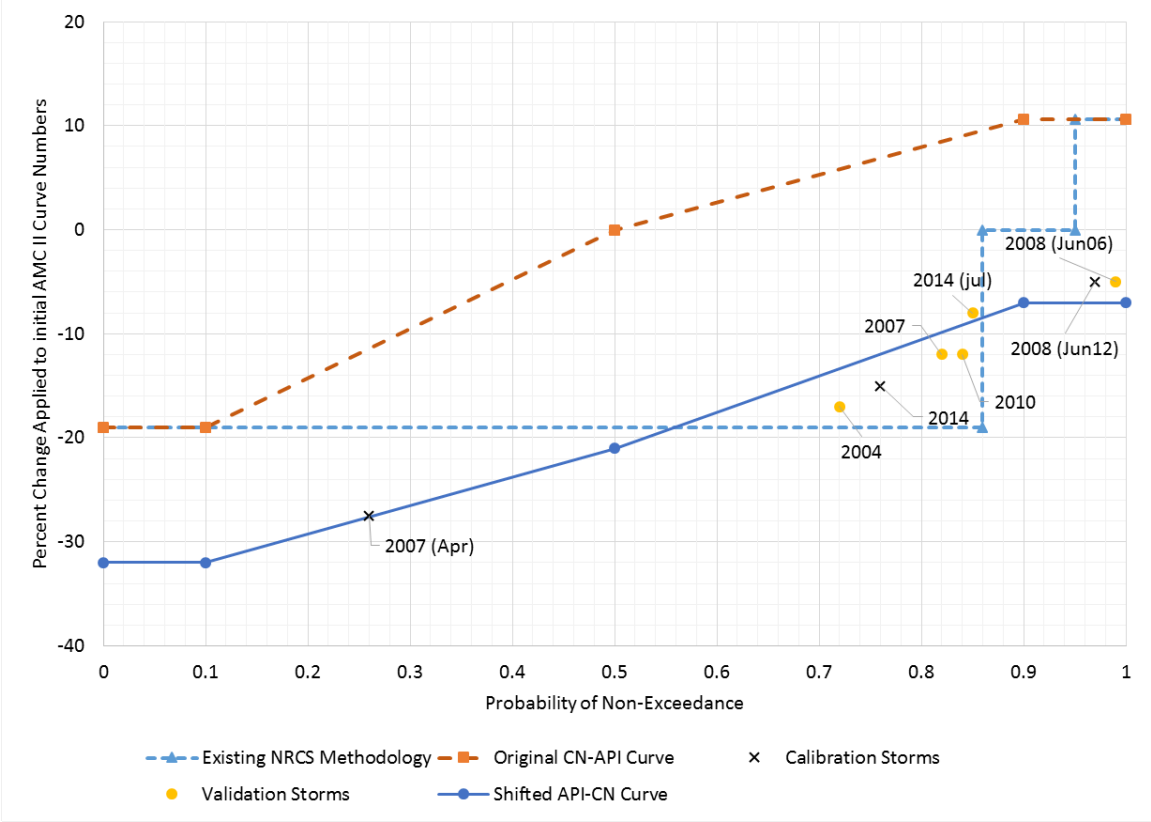

Figure B.2. Accounting for antecedent moisture conditions in the West Nishnabotna HMS model through use of the antecedent precipitation index (API). The researchers used precipitation gauge records to calculate the API prior to each historical storm event and applied a corresponding percent change to each subbasin Curve Number to account for the initial soil moisture conditions.

ii. Summary of Calibrated HMS Model Parameters

Table B.2 summarizes the final set of HMS model parameters determined through calibration for the West Nishnabotna River Watershed.

Parameter	*Initial Value*	*Calibrated Value*	*Comments*
Runoff Estimation			
Curve Number (CN)	Three discrete classes based on initial moisture state; subbasin CNs determined from Table 3.1	AMC II CNs reduced by 20%, AMC I reduced by 32%, and AMC III reduced by 17%	A continuous function to adjust CN values based on initial moisture state was developed.
Initial Abstraction (I_a)	20% of potential maximum retention (S)	20% of potential maximum retention (S)	
Subbasin Hydrograph Development			
Time of Concentration (T_c)	5/3 of subbasin lag time	5/3 of subbasin lag time	Lag time calculated using original uncalibrated CNs
Basin Storage Coefficient (R)	$\frac{T_c}{R} = 1.46 - 0.0867\frac{L^2}{A}$ (see Section 3.a.ii)	$\frac{T_c}{R} = 1.46 - 0.0867\frac{L^2}{A}$ (see Section 3.a.ii)	

River Routing			
Muskingum Flood Wave Travel Time (K)	Based on a velocity of 1.2 m/s (3.9 ft/s)	Based on a velocity of 1.8 m/s (5.9 ft/s)	
Muskingum Attenuation Factor (X)	0.2	0.2	
Muskingum-Cunge Routing Manning's Roughness - Channel	0.032	Upstream of Hancock – 0.032, Downstream of Hancock – 0.027	
Muskingum-Cunge Routing Manning's Roughness - Overbanks	0.06	Upstream of Hancock – 0.1, Downstream of Hancock – 0.06	
Baseflow			
Decay Constant (k)	0.8	0.8	Average value, varied with each storm event
Baseflow Reset on Receding Limb	0.07	0.07	Average value, varied with each storm event

iii. Calibration Storm Events

We calibrated the West Nishnabotna River Watershed HMS model to three storm events that occurred April 2007, June 2008, and June 2014. Figure B3 shows observed flow hydrographs at the Hancock and Randolph USGS gauging stations, with simulated flow hydrographs for the April 2007 event. The observations from the Riverton USGS gauging station began in 2010. Comparisons of simulated and observed peak discharge, time to peak discharge, and total streamflow volume are also shown in tabular format. Figures B4 and B5, respectively, show similar comparisons for the June 2008 and June 2014 events.

Figure B.3. Calibration Storm Events – April 23–29, 2007

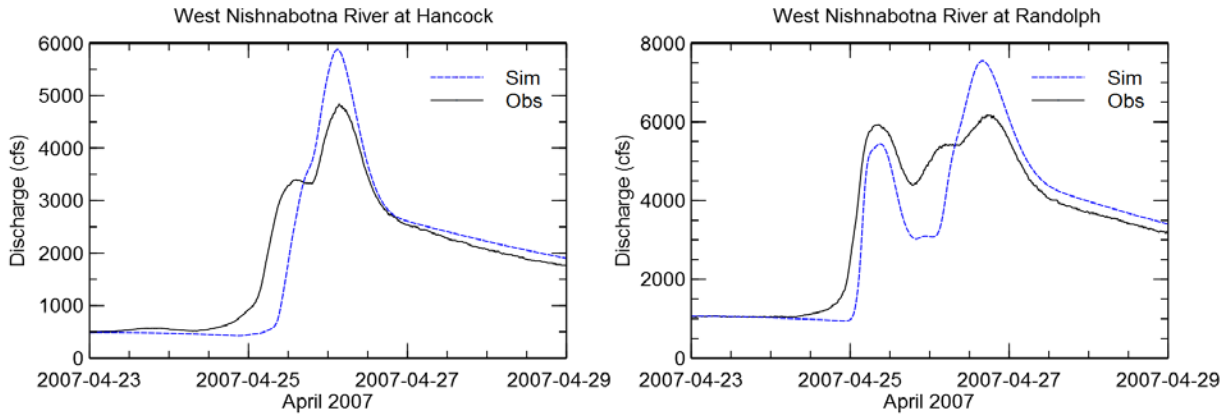

	Peak Discharge (cfs)	*Time of Peak*	*Total Volume (in)*
West Nishnabotna River at Hancock, USGS 06807410			
Simulated	5877.1	4/26/2007 02:50	0.71
Observed	4830.0	4/26/2007 03:16	0.72
West Nishnabotna River at Randolph, USGS 06808500			
Simulated	7548.9	4/26/2007 15:56	0.56
Observed	6180.0	4/26/2007 17:30	0.58

Figure B.4. Calibration Storm Events – June 10–14, 2008

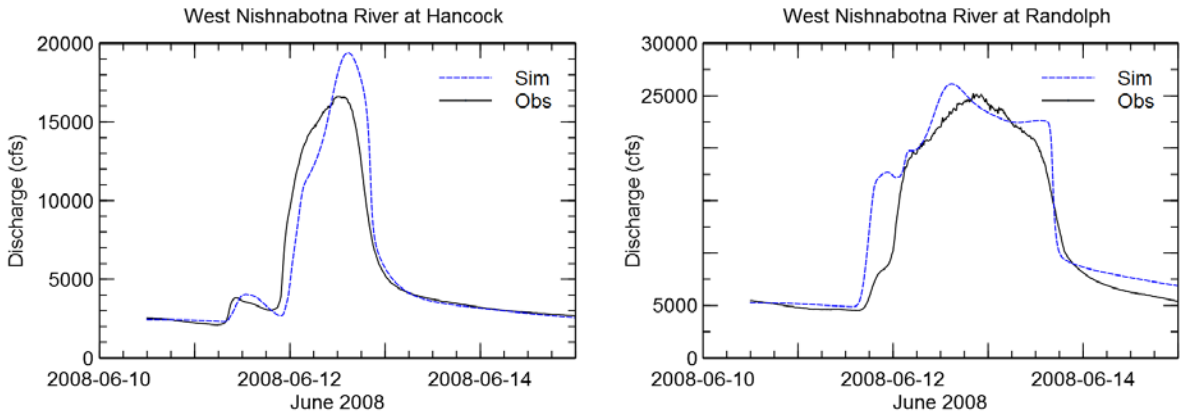

	Peak Discharge (cfs)	*Time of Peak*	*Total Volume (in)*
West Nishnabotna River at Hancock, USGS 06807410			
Simulated	19389.0	6/12/2008 14:40	1.48
Observed	16600.0	6/12/2008 11:46	1.48
West Nishnabotna River at Randolph, USGS 06808500			
Simulated	26123.9	6/12/2008 14:48	1.67
Observed	25173.3	6/12/2008 20:14	1.51

Figure B.5. Calibration Storm Events – June 3–6, 2014

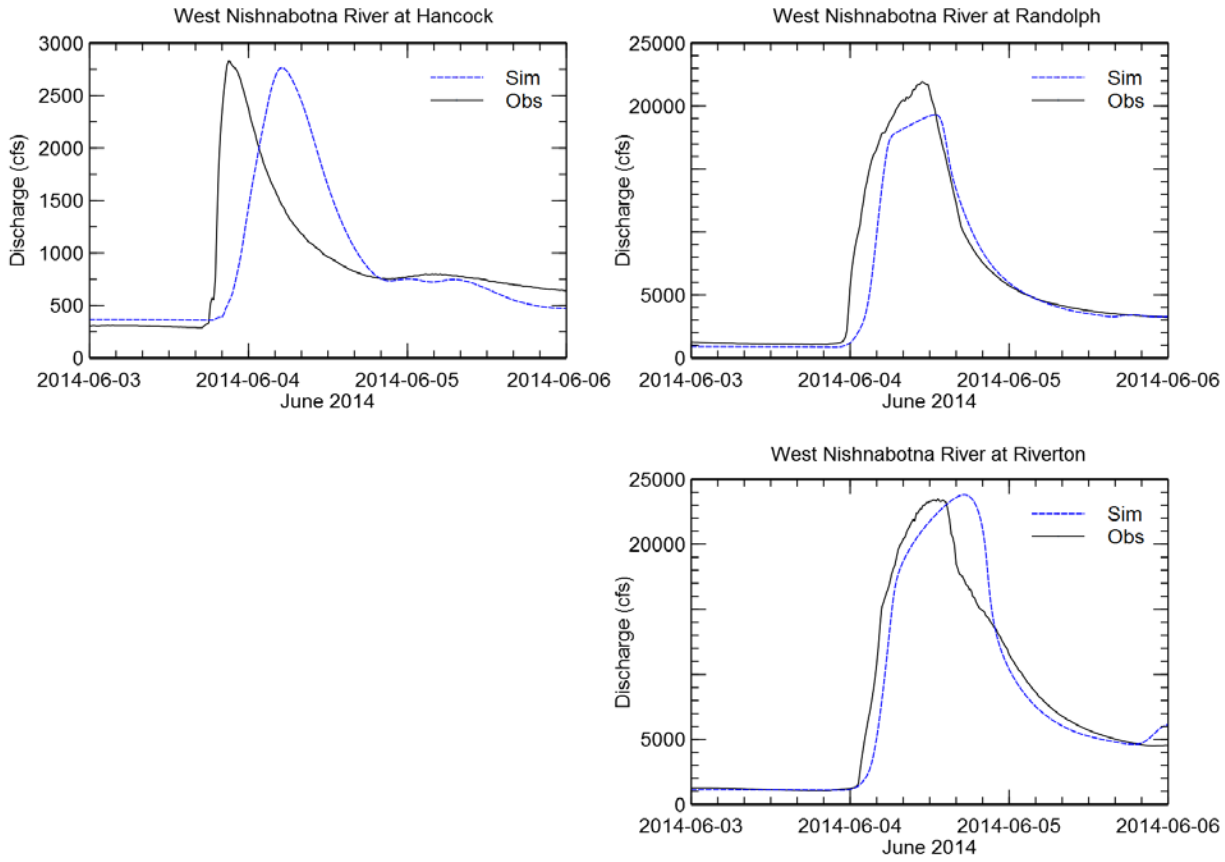

	Peak Discharge (cfs)	*Time of Peak*	*Total Volume (in)*
West Nishnabotna River at Hancock, USGS 06807410			
Simulated	2762.9	6/4/2014 05:02	0.16
Observed	2830.0	6/4/2014 21:00	0.16
West Nishnabotna River at Randolph, USGS 06808500			
Simulated	19301.2	6/4/2014 12:52	0.48
Observed	21900.0	6/4/2014 10:46	0.54
West Nishnabotna River at Riverton, USGS 06808820			
Simulated	23807.2	6/4/2014 17:12	0.52
Observed	23486.7	6/4/2014 13:14	0.53

iv. Validation Storm Events

Our team validated the West Nishnabotna River Watershed HMS model using five storm events between 2004 and 2014. Comparisons of simulated and observed peak discharges, time to peak discharge, and total streamflow volume for the May 2004, May 2007, June 2008, June 2010, and July 2014 events are shown in Figures B6 through B10, respectively.

Figure B.6. Validation Storm Events – May 22–28, 2004

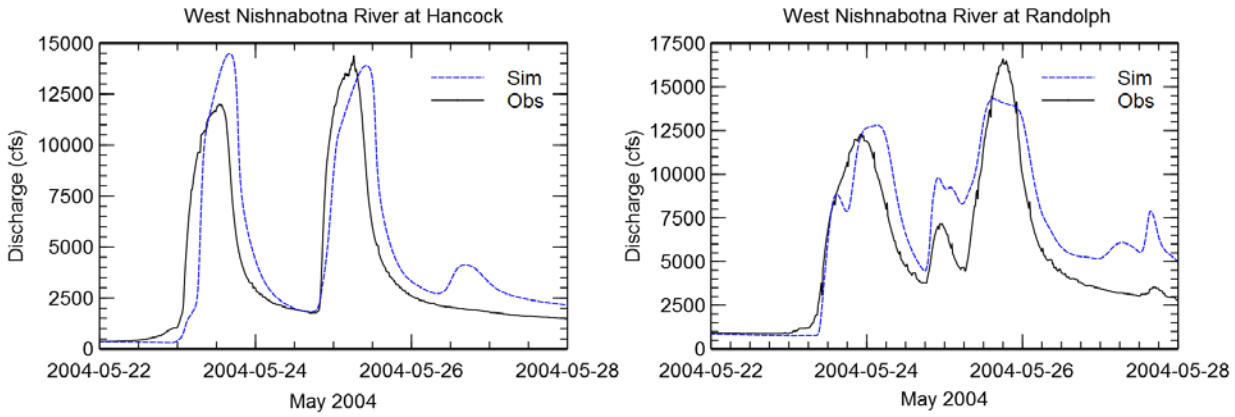

	Peak Discharge (cfs)	*Time of Peak*	*Total Volume (in)*
West Nishnabotna River at Hancock, USGS 06807410			
Simulated	14480.9	5/23/2004 16:02	1.61
Observed	11982.0	5/23/2004 13:02	1.40
Simulated (2nd Peak)	13889.0	5/25/2004 10:16	1.61
Observed (2nd Peak)	14380.0	5/25/2004 06:14	1.40
West Nishnabotna River at Randolph, USGS 06808500			
Simulated	12796.0	5/24/2004 03:12	1.13
Observed	12223.0	5/23/2004 22:24	0.93
Simulated (2nd Peak)	14294.0	5/25/2004 15:02	1.13
Observed (2nd Peak)	16600.0	5/25/2004 18:00	0.93

Figure B.7. Validation Storm Events – May 4–11, 2007

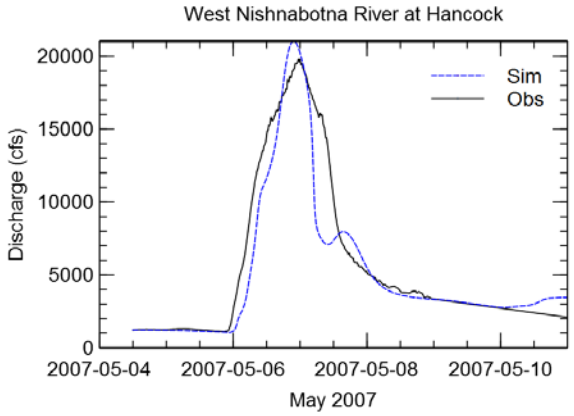

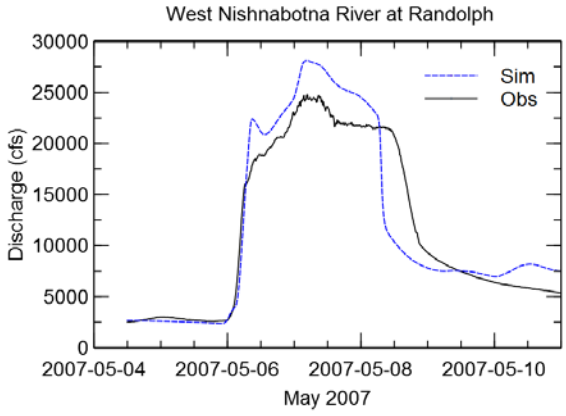

	Peak Discharge (cfs)	*Time of Peak*	*Total Volume (in)*
West Nishnabotna River at Hancock, USGS 06807410			
Simulated	21025.1	5/6/2007 21:42	2.00
Observed	19800.0	5/6/2007 23:30	2.19
West Nishnabotna River at Randolph, USGS 06808500			
Simulated	28090.5	5/6/2007 04:44	2.15
Observed	24793.3	5/6/2007 04:44	2.10

Figure B.8. Validation Storm Events – June 7–11, 2008

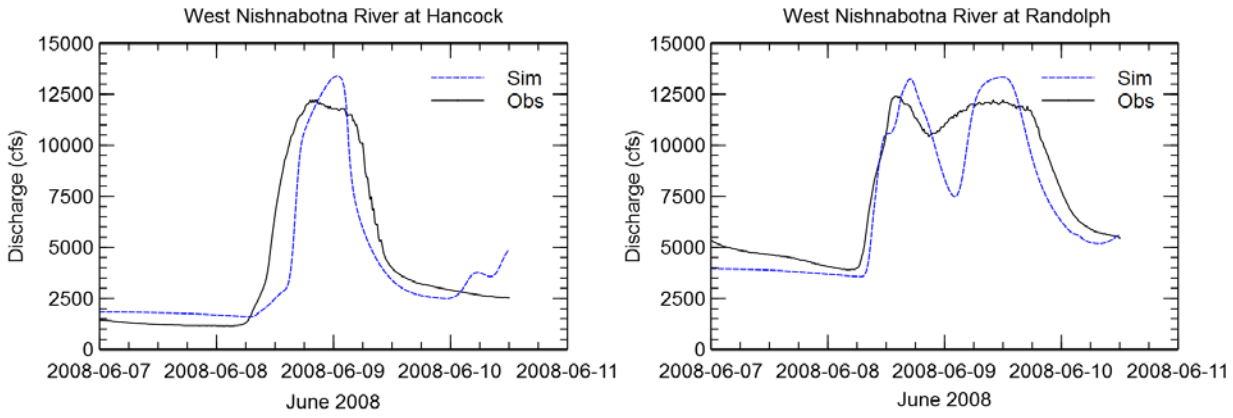

	Peak Discharge (cfs)	*Time of Peak*	*Total Volume (in)*
West Nishnabotna River at Hancock, USGS 06807410			
Simulated	13398.4	6/9/2008 00:48	0.84
Observed	12200.0	6/8/2008 20:16	0.92
West Nishnabotna River at Randolph, USGS 06808500			
Simulated	13350.1	6/9/2008 11:52	0.70
Observed	12400.0	6/8/2008 13:46	0.77

Figure B.9. Validation Storm Events – June 25–30, 2010

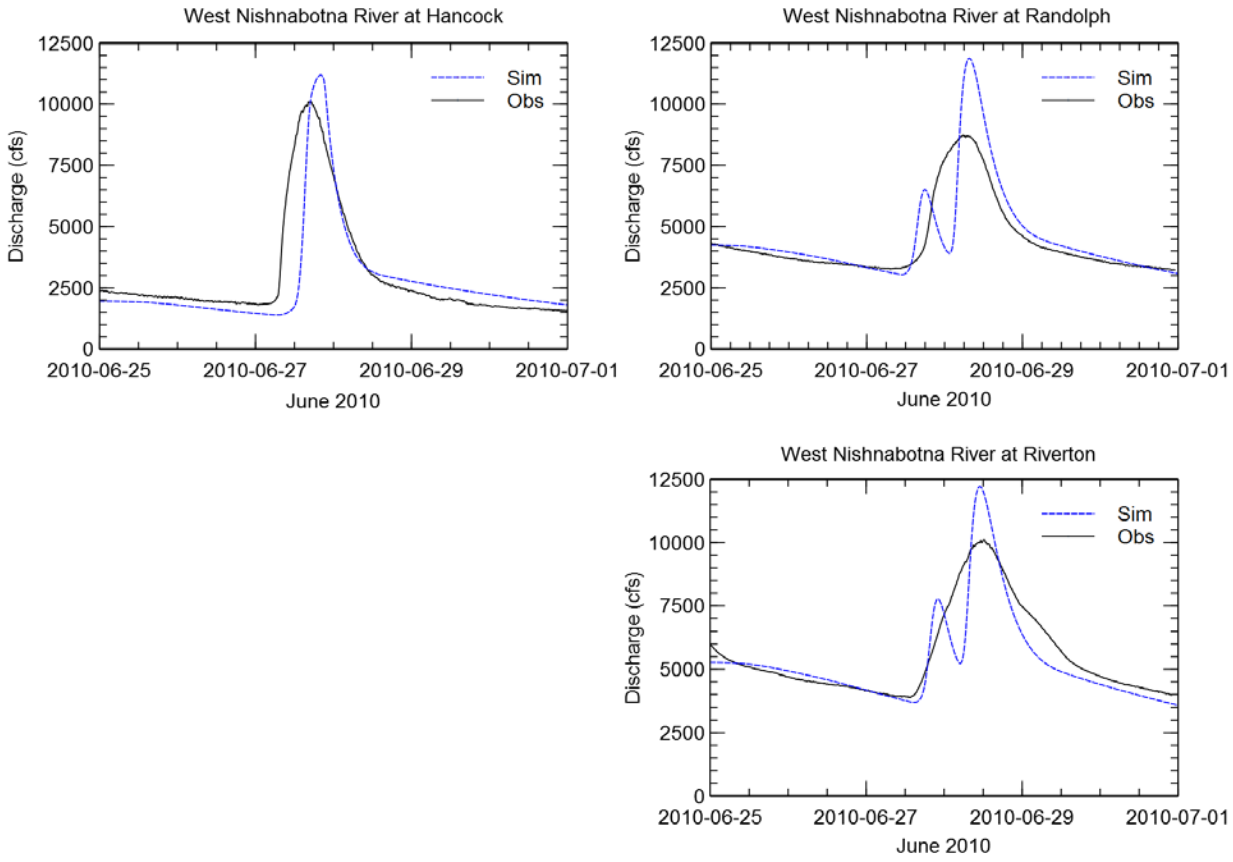

	Peak Discharge (cfs)	*Time of Peak*	*Total Volume (in)*
West Nishnabotna River at Hancock, USGS 06807410			
Simulated	11191.4	6/27/2010 20:04	1.01
Observed	10100.0	6/27/2010 16:16	1.09
West Nishnabotna River at Randolph, USGS 06808500			
Simulated	11874.1	6/28/2010 07:38	0.76
Observed	8738.7	6/28/2010 05:44	0.73
West Nishnabotna River at Riverton, USGS 06808820			
Simulated	12211.6	6/28/2010 11:00	0.72
Observed	10100.0	6/28/2010 12:00	0.74

Figure B.10. Validation Storm Events – July 3–7, 2014

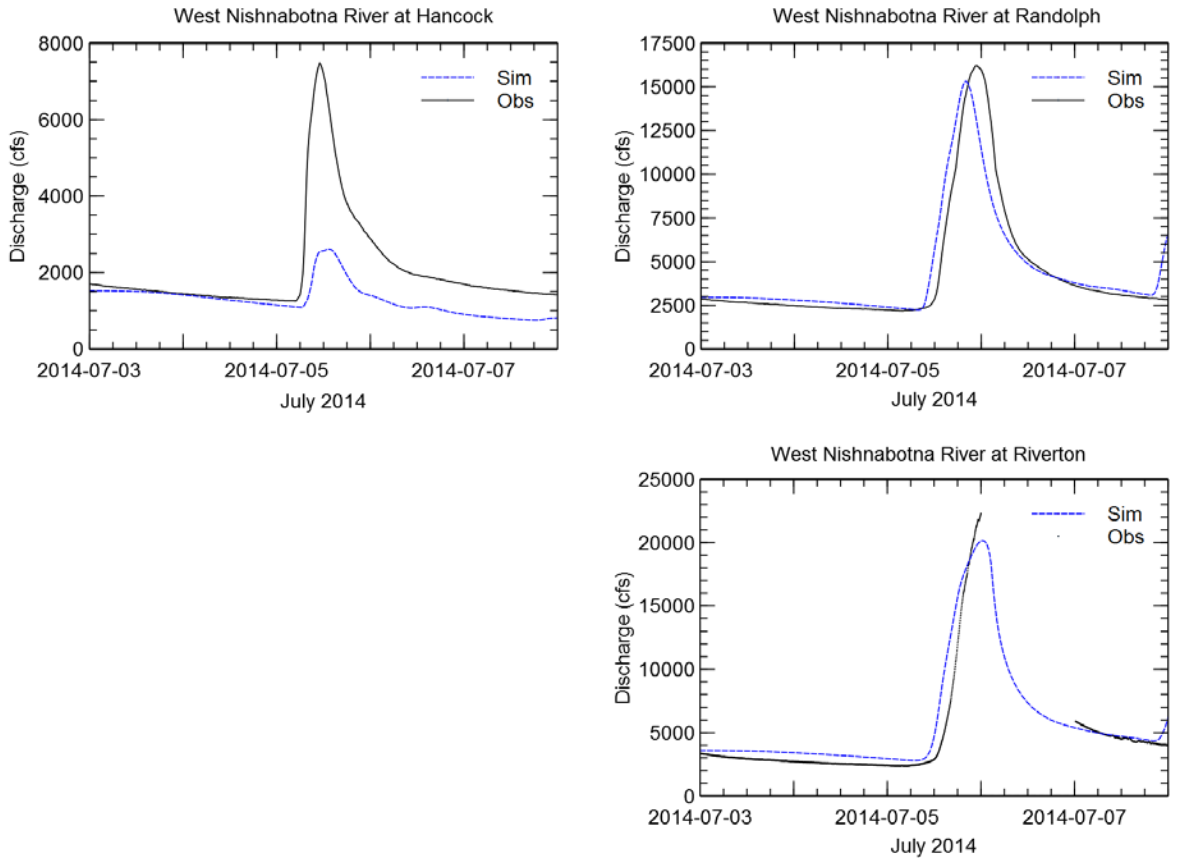

	Peak Discharge (cfs)	*Time of Peak*	*Total Volume (in)*
West Nishnabotna River at Hancock, USGS 06807410			
Simulated	2612.8	7/5/2014 13:26	0.39
Observed	7490.0	7/5/2014 11:00	0.63
West Nishnabotna River at Randolph, USGS 06808500			
Simulated	15302.7	7/5/2014 20:04	0.62
Observed	16200.0	7/5/2014 22:30	0.60
West Nishnabotna River at Riverton, USGS 06808820			
Simulated	20164.6	7/6/2014 00:26	0.67
Observed	22300.0 (missing data)	7/6/2014 00:00 (missing data)	n/a

v. Calibration/Validation Summary

We evaluated the West Nishnabotna River Watershed HMS model by comparing the simulated peak discharge, time to peak discharge, total streamflow volume, and general hydrograph shape to observations at the USGS stage/discharge gauges in the basin. Model performance varied for the calibration and validation storms.

Using the model parameters determined from calibration, we validated the West Nishnabotna River Watershed HMS model to five historical storm events. Validation is performed without adjusting transform or routing parameters beforehand to assess the predictive capability of the model. Our research team determined CNs at the beginning of each validation simulation using the API index discussed previously. Baseflow parameters were adjusted to closely reproduce observed baseflow prior to precipitation, and the transition back to baseflow following the passage of the flow wave.

The West Nishnabotna River Watershed HMS model has several strengths, weaknesses, and assumptions that should be reiterated. First, the HMS model is a surface water-only model, so subsurface and groundwater flow components are not accounted for explicitly. The HMS model represents baseflow with a first order exponential decay relationship, which represents the aggregated effects of all subsurface flow contributions (interflow and groundwater flow). Because this model is intended for event-based simulations, it does not account for evapotranspiration, which typically dwarfs infiltration and runoff volumes at large time scales. Additionally, the HMS model is only applicable for estimating the watershed response to storm events occurring between May and September. While flooding is common at other times of the year as well, particularly in March and April, this period was not considered during calibration for several reasons. Reasons include project goals (constructed projects are likely to perform better during the late spring to summer months), flood seasonality (the largest floods have occurred sporadically in the summer months), and model limitations (snowmelt was not considered in the model). Finally, the HMS model performs best when surface runoff is expected to dominate the partitioning of rainfall. This typically occurs for larger storm events when a greater overall amount of precipitation is converted to runoff or for near-saturated initial conditions.

Figure B11 compares the simulated and observed peak discharges at USGS stage/discharge gauge locations in the watershed for calibration and validation events. A line representing perfect agreement between simulated and observed peak discharges is also shown. Most of the validation data points lie on or near the line, indicating that the model is capable of reproducing observed peak discharges for a variety of storm events.

Figure B12 compares the simulated and observed runoff volumes at USGS stage/discharge gauge locations in the watershed for calibration and validation events. Once again, most of validation data points lie on or near the perfect agreement line, indicating that the model can reproduce observed runoff volumes for a variety of storm events.

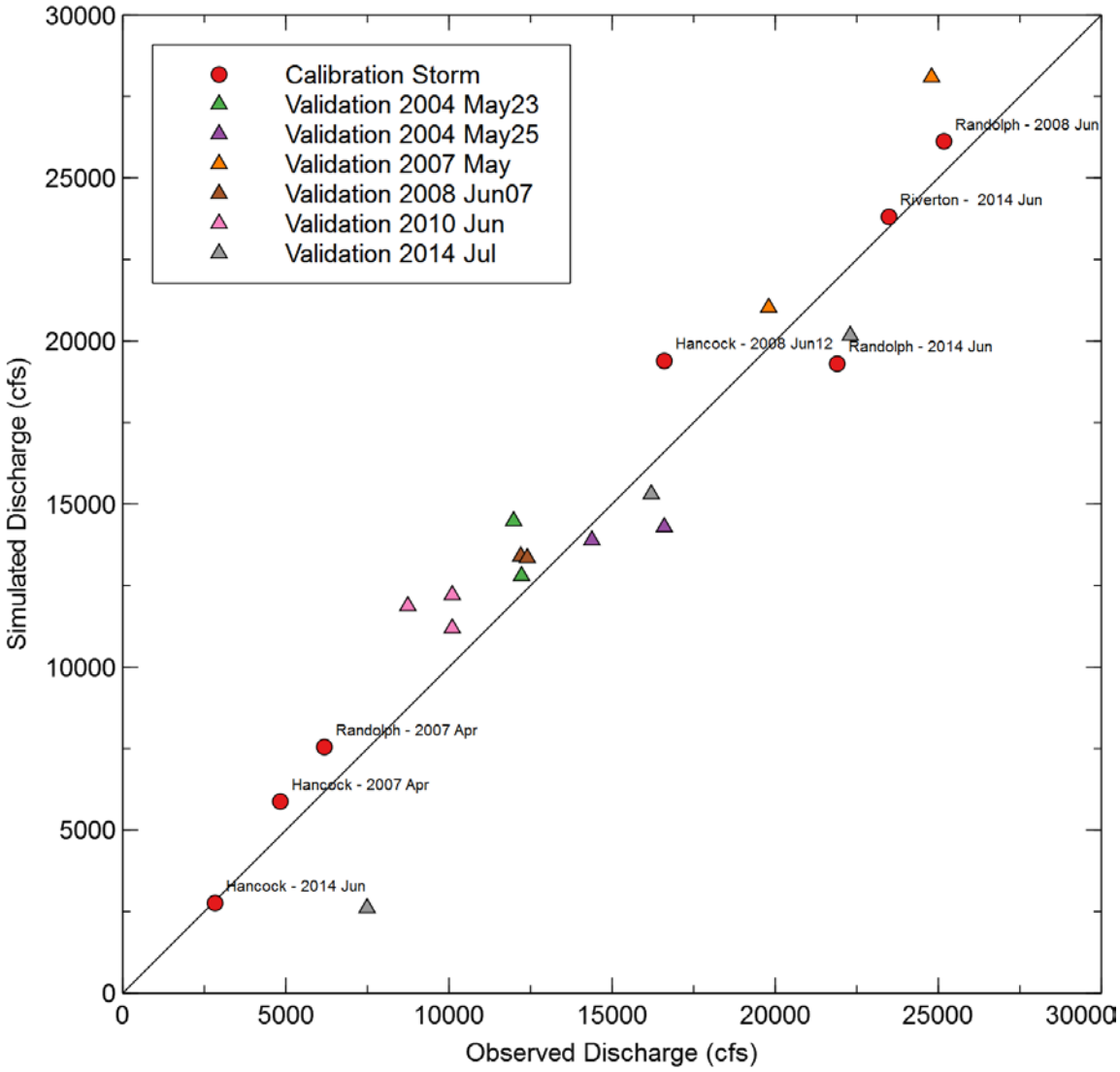

Figure B11. Comparison of simulated and observed peak discharges at USGS stage/discharge gauge locations in the West Nishnabotna River Watershed for calibration and validation events.

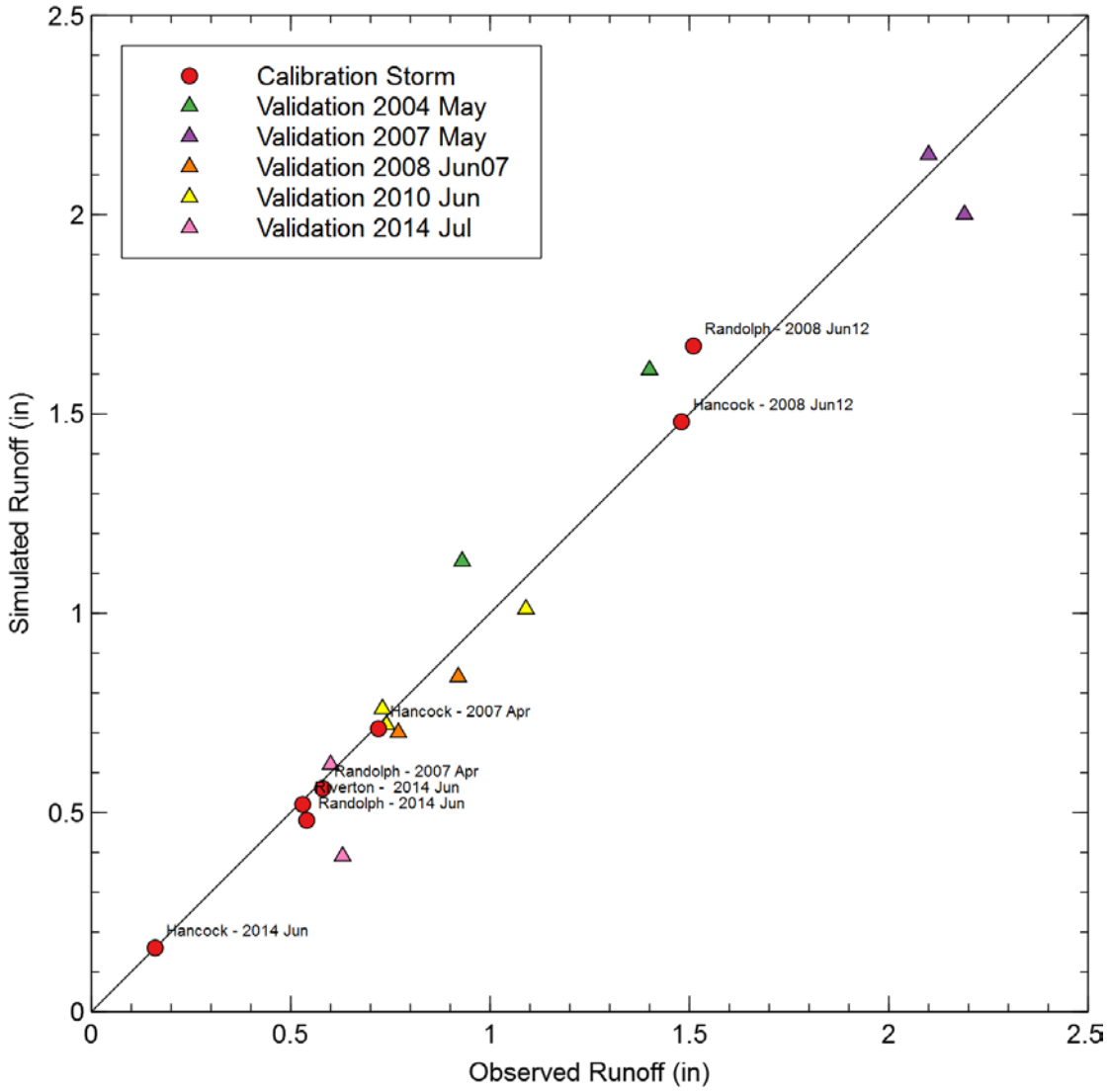

Figure B12. Comparison of simulated and observed runoff volumes at USGS stage/discharge gauge locations in West Nishnatbotna River Watershed for calibration and validation events

.

Appendix C – Incorporated Structures

Table C.1. Prairie Rose Lake Stage-Storage-Discharge Table

Elevation (ft)	*Storage (ac-ft)*	*Discharge (cfs)*	*Notes*
1228	3601.5	0	Principal Spillway
1230	3900	297	
1232	4350	840	
1234	4800	1543	
1236	5500	2376	
1238	6150	3320	
1240	6823.5	4365	Top of Embankment
1242	7800	13561	
1244	8700	29520	
1246	10000	49904	

Appendix D – References

Archuleta, Ray. "Cedar River Watershed Coalition Meeting – Cover Crops and Other Conservation Practices," Personal interview, April 2014.

Bharati, L., Lee, K.H., Isenhart, T.M., Schultz, R.C., (2002). "Soil-water infiltration under crops, pasture, and established riparian buffer in Midwestern USA," Agroforest. Syst. 56 (3), 249–257.

Bradley, A.A. (2010). "What Causes Floods in Iowa?" A Watershed Year: Anatomy of the Iowa Floods of 2008, C. Mutel (editor), University of Iowa Press, Iowa City, Iowa. 7 - 17.

Burkart, M. (2010). "The Hydrologic Footprint of Annual Crops," A Watershed Year: Anatomy of the Iowa Floods of 2008, C. Mutel (editor), University of Iowa Press, Iowa City, Iowa. 77 – 85.

Brye, K.R., Norman, J.M., Bundy, L.G., Gower, S.T., (2000). "Water-budget evaluation of prairie and maize ecosystems," Soil Sci. Soc. Am. J. 64 (2), 715–724

Chow, V.T., Maidment, D., and Mays, L. (1988). Applied Hydrology. McGraw-Hill, Inc.

Cohen, D. (1993). Iowa Prairies. Iowa Association of Naturalists. Biological Communities (IAN). Iowa State University Extension Service. Ames, Iowa.

Eash, D.A, Heinitz, A.J. (1991). Floods in the Nishnabotna River Basin, Iowa. Open-File Report 91-171. U.S. Geological Survey. 1991.

Easterling, D.R., K.E. Kunkel, J.R. Arnold, T. Knutson, A.N. LeGrande, L.R. Leung, R.S. Vose, D.E. Waliser, and M.F. Wehner, (2017). Precipitation change in the United States. In: Climate Science Special Report: Fourth National Climate Assessment, Volume I [Wuebbles, D.J., D.W. Fahey, K.A. Hibbard, D.J. Dokken, B.C. Stewart, and T.K. Maycock (eds.)]. U.S. Global Change Research Program, Washington, DC, USA, pp. 207-230, doi: 10.7930/J0H993CC.

Fischer, E.E. (1999). Flood of June 15-17, 1998 Nishnabotna and West Nishnabotna Rivers, southwest, Iowa. U.S. Geological Survey. Open-File Report 99-70.

Frans, C., Istanbulluoglu, E., Mishra, V., Munoz-Arriola, F., Lettenmaier, D.P. (2013). Are climatic or land cover changes the dominant cause of runoff trends in the Upper Mississippi River Basin? Geophysical Research Letters, Vol. 40 (17).

Galloway, G.E., (2010). "The Great Flood of 1993," A Watershed Year: Anatomy of the Iowa Floods of 2008, C. Mutel (editor), University of Iowa Press, Iowa City, Iowa. 227 – 233.

Hernandez-Santana, V., Zhou, X., Helmers, M., Kolka, R., & Tomer, M. (2013). Native prairie filter strips reduce runoff from hillslopes under annual row-crop systems in Iowa, USA. Journal of Hydrology, 94-103.

Iowa Department of Natural Resources (2018, January 16). 2016 305(b) Assessment Summary-2016 Impaired Waters List. https://programs.iowadnr.gov/adbnet/Assessments/Summary/2016. Accessed July 01, 2018.

Iowa Geological & Water Survey, Iowa Department of Natural Resources (2013). Landform Regions of Iowa. http://www.igsb.uiowa.edu/browse/landform.htm. Accessed January 2017.

Jackson, R.B., Canadell, J., Ehleringer, J.R., Mooney, H.A., Sala, O.E., Schulze, E.D. (1996). "A global analysis of root distributions for terrestrial biomes," Oecologia, 389-411.

Jones, C.S. and Schilling, K.E. (2011). "From Agricultural Intensification to Conservation: Sediment Transport in the Raccoon River, Iowa, 1916-2009," Journal of Environmental Quality, 40.

Knox, J.C. (2001). "Agricultural Influence on Landscape Sensitivity in the Upper Mississippi River Valley," Catena 42, 193-224.

Linhart, S.M., and Eash, D.A. (2010). Floods of May 30 to June 15, 2008, in the Iowa and Cedar River basins, eastern Iowa, Open-File Report 2010-1190, 99. U.S. Geological Survey.

Meierdiercks, K.L., Smith, J.A., Baeck, M.L., and Miller, A.J. (2010). "Analyses of Urban Drainage Network Structure and its Impacts on Hydrologic Response," Journal of American Water Resources Research, 14(4), 416-424.

Mejia, A.I., Moglen, G.E. (2010). "Impact of the Spatial Distribution of Imperviousness on the Hydrologic Response of an Urbanizing Basin," Hydrologic Processes, 24, 3353-3373.

Mora, C., Abby G. Frazier, A.G., Longman, R.J., Dacks, R.S., Walton, M.M., Tong, E.J., Sanchez, J.J., Kaiser, L.R., Stender, Y.O., Anderson, J.M., Ambrosino, C.M., Fernandez-Silva, I., Giuseffi, L.M. and Giambelluca, T.M. (2013). The projected timing of climate departure from recent variability, Nature, 502(7470).

Mutel, C.M. (2010). A Watershed Year: Anatomy of the Iowa Floods of 2008, C. Mutel (editor), University of Iowa Press, Iowa City, Iowa. 74.

National Oceanic and Atmospheric Administration (2013). NOAA Atlas 14 Point Precipitation Frequency Estimates. http://hdsc.nws.noaa.gov/hdsc/pdfs/pdfs_map_cont.html?bkmrk=ia.

National Oceanic and Atmospheric Administration (2017). National Centers for Environmental Information Map Application – Version 1.8.4 Monthly Summaries Map. https://gis.ncdc.noaa.gov/maps/ncei/summaries/monthly. Accessed April 2017.

North Central Region Water Network (2018). About the Agricultural Conservation Planning Framework (ACPF). https://northcentralwater.org/acpf/. Accessed July 01, 2018.

Papanicolaou, A.N., Wacha, K.M., Abban, B.K., Wilson, C.G., Hatfield, J.L., Stanier, C.O., Filley, T.R. (2015). "From soilscapes to landscapes: A landscape oriented approach to simulate soil organic carbon dynamics in intensively manage landscapes," Journal of Geophysical Research: Biogeosciences, 120, 2375-2401, doi:10.1002/2015JG003078.

Petersen W. (2010). "The Hydrology of Urban Landscape," A Watershed Year: Anatomy of the Iowa Floods of 2008, C. Mutel (editor), University of Iowa Press, Iowa City, Iowa. 87 – 95.

PRISM Climate Group. (2018). Oregon State University, http://prism.oregonstate.edu, created March 2018.

Sayre, R. (2010). "The Dam and the Flood: Cause of Cure," A Watershed Year: Anatomy of the Iowa Floods of 2008, C. Mutel (editor), University of Iowa Press, Iowa City, Iowa. 103 – 109.

Scharffenberg, W. (2013). HEC-HMS User's Manual 4.0. U.S. Army Corps of Engineers Hydrologic Engineering Center.

Schilling, K. (2000). "Patterns of Discharge and Suspended Sediment Transport in the Walnut and Squaw Creek Watersheds, Jasper County, Iowa: Water Years 1996-1998," Iowa Department of Natural Resources, Geological Survey Bureau, Iowa City, Iowa.

Schilling, K.E., Chan, K-S., Jha, M.K., Zhang, Y-K., and Gassman, P.W. (2008). "Impact of Land Use and Land Cover Change on the Water Balance of a Large Agricultural Watershed: Historical Effects and Future Directions," Water Resources Research, 44, doi: 10.1029/2007WE006644.

Schilling, K.E., Chan, K-S., Liu, K-S., and Zhang, Y-K., Gassman, P.W. (2008). "Quantifying the Effect of Land Use Land Cover Change on Increasing Discharge in the Upper Mississippi River," Journal of Hydrology 387, pp. 343-345.

Schottler, S.P., Ulrich, J., Belmont P., Moore, R., Lauer, J.W., Engstrom, D.R., Almendinger, J.E. (2013). "Twentieth Century Agricultural Drainage Creates More Erosive Rivers," Hydrological Processes, doi:10.1002/hyp.9738.

Smith, J. A., Baeck, M.L., Villarini, G., Wright, D.B., Krajewski, W.F. (2013). "Extreme flood response: The June 2008 flooding in Iowa." Journal of Hydrometeorology. 14(6). 1810-1825., doi: 10.1175/JHM-D-12-0191.1.

Sprague, L.A., Hirsch, R.M., Aulenbach, B.T. (2011). "Nitrate in the Mississippi River and its tributaries, 1980 to 2008: Are we making progress?" Environmental Science & Technology. 2011. August 9;45(17):7209–16.

Stolze, J.H. (2018). A Tale of Soap and Water: Soap Creek Leads the State in Flood Mitigation. Retrieved from http://www.iowawatershedapproach.org/2018/02/a-tale-of-soap-and-water-soap-creek-leads-the-state-in-flood-mitigation/

Takle, E.S. (2010). "Was Climate Change Involved?" A Watershed Year: Anatomy of the Iowa Floods of 2008, C. Mutel (editor), University of Iowa Press, Iowa City, Iowa. 111 – 116.

Thompson, J. (2003). "Wetlands Drainage, River Modification, and Sectoral Conflict in the Lower Illinois Walley," Southern Illinois University, Carbondale, IL.

Tomer, M.D., Porter, S.A, James, D.E., Boomer, K.M.B., Kostel, J.A., and McLellan, E. (2013). "Combining precision conservation technologies into a flexible framework to facilitate agricultural watershed planning" Journal of Soil & Water Conservation. 68:113A-120A.

United States Department of Agriculture-Iowa State University (2011). USDA-NIFA Award No. 2011-68002-30190. http://sustainablecorn.org/Weather&Agriculture/Pubs/IA-Northeast.pdf.

United States Department of Agriculture-National Resource Conservation Service (2007). National Engineering Handbook. Part 630. Chapter 7. http://directives.sc.egov.usda.gov/OpenNonWebContent.aspx?content=17757.wba

Urban, M.A. and Rhoads, B.L. (2003). "Catastrophic Human-Induced Change in Stream-Channel Planform and Geometry in an Agricultural Watershed, Illinois, USA", Annals of the Association of American Geographers, 93(4), 783-796.

Wang, C., Chan, K., Schilling, K.E. (2016). "Total Phosphorus Concentration Trends in 40 Iowa Rivers, 1999 to 2013." Journal of Environmental Quality. Madison, WI. doi: 10.2134/jeq2015.07.0365.

Weber, L.J., Muste, M., Bradley A.A., Amado Arenas, A., Demir, I., Drake, C.W., Krajewski, W.F., Loeser, T.J., Politano, M.S., Shea, B.R., Thomas, N.W. (2018). "The Iowa Watershed Project: Iowa's prototype for engaging communities and professionals in watershed hazard mitigation." International Journal of River Basin Management, 16:3, 315-328, doi: 10.1080/15715127.2017.1387127.

Wehmeyer, L.L., Weirich, F.H., and Cuffney, T.F. (2011). "Effect of Land Cover Change on Runoff Curve Number Estimation in Iowa, 1832–2001," Ecohydrol. 4, 315–321.

Winsor, R. (1975). "Artificial Drainage of East Central Illinois 1820-1920," PhD Thesis, Department of Geography, University of Illinois, Urbana-Champaign, Illinois.

Wuebbles, D.J., D.W. Fahey, K.A. Hibbard, B. DeAngelo, S. Doherty, K. Hayhoe, R. Horton, J.P. Kossin, P.C. Taylor, A.M. Waple, and C.P. Weaver, (2017). Executive summary. In: Climate Science Special Report: Fourth National Climate Assessment, Volume I [Wuebbles, D.J., D.W. Fahey, K.A. Hibbard, D.J. Dokken, B.C. Stewart, and T.K. Maycock (eds.)]. U.S. Global Change Research Program, Washington, DC, USA, pp. 12-34, doi: 10.7930/J0DJ5CTG

Yiping Wu, Y., Liu, S., Sohl, T.L., Young, C.J. (2013). Projecting the land cover change and its environmental impacts in the Cedar River Basin in the Midwestern United States, Environmental Research Letters, 8(2).

Zhang, Y. K. and Schilling, K.E. (2006). "Effects of Land Cover on Water Table, Soil Moisture, Evapotranspiration, and Groundwater Recharge: a Field Observation and Analysis," Journal of Hydrology, 319(1-4), 328-338.

Zhang, Y-K. and Schilling, K.E. (2006). "Increasing Streamflow and Baseflow in the Mississippi River since the 1940s:Effects of Land-use Change," Journal of Hydrology 325, doi:10.1016/j.jhydrol.200509.033, 412-42.